University of Natural Resources and Life Sciences, Vienna
Department of Water, Atmosphere and Environment
Institute for Soil Physics and Rural Water Management

Doctoral Thesis

Splash Erosion Affected by Rainfall Parameters and Soil Initial Conditions

submitted in partial fulfilment of the requirements to obtain the degree of "Doctor of Natural Resources and Life Sciences" (Dr.nat.techn.) at the University of Natural Resources and Life Sciences, Vienna

by

Nives Zambon

Vienna,
September 2020

Preface

The research for this thesis was carried out as a part of the Austrian-Czech Joint Research Project “Kinetic energy of rainfall as driving force of soil detachment and transport” (KERS) funded by the Austrian Science Fund (FWF): I 3049-N29.

One of the goals of this project was to investigate the relationship between rainfall kinetic energy and soil detachment under natural rainfall at the measurement sites in Central Europe and New Zealand and to relate differences in splash erosion to the surface conditions affected by rainfall kinetic energy.

The experiments of splash erosion under natural rainfall were carried out on the four measurement sites, three in Central Europe and one in New Zealand. Soil samples from the three sites in Central Europe were distributed between the sites. In order to ensure consistent comparison of soil erosion data, the measurements from New Zealand were not evaluated in this thesis due to different soil material used at this measurement site. Experiments investigating effect of surface condition on splash erosion were performed in laboratory using simulated rainfall at University of Natural Resources and Life Sciences (BOKU), in Vienna and Institute for Land and Water Management Research (BAW), in Petzenkirchen, Austria.

One part of my research was carried out at BAW, in Petzenkirchen where I operated the erosion measurement site in Hydrological Open Air Laboratory (TU Wien) and preformed the rainfall simulations in the institute`s laboratory. The other part of the research was based at the Institute for Soil Physics and Rural Water Management (SoPhy) at University of Natural Resources and Life Sciences, in Vienna where I was managing and performing the laboratory splash erosion experiments. As a part of my Ph.D. programme, I spent one abroad semester at the Department of Civil and Natural Resources Engineering at the University of Canterbury, Christchurch, New Zealand for research stay.

The doctoral thesis was completed under the academic supervision of:

Supervisor:
Ao.Univ.Prof. Dipl.-Ing. Dr.nat.techn. Andreas Klik

Advisory Team:
Dipl.-Ing. Dr.nat.techn. Peter Strauss
Doc. Dr. Ing. Tomáš Dostál
Dr. Thomas A. Cochrane

I hereby declare that I am the sole author of this work. No assistance other than that which is permitted has been used. Ideas and quotes taken directly or indirectly from other sources are identified as such. This written work has not yet been submitted in any part.

Vienna, September 2020

Nives Zambon

Acknowledgements

Completing the PhD was a challenging task, which required hard work and dedication. However, this would be even harder if there were not people, who provided their unselfish support and guidance and to whom I would like to express my deepest gratitude and appreciation.

First, I would like to thank Andreas Klik for supervising my thesis and giving his professional guidance during my doctoral study. I am grateful that he invested his trust, patience and time in my research, which greatly contributed to finalize my thesis. Furthermore, I would like to thank my supervisor for giving me an opportunity to present my research internationally on conferences and abroad Universities, which enabled me to meet international experts and colleagues.

My gratitude extends also to my co-supervisor Peter Strauss, who managed my experiments at BAW and provided his support during my stay in Petzenkirchen. Furthermore, I am thankful to my co-supervisor Tomas Dostal and David Zumr, who always provided their positive feedbacks and insightful ideas for the publications and experiments. I would like to thank KERS crew for great hospitality during visits in Prague at Czech Technical University.

I am thankful to my co-supervisor Thomas A. Cochrane for providing his support and warm hospitality during my abroad semester in New Zealand at Canterbury University in Christchurch. I would like to thank to Fabio for his help, positive energy and support during experiments and other Civil Postgrad students who made my stay in New Zealand unforgettable.

This work would not be possible without a finical support by Austrian Science Fond (FWF) under grant number: I 3049-N29. I am grateful that I was provided a continuous financial support by the project: "Kinetic energy of rainfall as driving force of soil detachment and transport".

I would like to thank my colleagues at SoPhy (BOKU) and BAW for an amazing team work, support and enjoyable working environment. Specially, thanks to Wolfgang Sokol for providing his IT and data management expertise and to Franz Aigner for helping me with the experiments.

Foremost, my thank you goes to Lisbeth Lolk Johannsen who was a great colleague, enjoyable to work and spend free time with. Thank you for sharing your honest opinion and feedback to my work and for the greatest time during our travel in New Zealand.

I would like to thank my family, who always believed in me and emotionally supported me along this journey. My special thanks to my friends Ivana and Anja for easing my troubles and keeping my thoughts positive. Finally, greatest thank to you Ivan, for giving me constant inspiration and encouragement to reach higher. Thank you for your endless love and understanding, which make everything possible.

Abstract

Soil erosion by water is one of the globally most threating soil degradation processes. Splash erosion begins with the first raindrop impact on the soil surface and represents the initial stage of soil erosion by water. The ability of rainfall to initiate splash erosion is highly dependent on its intensity and kinetic energy together with soil physical properties. Splash erosion is investigated either under natural or simulated rainfall. This thesis investigates the effect of rainfall erosivity on splash erosion under natural rainfall and possible effects of soil initial condition on splash erosion under simulated rainfall. First objective of this thesis is to test performance of different rainfall parameters in order to predict splash erosion for the three measurements sites in Central Europe. Second objective focuses on variations in splash erosion rates affected by different rainfall kinetic energy, soil moisture content and surface structure.

To obtain relationship between splash detachment and rainfall parameters (intensity, kinetic energy and rainfall erosivity factor (EI_{30})) experiments were arranged on two sites in lower Austria and one location in Czech Republic. Regression analysis suggested that the average rainfall intensity was the best erosivity parameter for splash erosion prediction, considering three soils tested in experiment. Cumulative rainfall kinetic energy and rainfall erosivity factor underestimated the splash erosion rate. Soil surface in the field is exposed to constant changes in the rainfall regime that affect directly soil moisture and surface structure. Rainfall simulations were performed to explore splash erosion development for different soil water content and surface condition. The largest decrease in splash erosion rates was evident for the samples with high initial water content and partly developed surface seals affected by high rainfall intensity. Surface seal formation was recognized through decrease in measured soil saturated hydraulic conductivity, which could be described as the function of rainfall kinetic energy.

The presented research highlighted complex interaction between rainfall and soil properties affecting splash erosion process. Monitoring of rainfall parameters on high temporal resolution and identifying the effect of rainfall on soil properties are crucial to describe underlying processes involved in splash erosion. The presented results are limited to conditions in the experiments. Further investigation on different locations using diverse soil types are recommended to extend the knowledge about splash erosion affected by raindrop impact.

Key words: splash erosion, rainfall intensity, rainfall kinetic energy, soil moisture, surface sealing

Zusammenfassung

Bodenerosion durch Wasser ist weltweit einer der bedeutendsten Prozesse, die zur Bodendegradation beitragen. Spritzerosion beginnt mit dem ersten Aufprall des Regentropfens auf der Bodenoberfläche und stellt die erste Phase der Bodenerosion durch Wasser dar. Das Potenzial von Regenfällen, Spritzerosion auszulösen, hängt stark von der Intensität und kinetischen Energie des Regens sowie von den physikalischen Eigenschaften des Bodens ab. Spritzerosion wird entweder bei natürlichem Regen oder mit Regensimulationen im Labor untersucht. Diese Doktorarbeit untersucht den Einfluss der Regenerosivität auf Spritzerosion bei natürlichem Regen sowie die möglichen Effekte des anfänglichen Bodenzustands auf Spritzerosion bei simuliertem Regen. Das erste Ziel dieser Arbeit ist es, die Anwendbarkeit verschiedener Regenparameter für die Vorhersage von Spritzerosion an drei Messstandorten in Zentraleuropa zu testen. Im zweiten Teil befasst sich die Arbeit mit den Schwankungen in Spritzerosionsraten und wie sie durch Unterschiede in der kinetischen Energie des Regens, der Bodenfeuchte und der Oberflächenstruktur beeinflusst werden.

Um einen Zusammenhang zwischen Spritzerosion und Niederschlagsparametern (Regenintensität, kinetische Energie und Erosivitätsfaktor (EI_{30})) zu erhalten, wurden die Experimente an zwei Standorten in Niederösterreich und einem Standort in Tschechien durchgeführt. Die Ergebnisse der Regressionsanalyse zeigen eine hohe Abhängigkeit der Spritzerosion mit der mittleren Regenintensität für die getesteten Böden. Die kumulative kinetische Energie des Niederschlags und der Erosivitätsfaktor des Niederschlags unterschätzten die Spritzerosionsrate. Die Bodenoberfläche auf dem Feld ist ständigen Änderungen des Niederschlagsregimes ausgesetzt, die sich direkt auf den Bodenwassergehalt und die Oberflächenstruktur auswirken. Um die Entwicklung der Spritzerosion bei unterschiedlichen Bodenwassergehalten und Oberflächenzuständen zu untersuchen, wurden Regensimulationen durchgeführt. Die Senkung der Spritzerosion war bei den Bodenproben mit hohem Wassergehalt und teilweise entwickelter Oberflächendichtung erkennbar. Die Oberflächendichtung des Bodens wurde durch Abnahme der gemessenen gesättigten Leitfähigkeit erkannt, die als Funktion der kinetischen Energie des Regens beschrieben werden konnte.

Die vorgestellte Studie betont die komplexe Interaktion zwischen Niederschlag und Bodeneigenschaften, die den Spritzerosionsprozess beeinflussen. Die Messungen der Niederschlagsparameter bei hoher zeitlicher Auflösung und die Ermittlung der Auswirkung des Niederschlags auf die Bodeneigenschaften sind entscheidend für die Beschreibung der zugrunde liegenden Prozesse bei der Spritzerosion. Die vorgestellten Ergebnisse beschränken sich auf die Bedingungen in den Experimenten. Weitere Untersuchungen an verschiedenen Standorten unter Verwendung verschiedener Bodentypen werden empfohlen, um das Wissen über die durch Regentropfeneinschläge beeinflusste Spritzerosion zu erweitern.

Schlüsselwörter: Spritzerosion, Regenintensität, kinetische Energie des Regens, Bodenfeuchte, Oberflächendichtung

Table of content

List of figures

1. Introduction

1.1. Motivation

Soil is essential resource for human needs in 21st century and main source for most of our food production. Further, soil is the medium trough, which atmospheric gasses are biologically cycled, and waters are filtered and stored (Koch et al., 2013). Soils have natural mechanisms of self-sustaining, which enable to retain their most important features such as thickness, carbon content and nutrients (Fig. 1). Human intervention in soil processes lower their capability to retain original properties (Amundson et al., 2015). United Nations (UN) recently reported that majority of the world's soils are in fair, poor or very poor condition due to soil degradation (FAO, 2015). Soil degradation by soil erosion is the major threat to global soil resources, according to this document. Extensive and unsustainable land use for agriculture, forestry, and grazing lead to accelerated soil erosion (Borrelli et al., 2017; Montgomery, 2007). The impacts of soil erosion are not only recognized on-site (land degradation, loss in soil fertility), but also off-site through the sedimentation, pollution and increased flooding of water aquifers (Boardman and Poesen, 2006). Furthermore, due to erosion, soils lose 75-85% of their carbon content, causing the carbon emission to the atmosphere (Morgan, 2005). According to the report from the WP2 of RECARE project (Stolte et al., 2016) eleven soil threats were identified: soil erosion by water, soil erosion by wind, decline of organic matter (*OM*) in peat, decline of *OM* in minerals soils, soil compaction, soil sealing, soil contamination, soil salinization, desertification, flooding, and landslides and decline in soil biodiversity. However, most of arable land is primary affected by water erosion (FAO, 2015).

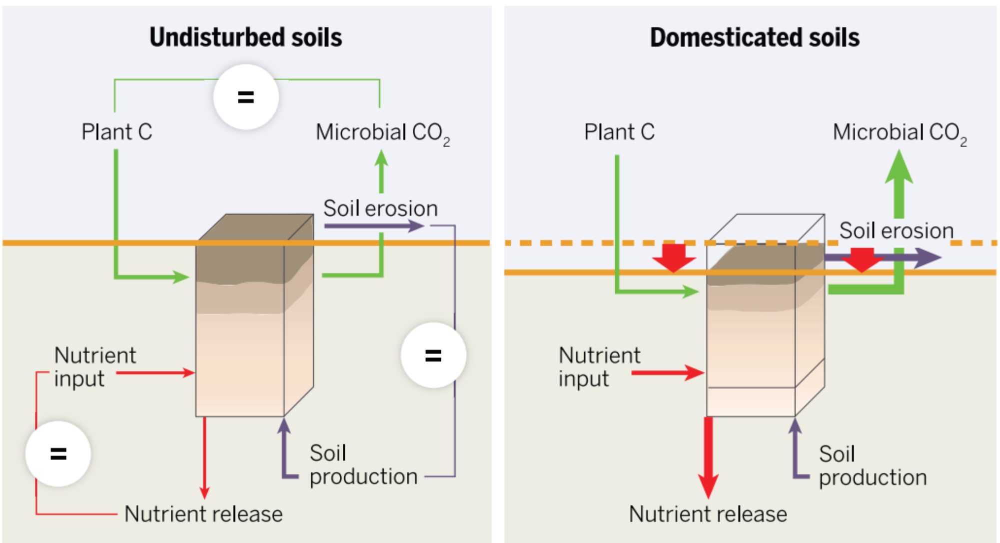

Figure 1. Changes in the balance of the important soil processes caused by human interaction (Amundson et al., 2015).

Morgan (2005) defined the soil erosion as the two-phase process consisting of the detachment of soil particles from the soil mass and their transport by erosive agents such as running water or wind. Most authors agree that the raindrop impact on the soil surface is a dominant agent of the soil erosion by water, where the overland flow is the principal transporting agent (Bauer, 1990; Mermut et al., 1997; Morgan, 1995; Rose, 1960). Raindrop impact starts with the first drops that strike the soil surface and results in splash erosion, first stage of soil erosion by water. The ability of rainfall to induce splash erosion (rainfall erosivity) is attributed to several variables, which are primary dependent on drop size and drop velocity (Salles and Poesen, 2000). Therefore, rainfall kinetic energy (*KE*) is commonly used as the main rainfall erosivity parameter since it is defined as the product of the raindrop mass and square of its fall velocity. Measurements of the drop size and velocity are crucial for assessment of actual energy load on soil surface. With the recent development of an optical laser precipitation monitors (disdrometers), measurements of raindrop size and velocity have become more available. Rainfall intensity is the simplest rainfall erosivity parameter and easier to measure (using rain gauge), than the rainfall *KE*. Rainfall intensity is strongly correlated to rainfall *KE*. Thus, when measurements of raindrop size and velocity are not available, rainfall *KE* is often estimated with the empirical *KE*-intensity relationships obtained from other studies. However, *KE* varies spatially and temporary, which could lead to uncertainty of rainfall erosivity estimation when using the empirical relationships. Number of studies concerning splash erosion in relation to rainfall parameters were conducted under simulated rainfall (Gilley and Finkner, 1985; Kinnell, 1982; Salles and Poesen, 2000). However, typical rainstorm is characterized by temporal changes in rainfall intensity and different drop sizes, which cannot be reproduced in the laboratory. To define the detachment power of rainfall attributed to certain geographical location, the rainfall parameters have to be determined directly and simultaneously with soil loss (Kinnell, 1973).

The ability of rainfall to detach soil particles depends also on soil conditions. Soil texture, soil chemistry and presence of *OM* dictate the response of the soil to raindrop impact (Fernández-Raga et al., 2017). Combination of high *OM* and higher soil moisture content contribute to formation of stable aggregates, which consequently increase soil resistance against raindrop impact (Le Bissonnais, 2016). The aggregate size and weight will determine the threshold value of *KE* to break or move soil aggregates (Leguédois et al., 2005; Salles et al., 2000; Salles and Poesen, 2000). The *KE* over threshold destroys the aggregates with concomitant surface compaction and sealing. Seal formation eventually reduces soil infiltration capacity resulting in surface ponding or runoff that may affect splash erosion rates (Ghahramani et al., 2012). Further, soil erodibility is related to soil inherent properties that dynamically vary during the storm events and in time and space (Wang et al., 2014). According to the literature, these factors are seldom evaluated and discussed in soil erosion studies. Therefore, a deeper understanding of interaction between the soil properties and raindrop impact would improve the ability to predict the potential splash erosion and to mitigate negative impacts on the environment.

1.2. State of the art

1.2.1. Rainfall parameters controlling splash erosion

Rainfall erosivity parameters affecting splash erosion are crucial for understanding the fundamental processes involved in soil detachment by raindrop splash. The ability of rainfall to cause soil detachment is attributed to rainfall intensity, but more commonly to *KE*, momentum or combination of these (Salles et al., 2001). Bubenzer and Jones (1971), Quansah (1981), Poesen (1985) and Morgan et al. (1998) represented the splash erosion by a nonlinear function of *KE* and soil detachment coefficient (K_d). In their laboratory experiments, Salles and Poesen (1999) found that the raindrop momentum multiplied with raindrop diameter better describes the splash erosion detachment. Rainfall intensity is easier to measure and often used as more direct parameter to reflect rainfall erosivity. Furthermore, it is strongly correlated to *KE* (Lim et al., 2015; Salles et al., 2002). The Water Erosion Prediction Project (WEPP) (Flanagan and Nearing, 1995) used the square intensity (I^2) for predicting a soil detachment, calculated as the combination of splash erosion and sheet flow (M. A. Nearing et al., 1989). When the raindrop size and velocity are not known, rainfall *KE* is commonly calculated from empirical *KE*-intensity relationships (e.g. Brown and Foster (1987); Kinnell (1981); Wischmeier and Smith (1958)). However, these empirical relationships are limited to geographic location where they were developed, therefore they are useful at locations with similar rainfall patterns (Kinnell, 1973). Rainfall intensity and drop size (crucial for *KE* estimation) interact together in such way that the raindrop size typically increases with intensity (Sharma and Gupta, 1989). Although, in natural conditions very low intensities can contain some erosive raindrops (Van Dijk et al., 2003) and increasing intensity cannot be always related to increasing raindrop size and velocity (Assouline, 2009). This indicates that the use of the rainfall intensity for *KE* estimation could lead to misinterpretation of rainfall erosivity characteristic to local conditions. Govers (1991) studied splash erosion in the field in Belgium. Results indicated that the rainfall *KE* underestimated splash erosion for high intensity rainfall. The intensity on the other hand, overestimated the detachment power for high intensity rainfall. Therefore, he concluded that the product of *KE* and drop circumference or an exponent value of 1.75 for intensity were better predictors of splash detachment. In the Universal Soil Loss equation (USLE) developed by Wischmeier and Smith (1958), rainfall erosivity is defined as the product of rainfall *KE* (in the literature *E*) and the maximum continuous 30 minute rainfall intensity (I_{30}) during the individual storm. The rainfall erosivity factor (EI_{30}) factor in Revised Universal Soil Loss Equation (RUSLE), by Renard et al. (1997), reflects the erosion for all the processes due to water: raindrop splash and runoff (sheet flow and concentrated flow). Effect of the EI_{30} on splash erosion was investigated in the field study by Van Dijk et al. (2003), however, low correlation was found. Better results were obtained in field experiments by Angulo-Martínez et al. (2012) where the rainfall erosivity factor was significant parameter for splash erosion prediction over *E* and I_{30} individually. However, the results could vary between different studies due to method used for estimating the rainfall *KE*, namely, empirical relationship between *KE* and intensity proposed in RUSLE, or direct measurements from the optical laser disdrometer.

Since the splash erosion is a raindrop-induced process many studies focused on soil detachment by a single raindrops. Using the combinations of different nozzle types, pressure and fall height, rainfall simulators in the laboratory can produce various ranges of raindrop size and velocity. Kinnell (1982) observed sand detachment using splash cups. The splash erosion during the initial phase of raindrop impact decreased after which the splash detachment per drop varied with the square of drop mass. Sharma and Gupta (1989) and Sharma et al. (1991) studied soil detachment by single raindrops of varying *KE*, where they established the critical *KE* of raindrop needed to initiate splash erosion. Further, the effect of raindrop size on splash detachment and transport has been studied by Fu et al. (2017). The amount of splashed soil increased with increasing raindrop diameter and significantly decreased relation to splash distance. However, it should be noted that the experiments with a single drop size do not reproduce the variations in the frequency of the raindrop impacts and the interactions due to simultaneous drops hitting the ground (Salles et al., 2000). Larger drops can produce higher splash in the beginning of the rainfall, however depending on surface roughness, they can impose grater surface compaction and result in final lower splash erosion rates due to surface sealing (Bradford and Huang, 1992).

According to current knowledge, a great number of the experiments studying splash erosion affected by rainfall were conducted under controlled conditions in laboratory using simulated rainfall. Unfortunately, the results of laboratory studies are not readily translated to field situations (Bradford and Huang, 1993). Rainfall produced by rainfall simulators is often characterized by uniform raindrops and constant rainfall rate. The natural rainfall is depended on raindrop size distribution (Van Dijk et al., 2003) and rainfall rate that varies temporally and spatially. When analysing *KE* of natural and artificial rainfall there are significant differences affected by raindrop properties. The velocity of the raindrops under rainfall simulator is lower than the terminal velocity of the natural drops (Iserloh et al., 2013). Splash erosion is a rainfall driven process, thus highly dependent on drop size and velocity. However, laboratory experiments with simulated rainfall can exclude some side effects, which cannot be controlled in field and reduce the duration of the experiments (Fu et al., 2019). The choice between simulated and artificial rainfall depends on the study objectives. When investigating the rainfall erosivity and its effect on the soil detachment in a certain region, the measurements under natural rainfall are indispensable (Fernández-Raga et al., 2017).

1.2.2. Soil properties controlling splash erosion

Soil erodibility is determining factor for splash erosion prediction. In order to overcome the weight and the binding forces of soil particles, raindrop must exceed the threshold kinetic energy (KE_0) to initiate splash erosion. This required amount of KE_0 is attributed to various soil properties above all soil texture, infiltration capacity, surface roughness, soil moisture and *OM* content. Salles et al. (2000) compared the KE_0 for silt loam and sandy soil. They related the KE_0 to median grain-size diameter (D_{50}), where the raindrop impact decreases with increasing D_{50}. Therefore, higher KE_0 is needed to initiate splash erosion for the silt loam soil with due to higher cohesion between soil particles than for the sandy soil with lower cohesion. Other than KE_0 required to induce the soil detachment, Goebes et al. (2014) showed that the soil texture is determining factor for choosing the relevant rainfall erosivity parameter to predict the splash erosion. Namely, they suggested that for heavier soil textures with greater particle size and density such as sand, *KE* multiplied by drop diameter is significant parameter for splash erosion prediction. Momentum divided by drop diameter on the power of 1.5 is more appropriate erosion predictor for the light textures such as silt.

Stable aggregates are crucial for protecting the soil surface against the raindrop impact and improving the water infiltration. Major role in aggregation play following soil properties: *OM*, clay, and $CaCO_3$ content or exchangeable sodium percent (Lado et al., 2004; Lado and Ben-Hur, 2004; Le Bissonnais et al., 1995). Le Bissonnais (2016) attributed higher aggregate stability to clay soils, which due to cementing effect have higher ability to form the stable aggregates. Furthermore, high soil *OM* content acts also as a bonding agent between the soil particles (Chenu et al., 2000; Haynes and Swift, 1990). Due to raindrop action the soil aggregate breakdown can be associated with several mechanisms: slaking, swelling, mechanical breakdown and physico-chemical dispersion (Le Bissonnais, 2016). Slaking occurs by the air compression entrapped inside of the aggregates due to fast wetting (Emerson, 1967). Slaking decreases with slow prewetting of soil due to reduction of volume entrapped during wetting and also reduction of gradients of matric potential (Truman et al., 1990; Vermang et al., 2009). In experimental study by Xiao et al. (2018) was found that the contribution of slaking to the splash erosion rates also decreases with the increasing *KE*, where mechanical breakdown increases with increasing *KE*. The swelling and shrinkage during the wetting and drying of soil can result in microcracking and reduction of the mean aggregate size (Le Bissonnais et al., 1993). Depending on soil in terms of clay content, breakdown by slaking decreases as the clay content increases, where swelling increases with increasing clay content (Le Bissonnais, 2016). Mechanical breakdown of aggregates by raindrop impact occurs when the *KE* of raindrop is high enough to cause disaggregation, but it usually occurs in interaction with other mechanisms (Bradford and Huang, 1992). Lastly, physico-chemical dispersion reduces the attractive forces between the clay particles, which migrate into to the soil with infiltrating water and clogs the pores beneath the surface to form the "washed-in" zone (Lado et al., 2004).

Clogging of the soil pores by fine material due to aggregate breakdown will result in formation of the structural seals (Assouline, 2004; McIntyre, 1958). Soil erodibility is closely related to aggregate stability and, therefore, ability of soils to form the seal. Formation of surface seals reduces the soil infiltration rate and increases the risk of runoff, which further transports soil particles (Assouline, 2013; Le Bissonnais et al., 1993). Depending on the rainfall and soil properties, seals can reach the thickness up to 20 mm (Bedaiwy, 2008) with the increase in the soil surface bulk density (Assouline and Mualem, 1997). Monitoring of soil seal development is directly measured by the microscope (Bresson and Boiffin, 1990; Cheng et al., 2008) or X-ray Computed

Tomography (CT) (Armenise et al., 2018; Bresson et al., 2004). Indirect evaluation of surface sealing is recognized through decrease in saturated hydraulic conductivity (K_s) (Pla, 1986), infiltration capacity (Poesen, 1986) or increase in surface strength (Bradford and Huang, 1992). With greater seal development soil detachment decreases due to higher surface strength (Lado et al., 2004; Vermang et al., 2009). McIntyre (1958) observed splash erosion for three soils where the fluctuations in splash rates were contributed to surface sealing. Cheng et al. (2008) concluded that the surface seal was related to reduction in splash erosion, where the developed seal was observed with micro-morphological photos. From several experimental studies it is obtained that the surface sealing is attributed to high silt content (Cheng et al., 2008; Truman et al., 1990), low clay content (< 200 g kg^{-1} according to Le Bissonnais and Singer (1993)) and low *OM* (Armenise et al., 2018) content. Furthermore, in the relation to abovementioned soil properties seal formation is related to raindrop impact. Agassi et al. (1985) investigated the seal formation on two soils. In the study was concluded that soil surface exposed to rainfall *KE* < 0.01 J m^{-2} mm^{-1} won't develop seal layer, where the soil surface exposed to *KE* of 23 J mm^{-1} m^{-2} will form seal with low hydraulic conductivity.

Effect of soil moisture on soil erodibility has been investigated by numerous authors (e.g. Le Bissonnais et al., 1994; Ryzak et al., 2015; Truman et al., 1990; Vermang et al., 2009). Soil water content (θ_a) can have effect on soil aggregate stability and on hydraulic properties that control splash erosion. Dry soil aggregates may have higher resistance against raindrop impact due to cementing effect and hydrophobic effects due to drying (Caron et al., 1992). However, dry aggregates can be affected by slaking during the fast wetting, which results in higher soil detachability and consequently greater seal formation. The study by Truman et al., (1990) showed that at prewetting of soils with rich clay content resulted in reduction of splash erosion rates and following surface runoff. In later study by Le Bissonnais and Singer (1992), and Le Bissonnais et al. (1995) was obtained that the effect of capillary rise during prewetting can reduce the slaking forces for soils with the high clay content. Lack of aggregate breakdown by slaking will consequently decrease the surface runoff and soil erosion. Some authors have reported different effects of θ_a on soil erosion. For instance, high θ_a was found to increase the soil erodibility due to lower cohesion between the particles (Al-Durrah and Bradford, 1981; Beczek et al., 2019). Furthermore, initial θ_a can induce faster surface runoff due to lower soil water potential pressure gradient and low storage capacity (Vermang et al., 2009). In this case, splash erosion will decrease due to accumulated water layer on soil surface (ponding or surface runoff), which protects it from raindrop impact (Torri et al., 1987). However, splash detachment will decrease if the thickness of the surface water layer is higher than the critical water depth. Studies show that critical depth is approximately equal to drop diameter (Palmer, 1964) or three diameter of the raindrops (Guy et al., 1987), depending on the conditions in the experiment. The contradictory results regarding splash detachment in relation to initial soil moisture are partly contributed to the fact that soil-moisture content interacts with soil properties which influence breakdown mechanisms and seal formation (Le Bissonnais et al., 1995).

1.2.3. Methods for splash erosion measurements

Different devices have developed in last few decades for splash erosion assessment depending on the experimental set up (field or laboratory experiments). The main difference between devices is whether they are collecting the splashed material from surrounding soil surface (unbounded splash traps) or they surround the soil surface from which the splash amount is collected (bounded splash traps) (Fig. 2) (Fernández-Raga et al., 2019).

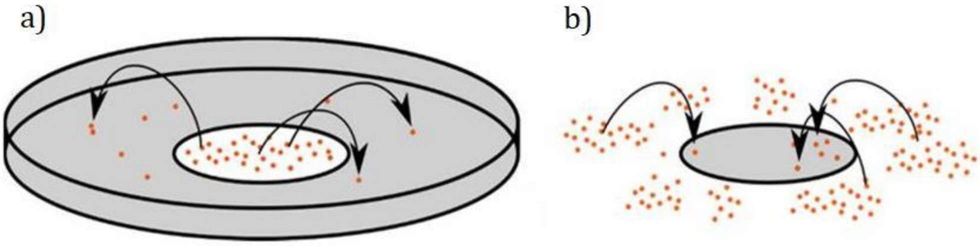

Figure 2. Two methods to collect detached soil particles: a) collector is around the soil sample; b) collector is surrounded by the sampled soil (Zumr et al., 2019).

Both trap approaches have advantages and disadvantages. The unbounded splash traps need to estimate the surface of the contributing area otherwise is not possible to estimate the amount of detached soil per specific area. In the case of bounded splash traps, splashed material can fall inside of the sampling area. Furthermore, some devices are installed directly on the soil surface without or minimum disturbance on the soil such as splash board (Ellison, 1944a, 1944b), collection troughs (Jomaa et al., 2010), splash cup (Fernández-Raga et al., 2010; Poesen and Torri, 1988), funnel (Fernández-Raga et al., 2010) and curtains of splash (Mermut et al., 1997). Few examples of the unbounded splash traps are shown on Fig. 3.

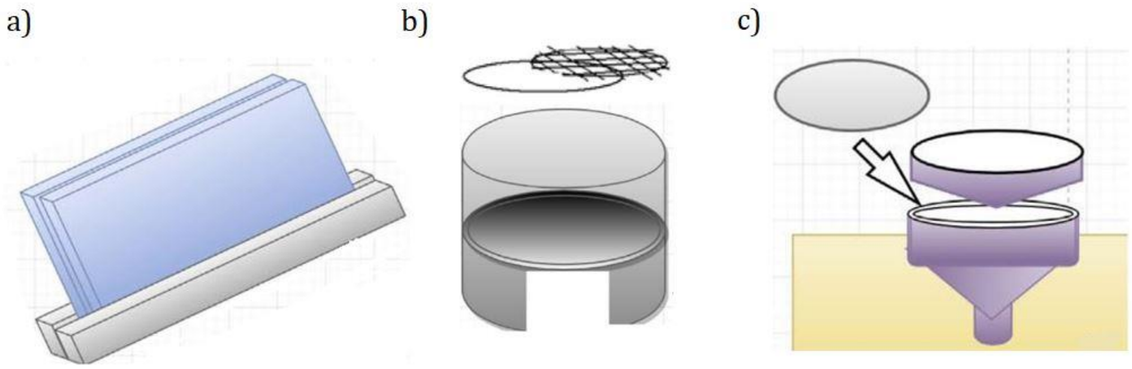

Figure 3. Unbounded splash erosion devices: a) splash board (Ellison, 1944a, 1944b), b) splash cup (Fernández-Raga et al., 2019; Poesen and Torri, 1988), and c)funnel (Fernández-Raga et al., 2010).

However, these device do not allow control of the soil conditions, but can provide more reliable results regarding attributed to certain location since soil properties are preserved (Zumr et al., 2019). The devices such as splash cups can be filled with certain amount of the soil and the remaining amount of soil after raindrop impact is measured (Fernández-Raga et al., 2019). In case of splash cup developed by Morgan (1978), splashed soil material is collected by circular catching tray, dried and weighted (Moghadam et al., 2015; Zumr et al., 2019). In the following paragraph, focus will be on splash cup, which has been used in the studies included in this thesis.

Recently developed, Tübingen splash cup (T splash cup) by Scholten et al. (2011) use standardized material (sand) to simplify comparison between study sites avoiding the differences between particular soils. Furthermore, T splash cup, on contrary measures the remaining material in splash cup ensuring the constant moist of the material by hydraulic connection between the soil sample and water in the plastic flask. By calibration of the splash cup with an optical laser disdrometer Scholten et al. (2011) showed that the T splash cup can be used as an optimal tool for estimating the rainfall *KE*. However, the use of the standardised materials cannot clarify the splash erosion attributed to soils, but only the response of the splash to rainfall *KE* (Fernández-Raga et al., 2017). For isolating the splash process, most researches (Lal, 1998; Morgan, 1978; Salles et al., 2000; Scholten et al., 2011) use the splash cup based on the design proposed by Ellison (1947). Described in Morgan (2005), splash cup by Ellison (Ellison, 1947) has 77 mm in diameter and 50 mm deep with a wire mesh base. A thin layer of cotton wool or sponge rubber is placed in the bottom of the cup, which is then filled with the soil, oven dried to a constant weight and weighed. The soil is levelled few millimetres below the rim to avoid surface runoff with soil material in the early stage of the rainfall (Mazurak and Mosher, 1968). The soil in the cup is brought to saturation prior to rainfall simulation. However, some limitations in splash cup design were reported in study by Kinnell, (1974). He observed that excessive amount of splash erosion in the initial stage of rainfall is attributed to the raindrop impact acting close to splash cup perimeter pushing the sand particles sideway eventually producing the "*wash-off*" effect. On the other hand, in the study by Salles et al. (2000) the sediment from *wash-off* was effectively separated from the areal splash by installing the cylindrical collecting device, 1 mm larger than the splash cup mounted concentrically to the splash cup. However, the authors reported small impact of the *wash-off* on soil detachment in the splash cup, due to small shear stress caused by thin sheet flow. Further issue reported by Kinnell (1974) was decrease in the splash erosion during the last stage of the rainfall simulation. According to author, this was attributed to fully developed surface roughness, enabling the drops to mobilize the sand particles. The decrease in splash erosion can be also contributed to lower level of soil in the splash cup due to extensive soil loss in the beginning and surface compaction by raindrop impact (Bisal, 1960). When using the splash cup as the toll for splash erosion assessment these factors should be considered during the experimental design development.

The size of the soil sample is another factor that should be considered using the bonded splash traps such as splash cups. Poesen and Torri (1988) used seven different cup diameters ranging between 0.7 and 24 cm in field measurements to establish the influence of cup diameter on mass of detached sediment per ground surface unit. They concluded that the mass of splashed soil is strongly influenced by the cup dimension and mean splash distance of the sediment. Other authors also suggest that the bigger-sized splash cups underestimate the splash erosivity (Leguédois et al., 2005; Van Dijk et al., 2003). Furthermore, Fu et al. (2017) reported that the splash distance depends on rainfall *KE* and Legout et al. (2005) reported that amount of the splash erosion exponentially decreases with increasing distance from the sample. Most of the splashed soil material is contracted within 20 cm from the soil sample where the transport distance decrease with increasing aggregate size (Fu et al., 2019). Depending on the rainfall characteristics and the size of soil aggregates, the splash cup design should be determined. Finally, splash colleting device must needs to have appropriate dimensions to capture most of the splashed particles and to provide the results comparable to other studies. However, due to lack of standardization the researchers manufacture the devices themselves according to the research objective, which hamper correct comparison of the results (Fernández-Raga et al., 2017; Rodrigo Comino et al., 2016).

According to literature, design based on Morgan splash cup (Morgan, 1978) can provide reliable results when measuring splash erosion in both outdoor and indoor experiments (Khaledi Darvishan et al., 2014; Vigiak et al., 2006, 2005). For this reason, in studies presented in this thesis, the modified splash cup base on design proposed by Morgan (1978) was used. To fulfil the purpose of the study objectives the original design was modified. The major modification is that the splash cup filled with soil was placed on holder in the centre of the splash collector. The splash holder has height of 12 mm and prevents the backsplash from the bottom of the container. Accordingly the adjacent tray rim was 30 mm high to capture the splash from the soil sample in the cup (Fig. 4). Details of the splash cup design used in the studies within this thesis are desribed in Zumr et al. (2019).

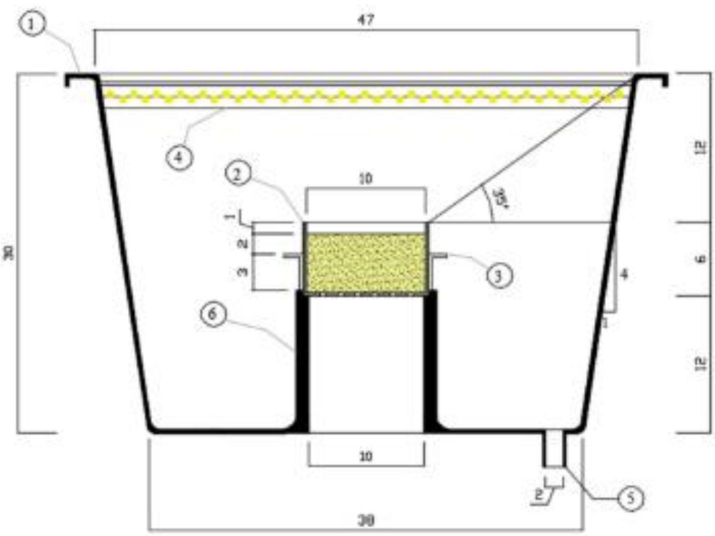

Figure 4. Splash cup and splash collector design with their dimensions in centimetres (Zumr et al., 2019).

1.3. Research gaps

During the last few decades considerable research has been done to define the role of splash erosion in soil erosion process. Splash detachment can contribute up to 95% of total material transported by water erosion (Van Asch, 1983). However, there are still many open research questions on the main processes affecting splash erosion, which require deeper and better understanding to predict further soil loss and to implement the appropriate measures for soil erosion prevention. The topic of splash erosion needs to be therefore further researched in order to fill the remaining gaps in knowledge.

Major limitation in splash erosion studies is high variability in space and time, which prevents to upscale the results to other conditions and situations (Fernández-Raga et al., 2017). Additional limitation is the inability to translate the results obtained in laboratory to situation in the field and vice versa. Natural rainfall is characterized with temporal changes in the intensity rate and variable drop size distribution. Spatial differences of natural rainfall are influenced by the altitude, temperature, wind speed and direction and land cover. Rainfall simulators produce uniform drop size distribution characterized by nearly constant rainfall intensity. The *KE* can vary by modifying rainfall intensity which affects the drop size distribution (*DSD*). Most researchers use the simulated rainfall in soil erosion studies, due to simplicity, ability to control the conditions and time needed for experiments. However, in order to define the impact of rainfall on splash erosion the experiments under natural rainfall are essential. Few studies measured the splash erosion under natural conditions (Govers, 1991; Morgan, 1978; Van Dijk et al., 2003). The measured rainfall parameters were rainfall intensity and rainfall depth, where the *KE* was calculated based on the empirical relationships between the *KE* and intensity from other studies. The role of *DSD* was not considered, since the measurement of raindrop size and velocity was not available. According to literature review, very few studies measured simultaneously splash erosion and rainfall characteristics, including the drop size and velocity, on the same location. With a recent development of optical laser disdrometer it is possible to measure the rainfall drop size and velocity in field and under simulated rainfall. Latest field studies about the raindrop impact on splash erosion were conducted by Angulo-Martínez et al. (2012) and Fernández-Raga et al. (2010). In their studies, rainfall *KE* was derived from the *DSD* measured by disdrometers. The authors, however, report limited data sets or high variability in splash amounts for individual rainstorms. To obtain stronger relationship between the splash erosion and rainfall parameters, measurements on larger temporal and spatial resolution are required. When focusing on Europe, such results have not been reported so far. In European Union 41% of total land is agricultural (The World Bank Group, 2016), which is most affected by soil erosion by water. According to data reported by Bauer (1990), most rainfall events in Central Europe do not generate overland flow. Therefore, erosion by raindrop impact contributes largely to total soil detachment rates. A rainfall erosivity data based on disdrometer measurements and splash erosion data are required to define the impact of rainfall on splash detachment in this area.

In the field, soil is exposed to constant changes in the rainfall regime, temperature, wind and humidity. These factors largely affect soil properties such as soil moisture and surface structure, which can eventually control the splash erosion rates. Splash erosion in relation to soil moisture and different hydraulic properties has been investigated by several authors (Romkens et al., 1990; Ryzak et al., 2015; Truman et al., 1990; Vermang et al., 2009), where depending clay content, *OM* and wetting rate different results were reported. The interaction between soil loss and antecedent θ_a is rather neglected in the soil erosion prediction models, such as Universal Soil Los Equation (USLE) by Wischmeier and Smith (1978) and Water Erosion Prediction Project (WEPP) (Flanagan and Nearing, 1995), although research show the correlation between the two parameters (Truman et al., 1990). Furthermore, long exposure to raindrop impact induces rapid changes in hydraulic properties and infiltration rate, due to crusting or/and surface sealing. These processes in relation to splash erosion were researched by Mcintyre (1957), Mermut et al. (1997), Truman et al. (1990), Vermang et al. (2009). The authors reported high variations in splash erosion affected by different seal formation stages. Most of presented studies concentrated either on different soil moisture content or susceptibility of soil to form a surface seal, to explain the variation in splash erosion rates. However neither of them took into account both factors, which mostly interact together in the field. Therefore, a new approach combining these two factors should be further investigated in attempt to closely describe undergoing processes affecting splash erosion in natural conditions.

2. Objectives and thesis structure

The aim of the thesis was to investigate main factors influencing splash erosion on arable land in Central Europe. In the first part of the study, focus was to quantify the effect of rainfall erosivity on splash erosion for the soil after seedbed preparation, when it is most susceptible to raindrop impact. During the field experiments splash erosion was measured together with rainfall intensity, drop size and velocity, with a goal to select significant rainfall parameter that describes splash erosion. The interaction between rain drop impact and soil properties is also crucial for splash erosion prediction. Therefore, effect of soil moisture and surface structure (seal and crust formation) on splash erosion was investigated under simulated rainfall. These experiments were conducted in laboratory to control soil initial conditions, namely soil moisture content and to effectively measure the changes in surface structure.

Following hypotheses were evaluated in the thesis:

i. Splash erosion is a raindrop induced process, which can be described as the function of rainfall erosivity parameters commonly used in literature such as *KE*, intensity or EI_{30}.

ii. Spatial and temporal rainfall variabilities affect splash erosion. The continuous measurements of the rainfall parameters, including rainfall intensity and *KE*, provide information based on which these differences can be evaluated in relation to splash erosion.

iii. Soil moisture and changes in surface structure by raindrop impact influence the soil erodibility and thus resulting different splash erosion rates. Therefore, an investigation is needed to quantify the effect of soil initial condition on splash erosion detachment.

iv. Differences in splash erosion between variable soils are related to soil inherent properties, which interact together with rainfall.

The stated objectives were evaluated trough two study cases, which were published as the research articles and summarized in the following chapters.

Study 1 describes the relationship between the splash erosion and rainfall erosivity parameters (rainfall intensity, *KE* and EI_{30}) measured on three locations in Central Europe under natural rainfall.

Study 2 presents impact of the soil moisture and surface condition affected by surface sealing and crusting on splash erosion, under the simulated rainfall using two rainfall simulators. The changes in surface structure were evaluated trough the changes in soil saturated hydraulic conductivity.

Overall discussion follows to relate the obtained results from the study cases with the state of the art. The conclusion and perspective highlight the main outcomes obtained in the thesis and to propose recommendations for further research. Lastly, a list of the publications and conference contributions is given. Complete publications based on the study cases can be found in the appendix along with the declaration of authorship.

3. Summary of Study 1

Summary of the Study 1 is based on the article **"Rainfall Parameters Affecting Splash Erosion under Natural Rainfall Conditions"** published in *Applied Sciences*. The complete publication can be found in the Appendix 1.

Nives Zambon, Lisbeth Lolk Johannsen, Peter Strauss, Tomas Dostal, David Zumr, Martin Neumann, Thomas A. Cochrane and Andreas Klik (2020): Rainfall Parameters Affecting Splash Erosion under Natural Rainfall Conditions, Applied Sciences, 10, 4103, DOI: 10.3390/app10124103.

3.1. Introduction

Splash erosion is the initial stage of soil erosion by water initiated with first raindrop impact on soil surface. The rainfall erosivity is the ability of rainfall to cause splash detachment. Depending on the experimental set up authors propose different rainfall erosivity parameters which determine the splash erosion detachment. Most commonly, authors use the parameters related to rain drop size and velocity such as kinetic energy (*KE*) (Morgan et al., 1998; Poesen and Savat, 1981; Walter H. Wischmeier and Smith, 1958), rainfall erosivity factor (EI_{30}) (Renard et al., 1997), raindrop momentum (Salles et al., 2001) or the rainfall intensity (Nearing and Bradford, 1985; Rose et al., 1983; Smith and Wischmeier, 1957). Splash erosion measurements are conducted under simulated or natural rainfall. The simulated rainfall often does not replicate the characteristics of natural rainfall due to limitations in rainfall simulator design (Iserloh et al., 2013) and the fact that the rainfall erosivity is spatially and temporally limited. Splash erosion is rainfall driven process largely dependent on size and velocity of raindrops, therefore, experiments under natural rainfall are crucial to explain the raindrop impact on initial soil detachment. To investigate the relationship between splash erosion and rainfall erosivity, Morgan (1978) conducted an experiment in the field using splash cups. He obtained significant relationship between the splash erosion of bare soil and rainfall *KE*. Further, Govers (1991) found in his field experiments that product of raindrop *KE* and drop circumference or rainfall intensity on power of 0.75 are better predictors of splash erosion, than *KE* and intensity independently. Both authors derived the *KE* either from the empirical relationships between the *KE* and intensity by Hudson (1965) or from the *DSD* and intensity relationships based on the data by Laws (1941) and Laws and Parsons (1943). However, the empirical relationships obtained from another studies could lead to misinterpret the realistic rainfall *KE* characteristic to certain location. Development of optical laser disdrometers (Hauser et al., 1984) enabled direct measurements of size, velocity and number of raindrops and improved the calculation of rainfall *KE*. Recent studies focusing on splash erosion and rainfall *KE* obtained from disdrometer was conducted by Fernández-Raga et al. (2010) in Portugal and Angulo-Martínez et al. (2012) in Spain. Authors obtained satisfied correlations between the splash erosion and rainfall *KE* or EI_{30}. However, the splash data were either limited or highly variable between the replicates, which suggested further measurements to statistically define relationship between splash erosion and rainfall erosivity parameters. Considering the local influences on rainfall erosivity and lack of the data sets on rainfall *DSD*, it is difficult to define the role of splash in soil erosion process and predict it relative to local conditions. This study presents the measurements of splash erosion and rainfall parameters, including the rainfall intensity and *KE*, on the three locations in Central Europe where most agricultural activity takes place. The objective is to compare relationships between splash erosion and rainfall erosivity parameters, expressed through rainfall *KE*, mean intensity and EI_{30}, and propose the rainfall parameter with highest ability to predict splash erosion.

3.2. Materials and Methods

The rainfall monitoring and splash erosion measurements were located on two sites in Lower Austria: Mistelbach and Petzenkirchen, and one site in Czech Republic: Prague. The monitoring period was each year from 2017 to 2019 during the late spring and summer. These seasons were selected according to findings from previous studies (Klik and Truman, 2003; Panagos et al., 2016b), which indicate that most erosive rainfall events occur during spring and summer in Central Europe. Soil samples were taken from the agricultural fields near to measurement sites in Lower Austria–Mistelbach (MI) and Zwerbach (ZW), and in Czech Republic from site in Central Bohemia Region–Bílkovice (BK). The samples were taken from the top 10 cm, after the seedbed preparation on all sites. Further, soil was air-dried and the samples from the three soils were distributed to three measurement sites. According to the soil particle distribution, determined soil textures were silt loam, for MI and ZW soil and loamy sand, for BK soil (Table 1 in Appendix 1). Splash erosion was measured with splash cups described in Zumr et al. (2019) based on design by Morgan (1978) (Fig. 5). Each soil was filled into splash cups, making sure that all aggregates (from finer to coarser) were equally arraigned on the soil surface. Splash cups were filled with soil samples and placed on the experimental sites afterwards. Sites were equipped with the automated rain gauge (tipping bucket or balance principle) and an optical laser disdrometer for drop size and velocity measurements. After the rainfall event with minimum rainfall depth of 5 mm, splashed soil was collected and the splash cups were replaced with new soil samples. The amount of splash erosion rate was calculated for each soil by dividing the collected splash material with the surface of splash cup surface (86.6 cm^2). Average rainfall intensity (I_{av}) was calculated as the total rainfall amount collected during rainfall event and divided by event duration. Rainfall KE was calculated from given raindrop and velocity distribution measured by disdrometers. The erosivity factor based on single rainfall event was calculated as the product of total KE (KE_{sum}) and 30 minute rainfall intensity (I_{30}). Regression analysis was performed in order to analyse relationship between splash erosion and rainfall parameters. Evaluated statistical parameters were coefficient of determination (R^2) and root mean square error ($RMSE$).

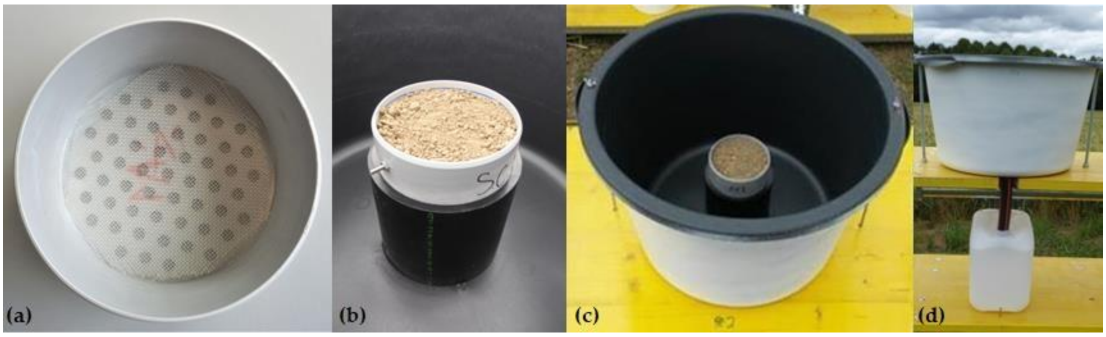

Figure 5. Experimental set-up for splash erosion measurements: a) splash cup with mesh at the bottom; b) splash cup filled with soil; c) splash collector; and d) connection with drainage pipe to water and soil collector.

3.3. Results

According to rainfall data selected over three seasons of measurement period average monthly rainfall precipitation was the greatest for Mistelbach site with 94 mm. Petzenkirchen and Prague followed with 68.7 and 46.5 mm, respectively. The highest average EI_{30} was also measured for Mistelbach site, with 378.9 MJ mm ha^{-1} h^{-1} and lowest for Petzenkirchen site, with 131.6 MJ mm ha^{-1} h^{-1}. Totally 80 records of complete splash and rainfall measurements from the three sites were selected for the data analysis. Average splash erosion varied between 4 and 2508 g m^{-2} depending on soil and corresponding rainfall event KE_{sum}, with range between 31 and 2722 J m^{-2}. Linear relationship was established between splash erosion and KE_{sum} for the three soils with highest R^2 of 0.52 for BK soil. High variations were found between the predicted splash erosion values by linear relationship and measured values, verified by high *RMSE* and the scattered data points. The analysis of the rainfall events revealed that higher splash erosion rates were attributed to higher rainfall intensity rather than KE_{sum}. To ensure the comparison of *KE* characterized by different rainfall intensity, the KE_{sum} was divided by rainfall duration. This parameter was defined as kinetic energy per hour (KE_h). Further regression analysis was obtained with KE_h, I_{av} and EI_{30}, as potential erosivity parameters to describe splash detachment. A power relationship was fitted between splash erosion and KE_h, with the R^2 of 0.76 for ZW and BK soil, and 0.75 for MI soil. The parameter KE_h indicated stronger correlation to splash erosion than KE_{sum}. Nevertheless, differences of 97% were noted for three splash erosion observations in close range of KE_h (220-280 J m^{-2} h^{-1}). These extreme measurements differed in either *DSD* or temporal distribution of rainfall, which possibly contributed to extreme low or high splash erosion. When performing the regression analysis without these observations, the linear relationship can be established between splash erosion and KE_h with R^2 of 0.91 for ZW and MI soil, and 0.90 for BK soil. Further, the 62% lower RMSE for this linear relationship indicated high influence of extreme observations on relationship between splash erosion and KE_h. Splash erosion detachment was further analysed in relation to I_{av} including and excluding the extreme observations. Linear relationship was obtained between the splash erosion and I_{av} for both data sets. Including the extreme observation the resulting R^2 amounts to 0.81, 0.82 and 0.86 for ZW, BK and MI soil, respectively. Relationship between splash erosion and I_{av} without extreme observations resulted in R^2 of 0.93 for the three soils. Similar to previous analysis with KE_h, better performance of a fitted linear function was obtained for the data without extreme observations. The splash erosion was described as the power-law function of EI_{30}, where the obtained R^2 was between 0.60 and 0.65 for the three soils, showing minor differences in both R^2 and *RMSE* between analysis with and without extreme observations.

3.4. Discussion

To characterize the impact of natural rainfall on splash erosion, similar studies to one presented above were done by Fernández-Raga et al. (2010) in Portugal and Angulo-Martínez et al. (2012) in Spain. Both studies used disdrometer to calculate rainfall *KE* from the raindrop size and velocity. In Portugal splash erosion was measured with splash cup and funnel, where in Spain authors used Morgan splash cup (described in Morgan, 1978). Fernández-Raga et al. (2010) found linear relationship between splash erosion and rainfall KE_{sum}, which was related to findings of this study case for the loamy sand soil (BK). However, the authors reported results based on only nine rainfall events where splash erosion rates were not comparable to the ones obtained for the BK soil. Lower splash erosion rates were probably attributed to low rainfall *KE* characterized with predominately small raindrops (<0.55 mm). In the study by Angulo-Martínez et al. (2012), authors proposed EI_{30} as a controlling factor of splash erosion under natural rainfall. The splash erosion was described as power function of EI_{30} and after reaching a certain amount of EI_{30}, splash erosion rate was constant. In the presented study case, splash erosion rates evidently increased with higher EI_{30}, resulting in higher power index. These differences could occur due to fact that the soil tested in presented study case was in seedbed condition exchanged after each rainfall event, where undisturbed soil used in Spain could indicate lower erodibility. Furthermore, the differences in soil condition could also apply for the study by Fernández-Raga et al. (2010). Data obtained in presented study revealed that splash erosion was attributed to the rainfall intensity, rather than other parameters analysed (KE_{sum}, KE_h and EI_{30}). Even though most authors propose the use of *KE* as the main parameter describing soil detachment, in the natural conditions rainfall *KE* is characterized by different intensity rates. Furthermore, for high intensity events use of the *KE* can underestimate the relative impact of rainfall on soil detachment (Govers, 1991). Considering that the *KE* in this study was obtained from *DSD* and drop velocity, there is also possibility that some limitations in the disdrometer measurements can influence the interpretation of *KE* (see L.L. Johannsen et al. (2020)). Nevertheless, strong agreement was found between the splash erosion and KE_h suggesting that *KE* is suitable parameter for splash erosion prediction. However, when events with different rainfall intensities are analysed, its erosive impact has to be expressed through rainfall duration. Soil characteristics largely influence soil erodibility. The splash erosion from the three soils used in the presented study did not show differences in regression analysis with rainfall parameters. However, positive correlation was found between splash erosion and soil sand content, and significantly ($p<0.05$) negative correlation was found for the clay content. The high splash detachability of soils with dominating sand content was also confirmed in experiments by Salles and Poesen (1999), Cheng et al. (2008), and Xiao et al. (2017). Other soil properties such as soil moisture could and surface condition could determine the final splash erosion rates under natural rainfall conditions. This could be applied to extreme events where some low splash erosion rates could be affected by surface sealing or crusting, as observed visually after the rainfall event. Apart from the differences in the rainfall characteristic and soil properties, the experimental design for splash erosion assessment plays an important role when comparing the results from different studies. As seen from the above described studies by Fernández-Raga et al. (2010) and Angulo-Martínez et al. (2012), the different devices used by different authors minimize the ability to compare the results between studies. However, low standard deviations in splash erosion rates between the replicates confirm that the modified version of the Morgan splash cup provided reliable results in this study case.

3.5.Conclusion

According to the results from the presented study, splash erosion is dependent on rainfall intensity for the conditions in this field experiments. The *KE* can be used as suitable parameter to describe rainfall erosivity; however it should be divided by the rainfall duration for the natural rainfall conditions. Minor differences between the replicates during splash erosion measurements indicate that the modified Morgan splash cup provides a good tool for soil erosion assessment.

4. Summary of Study 2

Summary of the Study 2 is based on the article **"Splash erosion affected by initial soil moisture and surface conditions under simulated rainfall"** published in *Catena*. The complete publication can be found in the Appendix 2.

Nives Zambon, Lisbeth Lolk Johannsen, Peter Strauss, Tomas Dostal, David Zumr, Thomas A. Cochrane and Andreas Klik (2020): Splash erosion affected by initial soil moisture and surface conditions under simulated rainfall, Catena, 196, 104827, DOI: 10.1016/j.catena.2020.104827

4.1. Introduction

Soil surface exposed to direct raindrop impact cause the destruction of soil aggregates resulting in splash erosion. When deposited on soil surface, detached soil particles can cause the pore filling and wash-in of fine particles (Assouline, 2004; McIntyre, 1958). Soil infiltration is then reduced with incipient surface ponding followed by run-off. During ponding soil surface is rapidly sealed and further seal formation depends on rainfall *KE* (Baumhardt et al., 1990). Splash erosion rates affected by surface sealing can temporary vary, depending on the stage of surface seal development (Cheng et al., 2008; McIntyre, 1958). Surface ponding can either reduce or increase the splash erosion rates. According to Gao et al. (2003), ponding can accelerate the raindrop impact on the soil until the water on the surfaces reaches a critical depth, when soil detachability decreases. Proposed by Guy et al. (1987), critical ponding depth is equal to three drop diameter. After the critical ponding depth is reached, the splash detachment by raindrop impact is hindered by the accumulated layer of water on the soil surface (Vermang et al., 2009). Soil detachment is also dependent on soil initial water content, which reflects on aggregate stability (Le Bissonnais and Singer, 1992), ability of soil to form crusts and infiltration capacity. Few authors (Beczek et al., 2019; Truman et al., 1990; Vermang et al., 2009) investigated the effect of different soil moisture on splash erosion, however, contradictory results reported could be contributed to a particular conditions in the experiment. Dynamic changes in moisture content, surface sealing and crusting effect are mostly not considered in splash erosion studies. However, these processes are widely present especially in the natural conditions where soil is constantly exposed to different weather conditions. Lack of current knowledge about the effect of soil moisture, surface sealing and crusting on splash erosion hinders the ability to predict splash erosion. The main aim of this study is to investigate the effect of different soil moisture content and surface condition (seal formation) on splash erosion for three soils under simulated rainfall. The changes on soil surface were related to changes in soil saturated hydraulic conductivity. Consequently, second objective is to quantify the differences in soil saturated hydraulic conductivity affected by different rainfall intensities and corresponding *KE*. Considering the possibility that the rainfall characteristics can vary for different rainfall simulators, in this study the results were obtained using two rainfall simulators. Therefore, a third objective is to quantify the differences between rainfall characteristics produced by two different rainfall simulators and their impact on soil splash erosion affected by different initial conditions.

4.2. Materials and methods

Soil samples for splash erosion measurements were taken from three locations in Lower Austria (Zwerbach and Mistelbach) and one location in Central Bohemia (Bílkovice) of Czech Republic. The samples were taken in first 10 cm of soil surface, air dried and sieved trough 10 mm sieve. Determined soil textures by particle size distribution analysis were silt loam for Zwerbach (ZW) and Mistelbach (MI) soil, and loamy sand for Bílkovice (BK) soil. The amount of stable aggregates determined with method by Kemper and Rosenau (1986) was 18, 41 and 63% for MI, ZW and BK soil, respectively (Table 1 in Appendix 2). Each soil was filled into the splash cups (Fig. 5) and placed under the rainfall simulator. The rainfall simulators were located at the Institute for Soil Physics and Rural Water Management at University of Natural Resources and Life Sciences in Vienna, Austria (BOKU) and the Institute of Land and Water Management Research in Petzenkirchen, Austria (BAW). Norton Ladder type rainfall simulator at BOKU was equipped with four VeeJet nozzles with operating pressure of 0.45 bar. Total nine positions were arranged under rainfall simulator for the splash erosion measurements. The rainfall simulator at BAW had one FullJet nozzle with operating pressure of 0.25 bar where six positions were arranged for splash erosion measurements. The intensity was controlled by discontinuous spraying.

Both rainfall intensity and *KE* were measured for each splash cup position under both rainfall simulators. *KE* was calculated from drop size distribution measured by an optical laser disdrometer OTT Parsivel. Splash cups filled with air dried soil samples were exposed to rainfall three times for 30 minutes under constant intensity. Intensity depended on the positon under two rainfall simulators (see the 4.3. Results). Time intervals between the simulations were defined to reach certain θ_a. Different initial conditions were determined due to different θ_a and the surface condition of the soil samples. Namely, first simulation was performed on air-dried (AD-initial condition) (θ_a~5%), second simulation on wet-sealed (WS) (θ_a~30%) and third simulation on dry-crusted (DC) soil samples (5%<θ_a<10%). The representative soil sample with the three initial conditions is presented on Fig. 6.

a) b) c)

Figure 6. Photos of the soil surface in splash cups for three initial conditions: a) air-dried (AD); b) wet-sealed (WS) and c) dry-crusted (DC).

After each simulation, splashed soil particles from the splash cups were collected, oven-dried and weighted. Totally three replicates were done for each soil and initial condition. Saturated hydraulic conductivity (K_s) of soil samples in splash cups was measured after each simulation. The constant head method provided by Klute and Dirksen (1987) was used for establishing the K_s. Only the samples in splash cups tested under BAW rainfall simulator were evaluated. Results of K_s were based on three replicates. The flow chart of the conducted experiments is shown in Fig. 7. Time to ponding (t_p) in minutes was additionally measured for the samples tested under BAW rainfall simulator. Aim was to validate the measurements of the K_s, relating the reduction in infiltration rate (trough t_p) to reduction in soil K_s.

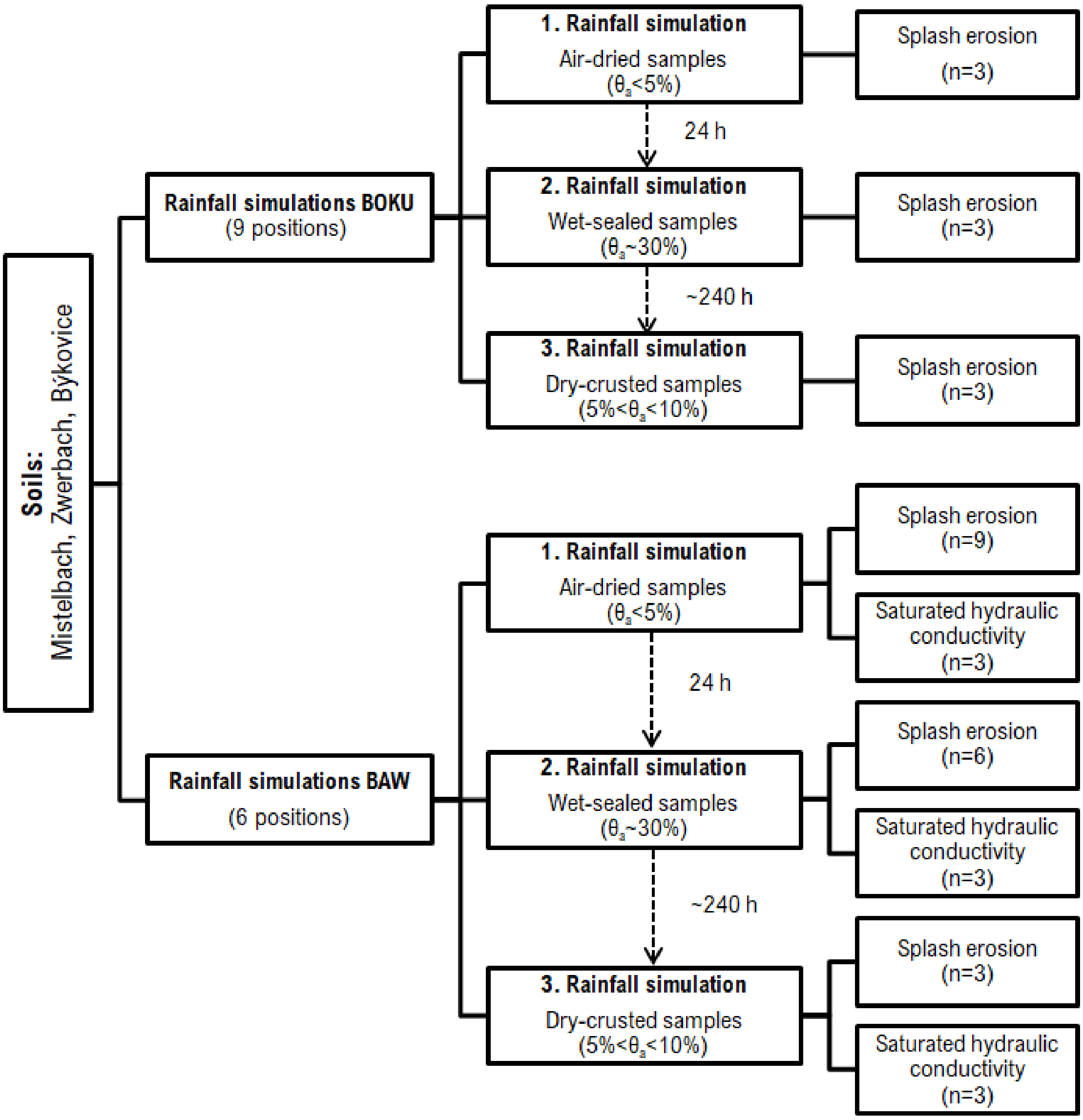

Figure 7. Schematic overview of the splash erosion experiments for two rainfall simulators. The numbers in the parenthesis under splash erosion and saturated hydraulic conductivity indicate the number of replications per each soil. θ_a denotes the initial soil water content

4.3. Results

Intensities measured for the selected positions under rainfall simulator at BOKU ranged from 28 to 54 mm h^{-1} and at BAW from 35 to 81 mm h^{-1}. The *KE* obtained for the same positions ranged between 504 and 923 J m^{-2} h^{-1} for BOKU and between 376 and 962 J m^{-2} h^{-1} for BAW rainfall simulator. Although higher rainfall intensities were recorded under BAW rainfall simulator, the *KE* per mm of rainfall was 62% higher for the rainfall simulator at BOKU. Higher velocities obtained for the larger drops under rainfall simulator at BOKU contributed to higher *KE* for the same amount of rainfall. Therefore, twice as high splash erosion rates were measured under rainfall simulator at BOKU, considering most cases with different soils and initial conditions. Splash erosion of three soils was described as the linear (BOKU) or power function (BAW) of rainfall *KE* for the AD initial condition. For WS soil samples, splash erosion was 60 and 72% lower considering both rainfall simulators. This reduction concerns the soil samples exposed to high intensities (45-80 mm h^{-1}) with developed surface ponding. Resulting relationship between the splash erosion and *KE* was therefore negative for all soils. Samples exposed to lower intensities showed increase in splash rate compared to AD surface condition. This increase was evident for the MI and ZW soil under rainfall simulator at BOKU. During the simulation with the DC soil samples, splash erosion increased positively with increasing *KE*. Similarly to WS simulation 50% more splash erosion was noted for the samples exposed to lower intensities. Generally, the BK soil (loamy sand) had highest splash erosion rates for AD and DC initial condition and the lowest for WS initial condition, obtained under both rainfall simulators. The soil K_s decreased between the simulations affected by increasing rainfall intensity and cumulative *KE* imposed on soil samples. The highest K_s values were obtained for the ZW soil and lowest for the BK soil. The decrease in the K_s between the rainfall simulations with different initial conditions is described as the negative power function of the accumulated *KE*. This relationship was significant for the MI and ZW soil, where the BK soil did not show any variation in K_s between the simulations or the rainfall intensities. The reduction of K_s values between the simulations indicated surface sealing due to raindrop impact. From the obtained relationship between the K_s and accumulated rainfall *KE*, a threshold value for *KE* needed to develop stable seal was obtained for MI and ZW soil. Correspondingly, the t_p measurements showed similar trend to K_s considering plotted against rainfall intensity. Higher t_p values were obtained for simulation with AD surface condition and lower rainfall intensity, due to higher soil infiltration capacity. The relationship between the t_p and rainfall intensity resulted in power function with the R^2 of 0.90, 0.91 and 0.44 for MI, BK and ZW soil, respectively. The correlation between K_s could not be obtained due to high deviations between replicates of K_s measurements for individual positions.

4.4. Discussion

Rainfall *KE* produced by different rainfall simulators resulted in different splash erosion rates. Even though the rainfall simulators are often used in soil erosion studies, the differences in the design and operating principle result in different drop spectrum, which can violate the comparison of the results obtained with other rainfall simulators (Iserloh et al., 2013). Furthermore, it is already recognized that the rainfall produced by rainfall simulator is often characterized by uniform drops of different sizes and fall velocities. In natural conditions, the rainfall *KE* is primarily dependent on drop size distribution and velocity (Van Dijk et al., 2003). Larger drops (>1.3 mm) produced by rainfall simulators in this study were markedly under their terminal velocity defined by Atlas et al. (1973). This findings further confirm that rainfall *KE* produced by rainfall simulators cannot reflect the *KE* of natural rainfall. Nevertheless, to control the conditions of soil properties in this study the use of the artificial rainfall was essential. Variations in splash erosion between the three rainfall simulations were affected by the soil moisture content and surface ponding followed by seal development. Splash erosion for soil samples with AD initial condition and low θ_a increased with increasing *KE*. However, the appearance of surface ponding in the last stage of the rainfall simulation indicated the reduction in soil infiltration rate. This reduction was attributed to lower soil permeability due to surface sealing (Assouline, 2004; Liu et al., 2011; Sharma et al., 1995). The surface sealing was further evident trough the reduction in the soil K_s for samples exposed to higher intensities and visible smooth surface after the rainfall simulation. In the following simulation with WS soil samples, early surface ponding (evident trough t_p) and partly formed seals from the previous simulation were observed. High θ_a mostly contributed to reduction of t_p for intensive rainfall. Short t_p was result of decline in hydraulic gradient and water storage capacity (Liu et al., 2011; Vermang et al., 2009). During the ponding, splash erosion was prevented by water layer, which lowered the raindrop impact on the soil surface (Poesen, 1981). The influence of the θ_a on t_p could be excluded for the simulation with DC initial condition since the initial θ_a was approximately three times lower. Earlier surface ponding (compared to t_p for AD initial condition) was probably affected by already developed seals from previous simulations. Generally splash erosion increased or did not vary between the simulations on samples with different initial condition, which were not regularly affected by surface ponding. The increase in splash erosion during rainfall simulation with DC samples was noticed for MI and ZW soil samples exposed to low intensities. Considering low θ_a, this could indicated higher effect of destructive slaking forces acting on aggregates (Lado et al., 2004). Evidently, samples exposed to lower intensities and *KE* showed increase of almost 50% in splash erosion rates for WS initial condition. Detachability by rain drop impact could be accelerated due to lower cohesion of the soil particles affected by high θ_a (Beczek et al., 2019; Gao et al., 2003). Other soil properties that contribute to soil detachment and surface seal formation are aggregate stability and soil texture (Le Bissonnais, 2016). Between the three soils the BK soil had highest aggregate stability; however it showed highest splash erosion detachment for lower θ_a and lowest K_s compared to the other soils. Furthermore, K_s for BK soil did not significantly decrease between the rainfall simulations. This might indicate that stable seals were formed already after the first simulation, which is typical for loamy soils according to observations by Morgan (1995). However, visibly smaller aggregates for BK soil and lower surface roughness could contributed to shorter t_p, since lower depression storage for water was available (Truman et al., 1990). The highest decrease in K_s was noted for MI soil, where rapid formation of the surface seals was attributed to high silt content. This results were equivalent to findings from several studies (Cheng et al., 2008; Comino et al., 2016; Truman et al., 1990). The obtained threshold values for *KE* to from stable seals (in case of MI and ZW soil) indicated that the seal formation highly dependent on rainfall *KE*. However, high variability between the replicates in the measurements for K_s would suggest that larger data set is needed to precisely describe seal development stages and its effect on splash erosion for certain scenarios.

4.5. Conclusion

Splash erosion measured under two different rainfall simulators is highly affected by rainfall characteristics produced by different rainfall simulators. The higher splash erosion rates are attributed to higher raindrop velocities produced by rainfall simulator.

Higher initial soil moisture content contributes to the reduction of splash erosion rate due to faster surface ponding. The formed seal layer can be reflected on decrease in saturated hydraulic conductivity, where the predominant factor for its reduction was kinetic energy. Considering high variability among replicates for saturated hydraulic conductivity measurements, it is difficult to identify clear relationship for some soils. Nevertheless, this study presented that there is a complex interaction between the rainfall and soil physical parameters in the soil erosion process, which should be more investigated in order to apply these findings to more complex soil erosion prediction models.

5. Overall discussion

5.1. Rainfall erosivity parameters for splash erosion prediction

The splash erosion has been one of most intensively researched soil erosion process. However, there is still no general agreement which rainfall properties actually best describes the detachment rate of the soil by raindrop impact (Salles et al., 2000). This is principally attributed to different approaches that researchers use to determine the relationship between the soil detachment and rainfall erosivity. In the experiments with simulated rainfall the rainfall conditions are constant and splash is observed often on sand not on soils. However, under natural rainfall conditions the rainfall is highly temporary and spatially variable, which introduces additional difficulty in choosing the right parameter for splash erosion prediction. In the Study 1 was shown that same amount of total rainfall *KE* wont necessary produce same splash erosion rate when observed on different sites. Higher splash erosion rates were attributed to site with intensive short storms and larger drop diameter. Govers (1991) suggested that splash erosion was underestimated for higher rainfall intensity when using the *KE,* which was also the case for the observed splash rates in Study 1. Furthermore, the results obtained in Belgium were based on events with lower intensities. The author suggested that rainfall intensity is more appropriate erosivity parameter when low intensity rainfall prevails. This could be one of the reasons that in Study 1 splash erosion was better described trough rainfall intensity rather than gross *KE*. van Dijk (2003) on the other hand, suggested for his data observed in West Java, Indonesia to use the *KE* of rainfall falling at the intensities higher than 25 mm h^{-1}. However, for temperate climates, lower thresholds were suggested. For instance 10 mm h^{-1} in Britain (Morgan, 1977), 6 mm h^{-1} in Germany (Richter and Negendank, 1977) and 2-5 mm h^{-1} in Netherlands (Van Asch, 1983). From the relationship between splash erosion and rainfall intensity obtained in the Study 1 was shown that already low intensities produced significant amount of splash. Therefore, no such a threshold was applied in the analysis with *KE*. However, strong relationship (R^2=0.90) obtained between splash erosion and *KE* per time unit (KE_h) enabled to discern the rainfall events with low and high intensity rate.

Considering the variable rainfall distribution of storms in the field, the duration of the rainfall is crucial parameter when analysing the splash erosion. The erosivity of rainfall should be attributed to rainfall intensity as the raindrop erosion increases with rainfall intensity. For this reason the factors combining the intensity with rainfall *KE*, such as EI_{30}, has been widely used for prediction of soil erosion by water (Panagos et al., 2016a; Renard et al., 1997; Walter H. Wischmeier and Smith, 1958; Yin et al., 2015). The EI_{30} is a statistical interaction how total *KE* and peak intensity are combined in each particular storm (Renard et al., 1997). The EI_{30} results in detachment of soil particles and their detachment by runoff. Direct application of the EI_{30} as the splash erosion prediction factor was elaborated in the study by Angulo-Martínez et al. (2016). The author obtained good relationship between the splash erosion and the EI_{30} factor, also using the *KE* calculated from *DSD*. According to data obtained in Study 1, the EI_{30} was found to underestimate the soil detachment by splash. The lower splash erosion rates predicted by the EI_{30} factor could be attributed to low I_{30} values from the minute data. Furthermore, slightly better correlation was obtained with maximum 15- or 5-minute intensity, but not significantly (not shown in the results). However, it should be considered that the EI_{30} as a part of USLE was primarily created to predict annual rainfall erosivity based on large time scale data and potential soil loss, but not soil detachment based on one event (Wischmeier, 1976). The EI_{30} for splash erosion prediction in the Study 1 was therefore not appropriate factor. The splash erosion is primarily attributed to rainfall *DSD*, which is highly sensitive to temporal variability of rainfall within the rainfall event. Furthermore, Nearing et al. (2017) also implied that the EI_{30} can be used in terms of quantifying the relative spatial or temporal differences in rainfall erosivity on annual or monthly basis, but it can underestimate the erosivity of rainfall for splash erosion prediction.

The choice of the appropriate rainfall parameter for splash erosion prediction must be based on the on high temporal resolution data in order to evaluate the differences between the individual rainfall events or sites. The data analysis should include parameters relative to the specific conditions in the experiments. In case of the experiments under natural rainfall such as presented in Study 1, the disdrometer measurements are necessary to evaluate the raindrop impact on splash erosion. Even though in the presented study, splash erosion was more related to rainfall intensity, these results are based on a given experimental set conditions and cannot be extracted to different conditions. The rates of splash erosion were very significant, according to the given results in the Study 1 and comparing the splash erosion rates to similar studies (Angulo-Martínez et al., 2012; Fernández-Raga et al., 2010). Therefore, the choice of the relevant factor for splash erosion prediction is important for more precise evaluation of the potential risk of soil erosion on the investigated sites in Central Europe.

5.2. Initial soil water content and soil properties affecting splash erosion

The bare soil exposed to consecutive rainfall events will influence soil erodibility by changes in soil moisture and surface roughness. Accordingly, the splash erosion will increase until reaching full soil saturation with following surface runoff. These factors can affect, or in turn, be affected by other phenomena directly related to raindrop impact, such as the formation of the seal layer on the bare soil surface exposed to high intensities (Assouline and Ben-Hur, 2006). Soil moisture affects not only the infiltration and runoff rates, but also the cohesion forces between the soil aggregates. The interaction of splash erosion with the above-described effects (except surface runoff) was investigated in the Study 2 under controlled conditions in laboratory. The soil water content (θ_a) played major role in the soil infiltration responses observed for the soil samples under different intensities. Higher soil θ_a initiated earlier surface ponding due to reduction in soil infiltration capacity. This was expected considering reduced soil water storage capacity and lower matric potential gradient (Lado et al., 2004; Vermang et al., 2009). The final splash erosion rates for the samples with wet-sealed condition were lower compared to air-dried initial condition due to surface ponding, which prevented further soil detachment (Mermut et al., 1997). For air-dried and dry-crusted conditions the splash erosion increased with higher rainfall *KE*. However, the reduction in infiltration rate for air-dried (seed bed condition) soil samples differed between soils used in the experiment. According to K_s measurements the lowest infiltration was attributed to loamy sand soil with lowest clay content and highest to silt loam soil with highest clay content among the soils. The higher sand content (45%) of the loamy sand soil would indicate greater K_s compared to silt loam samples according to García-Gutiérrez et al. (2018). The reason for lower K_s and earlier reduction in the infiltration capacity of the loamy sand soil could be attributed to higher capability to aggregate destruction followed by surface sealing. Significantly ($p<0.05$) higher splash erosion rates for air-dried condition of loamy sand also confirmed the assumption lower resistance of soil surface to raindrop impact in the initial phase of rainfall simulation. The aggregate stability measurements for the three soils could not confirm these findings, since the highest percentage of the stable aggregates was measured for loamy sand soil (63.3%). However, its visibly finer aggregates compared to other soils with coarser aggregate structure (silt loams) might indicate higher ability of raindrops to destroy aggregates resulting in higher splash erosion and reduction in surface infiltration. The findings by Fox et al. (2007) indicate that smaller fractions were more susceptible to surface crusting and splash erosion than the coarser fractions. Furthermore, lower surface roughness due to smaller aggregates is characterized with lack of depressional storage, which possibly induced earlier surface ponding (Truman and Bradford, 1990).

Silt content is commonly considered as the key factor for fast surface seal development (Cheng et al., 2008; Rodrigo Comino et al., 2017; Truman et al., 1990). The silt loam soil from Mistelbach with the highest silt content (70.4%) had the greatest reduction in K_s for soil samples exposed to highest intensities. Consequently the seal formation during the rainfall simulation reduced the surface erodibility and final splash erosion rates. Strong relationship was found between the K_s for silt loam soils and the accumulated rainfall *KE*, where the K_s was decreasing with increasing *KE* until reaching a constant value. Therefore, it can be stated that stable seal development will depend on the applied rainfall *KE*. Lack of the significance found between K_s and *KE* for loamy sand soil could be attributed to early stable seal formation during the first simulation with air-dried samples or inability of loamy sand soil to form stable seals. Additional micro-morphological measurements are necessary to establish the presence of developed seal. However, the indirect measurements such as time to ponding and soil K_s indicated lower infiltration capacity of loamy sand soil compared to silt loams. In addition to this it should be noted that measurements of the K_s for the specific samples showed high variations, therefore more replications (n>3) should be performed in order to make stronger conclusions.

Observing the three subsequent rainfall simulations increase in splash erosion rates was noted for samples exposed to lower intensities (<35 mm h^{-1}) and less affected by surface ponding. Evident increase in splash erosion compared to air-dried surface condition was detected for the samples with higher initial θ_a. Lower cohesion between the particles contributes to higher detachability affected by raindrop impact (Beczek et al., 2019; Gao et al., 2003). This increase in detachability was in particular noted for the silt loam soils for the wet-sealed initial condition. As seen from the results obtained in Study 2 the soil initial conditions and dynamic changes in soil structure caused by rainfall largely affect the splash erosion process. These results partly reflect the conditions in the field where soil surface is exposed to different rainfall intensities and weather conditions, which foremost affect the soil moisture and surface structure. However, due to certain limitations in the filed Study 1, such as inability to temporally monitor soil moisture or surface structure, the results from the laboratory measurements cannot be exactly translated to outdoor experiments. Still, the experimental study present that the soil initial properties must be considered in order to precisely predict splash erosion at the scale of a single rainfall event.

5.3. Uncertainties in splash erosion research approaches

Splash erosion has been widely studied over last few decades; still understanding the splash erosion from a physical point of view is associated with many uncertainties concerning different research approaches. One of the most disputable is the choice between field and laboratory study or natural and simulated rainfall. The rainfall parameters causing the splash erosion have been widely studied in the laboratory (Ghadiri and Payne, 1977; Poesen and Savat, 1981; Salles and Poesen, 2000; Sharma and Gupta, 1989). However, the laboratory studies cannot directly reproduce the conditions in the field (Van Dijk et al., 2003). Variability in *DSD* is the main factor defining splash erosion in the field where in laboratory uniform drop size and constant intensity is used. Accordingly, the results obtained from Study 1 and Study 2, showed evidently higher splash erosion rates measured in the field compared to ones obtained in the laboratory, considering similar range of *KE* and soil initial condition. Together with *DSD*, the raindrop velocity is dominant factor controlling splash erosion detachment. Drops accelerated by the two rainfall simulators used in Study 2 were under the terminal drop velocity defined by Atlas et al. (1973). Lower drop velocities can significantly reduce the rainfall potential to detach soil particles. The results published by Iserloh et al. (2013) revealed that rainfall drop velocities produced by thirteen different rainfall simulators is generally lower than calculated terminal velocity mostly due to technical limitations such as height of the rainfall simulator. Furthermore, the differences between rainfall simulators can also reflect on experiment outcome. Two rainfall simulators used in Study 2 showed significant differences in the rainfall *KE* comparing same rainfall amounts. Consequently, the rainfall simulator with higher *KE* per rainfall unit (mm) contributed to higher splash erosion rates. Considering the variabilities in rainfall character between the natural and simulated rainfall, and simulated rainfall produced by different simulators, special attention needs to be payed when comparing the splash erosion results obtained under different conditions.

Monitoring of splash erosion together with the rainfall erosivity requires extensive instrumental effort (Angulo-Martínez et al., 2012). Due to spatial differences attributed to certain location rainfall parameters need to be closely monitored (Angulo-Martínez and Barros, 2015). Splash erosion is raindrop induced process where *DSD* is crucial for precise calculation of *KE* and prediction of total soil detachment rate by splash. Raindrop size and velocity measurements require instruments such as optical laser disdrometer or acoustic disdrometer. When the measurements of the drop size and velocity spectrum are not available the rainfall *KE* is calculated from the rainfall intensity. From the literature exponential (Brown and Foster, 1987; Petan et al., 2010), logarithmic (Brandt, 1990; Wischmeier and Smith, 1978) and linear (Sempere Torres et al., 1992) relationships between *KE* and intensity are known. These empirical relationships represent the rainfall erosivity of the location where the data was measured. Therefore, they cannot completely reflect the rainfall conditions of other regions with different geographical and meteorological characteristics. For e.g. Brown-Foster equation (Brown and Foster, 1987) is valid for continental United States. Researchers validated empirical *KE* intensity relationships from literature with their data sets measured with disdrometer (Angulo-Martínez et al., 2016; Lisbeth Lolk Johannsen et al., 2020), but there is still no general agreement which empirical relationship preforms the best due to differences in rainfall regime and the instrument used. The empirical relationships are important tool for soil erosion prediction (Morgan et al., 1998; Renard et al., 1997; Walter H. Wischmeier and Smith, 1958). However, empirical relationships could reduce ability to correctly estimate rainfall *KE* on event basis and consequently predict splash erosion detachment. For the data collected at experimental sites described in Study 1 different *KE* and intensity relationships from the literature were validated in the research by Johannsen et al. (2020). Results have shown that the best fit *KE* and intensity relationships from the literature varied according to site and disdrometer type used. Furthermore use of disdrometer by different producers for classifying drop size and velocity can also introduce certain uncertainty in the *KE* measurements. The results from the study by Angulo-Martínez et al. (2018) and Johannsen et al. (2020) clearly demonstrate the influence of the disdrometer by different producer on the *KE* calculation. In the Study 1 the *KE* measured by different disdrometers was modified using the correction factor obtained in L.L. Johannsen et al., (2020) in order to ensure more consistent comparison between the devices. The reference used for developing correction factor was the device with measured rainfall amount close to one measured by rain gauge, on event basis. In the field experiments for splash erosion monitoring the correct interpretation of the rainfall *KE* is one of the most important factors. When neglecting the spatial and temporal differences of rainfall and differences between instruments for drop size and velocity detection, the accurate comparisons between studies could be violated.

Another critical point in the splash erosion studies that can affect the result interpretation is the method or device used for splash erosion measurements. Splash cup by Morgan (1978) is commonly used in many studies (Angulo-Martínez et al., 2012; Fernández-Raga et al., 2010; Zumr et al., 2019). Authors usually apply different devices or modify the ones proposed in the literature to reach the objectives of the presented study. Accordingly, the comparison of results between the studies that use different methods for splash erosion assessment is highly uncertain (Fernández-Raga et al., 2019). The results obtained in the Study 1 were compared with studies using the similar method for splash erosion measurements. However, due to differences in the soil condition (disturbed, undisturbed) splash erosion rates were difficult to compare. Additional factor that needs to be considered is spatial upscaling. In the Study 1 the splash erosion was measured on the surface of 84 cm^{-2}, however upscaling the results on m^2 or ha can introduce uncertainties. Splash erosion varies according to geographical conditions affected by the slope steepness (Torri and Poesen, 1992; Wu et al., 2019) and surface roughness (Römkens et al., 2002; Wu et al., 2016). For the given conditions in the Study 1 and Study 2, splash erosion measured by splash cup based on Morgan (1978) design gave acceptable results showing minor variabilities between the replicates.

6. Conclusions

This thesis aims to investigate the performance of different rainfall parameters for more accurate prediction of splash erosion under natural rainfall conditions on sites in Central Europe. Furthermore, it aims to relate the differences in splash erosion rates to soil properties affected raindrop impact.

The results of splash erosion measurements under natural rainfall suggested that splash erosion can be described as the linear function of the rainfall intensity, for the three monitored sites. Cumulative rainfall kinetic energy underestimated splash erosion; however, better results were obtained when splash erosion and rainfall kinetic energy were divided by rainfall duration. Temporal variations in rainfall intensity are typical characteristic of natural rain storms. Therefore, gross rainfall kinetic energy was not appropriate parameter to describe these variations and their affect on splash erosion. Rainfall erosivity factor, commonly used in soil erosion prediction models, underestimated the splash erosion on the rainfall event basis. Data show that spatial rainfall characteristics reflected on splash erosion detachment between the sites. Monitoring of the rainfall drop size and velocity on high temporal resolution enabled to distinguish the differences in the rainfall characteristics between individual rainfall events and the variabilities specific to local conditions (only for the sites with same disdrometer type). However, different locations require independent investigation of parameters controlling splash erosion.

Effect of initial soil moisture and surface structure on splash erosion was investigated using simulated rainfall. Combination of soil initial water content and surface seal formation highly affected final splash erosion rates. The reduction in final splash erosion rates was characteristic to samples exposed to high intensity rainfall affected by surface ponding. During ponding, surface was protected from further raindrop impact. High initial water content contributed to early surface ponding due to lower soil infiltration capacity. Surface ponding indicated also the beginning of surface seal formation for the samples exposed to high rainfall intensities. Measurements of saturated hydraulic conductivity enabled to track temporal development of surface sealing between the consecutive rainfall simulations. The reduction in soil saturated hydraulic conductivity can be described as the power function of increasing cumulative rainfall kinetic energy. The samples with dry-crusted surface and fully developed seals had lower erodibility and infiltration capacity. However, the samples without developed surface seals, exposed to lower intensities, had higher detachment capacity due lower cohesion of soil particles. Initial soil conditions dictate the dynamics of splash erosion development, which could highly affect soil erosion process. These factors have to be considered, not only in experiments similar to presented one, but also in more complex soil erosion prediction models.

Splash erosion is highly affected by rainfall properties. The simulated rainfall cannot reflect the natural rainfall characteristics which highly affect the final splash erosion rates. The relation between splash erosion and soil texture confirmed that splash erosion is positively correlated to sand content and negatively to clay content. Detail knowledge of parameters defining splash erosion contributes to higher ability of predicting the potential risks caused by soil erosion water. Complete study of splash erosion should investigate the potential of rainfall to cause soil detachment in relation with soil properties that define the soil erodibility.

7. Perspectives

Splash erosion is one of the dominant processes of soil erosion by water on arable land. Accurate prediction of splash erosion provides better application of the soil management techniques, which prevent excessive soil erosion by water. For this reason, monitoring of rainfall properties together with soil erosion is essential, especially in the field studies. In the presented research, the temporal monitoring of rainfall properties with rain gauge and disdrometers enabled to discern the differences between the rainfall events and to relate them to resulting splash erosion rates. However, the monitoring of the temporal resolution of splash erosion was not conducted in the presented experimental design, only the final splash erosion rates were analysed. The temporal splash distribution could provide information on direct splash erosion response to changes in rainfall pattern in the field studies. The changes in rainfall patterns could be, however, simulated in controlled laboratory conditions and thus provide theoretical background of the temporal resolution of splash erosion affected by different rainfall patterns. The spatial character of splash erosion is additional topic that requires more research. With an application of a similar model of splash cup installed directly into soil, differences between the splash erosion upslope and downslope could be quantified on site. Further, the spatial differences in splash erosion could be accessed by measurements on more sites using the same measurement technique.

The soil detachability is closely correlated to soil texture, structure, composition and physical characteristics. Lack of information about the soil characteristics can lead to misinterpretation of the results and the inability to compare the results from the similar studies. Analysed soils in this research showed similarity in the soil texture, however different response to the rain-drop impact. These differences could be affected by other soil characteristics (such as clay minerology, iron oxides, infiltration capacity, aggregate size etc.), which were not directly measured. Furthermore, more analysed soils would provide larger data set, which could enable to statistically define the crucial soil properties affecting splash erosion. These results would provide necessary data basis for developing splash erosion model, which could be applied for the studied area.

Lack of standardized methods for splash erosion measurements often leads to inconsistent output from different studies. The results obtained with splash cup method for splash erosion measurement provided reliable information about the splash erosion under natural and controlled conditions. However, the application of different method could be researched in order to investigate the impact of sample size and the concept of the measurement method on the results.

Further research can focus on the investigation of other soil processes, such as rill and interill erosion using runoff plots studies. With combination of the measurements from splash cups and those from plots would be possible determine the potential amount of soil, which could be detached by raindrop impact, overland flow and rill erosion. Such research would provide more guidance on soil and water conservation on the arable land. Furthermore, the results of the presented study reveal that the splash erosion dynamic physical process, affected by complex interaction between rainfall and inherent soil properties. For more reliable results prediction models of splash erosion on the scale of the single event must take into account these interactions.

References

Agassi, M., Morin, J., Shainberg, I., 1985. Effect of Raindrop Impact Energy and Water Salinity on Infiltration Rates of Sodic Soils. Soil Sci. Soc. Am. J. https://doi.org/10.2136/sssaj1985.03615995004900010037x

Al-Durrah, M., Bradford, J.M., 1981. New Methods of Studying Soil Detachment due to Waterdrop Impact. Soil Sci. Soc. Am. J. https://doi.org/10.2136/sssaj1981.03615995004500050026x

Amundson, R., Berhe, A.A., Hopmans, J.W., Olson, C., Sztein, A.E., Sparks, D.L., 2015. Soil and human security in the 21st century. Science (80-.). https://doi.org/10.1126/science.1261071

Angulo-Martínez, M., Barros, A.P., 2015. Measurement uncertainty in rainfall kinetic energy and intensity relationships for soil erosion studies: An evaluation using PARSIVEL disdrometers in the Southern Appalachian Mountains. Geomorphology

228. https://doi.org/10.1016/j.geomorph.2014.07.036
Angulo-Martínez, M., Beguería, S., Kyselý, J., 2016. Use of disdrometer data to evaluate the relationship of rainfall kinetic energy and intensity (KE-I). Sci. Total Environ. 568, 83–94. https://doi.org/10.1016/j.scitotenv.2016.05.223
Angulo-Martínez, M., Beguería, S., Latorre, B., Fernández-Raga, M., 2018. Comparison of precipitation measurements by OTT Parsivel2 and Thies LPM optical disdrometers. Hydrol. Earth Syst. Sci. 22, 2811–2837. https://doi.org/10.5194/hess-22-2811-2018
Angulo-Martínez, M., Beguería, S., Navas, A., Machín, J., 2012. Splash erosion under natural rainfall on three soil types in NE Spain. Geomorphology. https://doi.org/10.1016/j.geomorph.2012.06.016
Armenise, E., Simmons, R.W., Ahn, S., Garbout, A., Doerr, S.H., Mooney, S.J., Sturrock, C.J., Ritz, K., 2018. Soil seal development under simulated rainfall: Structural, physical and hydrological dynamics. J. Hydrol. 556, 211–219. https://doi.org/10.1016/j.jhydrol.2017.10.073
Assouline, S., 2013. Infiltration into soils: Conceptual approaches and solutions. Water Resour. Res. 49, 1755–1772. https://doi.org/10.1002/wrcr.20155
Assouline, S., 2009. Drop size distributions and kinetic energy rates in variable intensity rainfall. Water Resour. Res. https://doi.org/10.1029/2009WR007927
Assouline, S., 2004. Rainfall-Induced Soil Surface Sealing: A Critical Review of Observations, Conceptual Models, and Solutions. Vadose Zo. J. 3, 570–591. https://doi.org/10.2113/3.2.570
Assouline, S., Ben-Hur, M., 2006. Effects of rainfall intensity and slope gradient on the dynamics of interrill erosion during soil surface sealing. Catena 66, 211–220. https://doi.org/10.1016/j.catena.2006.02.005
Assouline, S., Mualem, Y., 1997. Modeling the dynamics of seal formation and its effect on infiltration as related to soil and rainfall characteristics. Water Resour. Res. https://doi.org/10.1029/96WR02674
Atlas, D., Srivastava, R.C., Sekhon, R.S., 1973. Doppler radar characteristics of precipitation at vertical incidence. Rev. Geophys. 11, 1–35. https://doi.org/10.1029/RG011i001p00001
Bauer, B., 1990. Soil splash as an important agent of erosion. Geogr. Pol. 58, 99–106.
Baumhardt, R.L., Römkens, M.J.M., Whisler, F.D., Parlange, J. -Y, 1990. Modeling infiltration into a sealing soil. Water Resour. Res. https://doi.org/10.1029/WR026i010p02497
Beczek, M., Ryżak, M., Sochan, A., Mazur, R., Bieganowski, A., 2019. The mass ratio of splashed particles during raindrop splash phenomenon on soil surface. Geoderma. https://doi.org/10.1016/j.geoderma.2019.03.028
Bedaiwy, M.N.A., 2008. Mechanical and hydraulic resistance relations in crust-topped soils. Catena 72, 270–281. https://doi.org/10.1016/j.catena.2007.05.012
Bisal, F., 1960. The effect of raindrop size and impact velocity on sand-splash 88–91.
Boardman, J., Poesen, J., 2006. Soil Erosion in Europe, Soil Erosion in Europe. https://doi.org/10.1002/0470859202
Borrelli, P., Robinson, D.A., Fleischer, L.R., Lugato, E., Ballabio, C., Alewell, C., Meusburger, K., Modugno, S., Schütt, B., Ferro, V., Bagarello, V., Oost, K. Van, Montanarella, L., Panagos, P., 2017. An assessment of the global impact of 21st century land use change on soil erosion. Nat. Commun. 8. https://doi.org/10.1038/s41467-017-02142-7
Bradford, J.M., Huang, C., 1993. Comparison of interrill soil loss for laboratory and field procedures. Soil Technol. https://doi.org/10.1016/0933-3630(93)90003-W

Bradford, J.M., Huang, C., 1992. Mechanisms of crust formation: physical components., in: Stewart, M.A., Summer, B.A. (Eds.), Soil Crusting: Physical and Chemical Processes. Lewis Publishers, Boca Raton, Florida, pp. 55–72.
Brandt, C.J., 1990. Simulation of the size distribution and erosivity of raindrops and throughfall drops. Earth Surf. Process. Landforms. https://doi.org/10.1002/esp.3290150803
Bresson, L.M., Boiffin, J., 1990. Morphological characterization of soil crust development stages on an experimental field. Geoderma. https://doi.org/10.1016/0016-7061(90)90035-8
Bresson, L.M., Moran, C.J., Assouline, S., 2004. Use of Bulk Density Profiles from X-Radiography to Examine Structural Crust Models. Soil Sci. Soc. Am. J. 68, 1169–1176. https://doi.org/10.2136/sssaj2004.1169
Brown, L.C., Foster, G.R., 1987. STORM EROSIVITY USING IDEALIZED INTENSITY DISTRIBUTIONS. Trans. Am. Soc. Agric. Eng. https://doi.org/10.13031/2013.31957
BUBENZER GD, JONES, B., 1971. Drop size and impact velocity effects on the detachment of soils under simulated rainfall. Trans. Am. Soc. Agric. Eng. https://doi.org/10.13031/2013.38353
Caron, J., Kay, B.D., Stone, J.A., 1992. Improvement of Structural Stability of a Clay Loam with Drying. Soil Sci. Soc. Am. J. https://doi.org/10.2136/sssaj1992.03615995005600050041x
Cheng, Q., Cai, Q., Ma, W., 2008. Comparative study on rain splash erosion of representative soils in China. Chinese Geogr. Sci. 18, 155–161. https://doi.org/10.1007/s11769-008-0155-9
Chenu, C., Le Bissonnais, Y., Arrouays, D., 2000. Organic Matter Influence on Clay Wettability and Soil Aggregate Stability. Soil Sci. Soc. Am. J. https://doi.org/10.2136/sssaj2000.6441479x
Comino, J.R., Iserloh, T., Morvan, X., Issa, O.M., Naisse, C., Keesstra, S.D., Cerdà, A., Prosdocimi, M., Arnáez, J., Lasanta, T., Ramos, M.C., Marqués, M.J., Colmenero, M.R., Bienes, R., Sinoga, J.D.R., Seeger, M., Ries, J.B., 2016. Soil erosion processes in European vineyards: A qualitative comparison of rainfall simulation measurements in Germany, Spain and France. Hydrology. https://doi.org/10.3390/hydrology3010006
Ellison, W.D., 1947. Soil erosion studies - Part II: Soil detachment hazard by raindrop splash. Agric. Eng. 28, 197–201.
Ellison, W.D., 1944a. Studies of raindrop erosion. Agric. Eng. 25, 181–182.
Ellison, W.D., 1944b. Two devices for measuring soil erosion. Agric. Eng. 25, 53–55.
Emerson, W.W., 1967. A classification of soil aggregates based on their coherence in water. Aust. J. Soil Res. https://doi.org/10.1071/SR9670047
FAO, 2015. Status of the World's Soil Resources., Intergovernmental Technical Panel on Soils.
Fernández-Raga, M., Campo, J., Rodrigo-Comino, J., Keesstra, S.D., 2019. Comparative analysis of splash erosion devices for rainfall simulation experiments: A laboratory study. Water (Switzerland) 11, 1–21. https://doi.org/10.3390/w11061228
Fernández-Raga, M., Fraile, R., Keizer, J.J., Varela Teijeiro, M.E., Castro, A., Palencia, C., Calvo, A.I., Koenders, J., Da Costa Marques, R.L., 2010. The kinetic energy of rain measured with an optical disdrometer: An application to splash erosion. Atmos. Res. 96, 225–240. https://doi.org/10.1016/j.atmosres.2009.07.013
Fernández-Raga, M., Palencia, C., Keesstra, S., Jordán, A., Fraile, R., Angulo-Martínez, M., Cerdà, A., 2017. Splash erosion: A review with unanswered questions. Earth-Science Rev. 171, 463–477. https://doi.org/10.1016/j.earscirev.2017.06.009

Flanagan, D., Nearing, M., 1995. USDA water erosion prediction project: Hillslope profile and watershed model documentation, NSERL Rep. 10. Agric. Res. Serv., West Lafayette, Indiana.
Fox, D.M., Darboux, F., Carrega, P., 2007. Effects of fire-induced water repellency on soil aggregate stability, splash erosion, and saturated hydraulic conductivity for different size fractions. Hydrol. Process. https://doi.org/10.1002/hyp.6758
Fu, Y., Li, G., Wang, D., Zheng, T., Yang, M., 2019. Raindrop energy impact on the distribution characteristics of splash aggregates of cultivated dark loessial cores. Water (Switzerland) 11. https://doi.org/10.3390/w11071514
Fu, Y., Li, G., Zheng, T., Li, B., Zhang, T., 2017. Splash detachment and transport of loess aggregate fragments by raindrop action. Catena 150, 154–160.
Gao, B., Walter, M.T., Steenhuis, T.S., Parlange, J.Y., Nakano, K., Rose, C.W., Hogarth, W.L., 2003. Investigating ponding depth and soil detachability for a mechanistic erosion model using a simple experiment. J. Hydrol. 277, 116–124. https://doi.org/10.1016/S0022-1694(03)00085-4
García-Gutiérrez, C., Pachepsky, Y., Ángel Martín, M., 2018. Technical note: Saturated hydraulic conductivity and textural heterogeneity of soils. Hydrol. Earth Syst. Sci. 22, 3923–3932. https://doi.org/10.5194/hess-22-3923-2018
Ghadiri, H., Payne, D., 1977. RAINDROP IMPACT STRESS AND THE BREAKDOWN OF SOIL CRUMBS. J. Soil Sci. https://doi.org/10.1111/j.1365-2389.1977.tb02233.x
Ghahramani, A., Yoshiharu, I., Mudd, S.M., 2012. Field experiments constraining the probability distribution of particle travel distances during natural rainstorms on different slope gradients. Earth Surf. Process. Landforms 37, 473–485. https://doi.org/10.1002/esp.2253
Gilley, J.E., Finkner, S.C., 1985. Estimating soil detachment caused by raindrop impact. Trans. ASAE 28, 140–146.
Goebes, P., Seitz, S., Geißler, C., Lassu, T., Peters, P., Seeger, M., Nadrowski, K., Scholten, T., 2014. Momentum or kinetic energy - How do substrate properties influence the calculation of rainfall erosivity? J. Hydrol. https://doi.org/10.1016/j.jhydrol.2014.05.031
Govers, G., 1991. Spatial and temporal variations in splash detachment: a field study. Catena Suppl. 20, 15–24.
Guy, B.T., Dickinson, W.T., Rudra, R.P., 1987. ROLES OF RAINFALL AND RUNOFF IN THE SEDIMENT TRANSPORT CAPACITY OF INTERRILL FLOW. Trans. Am. Soc. Agric. Eng. https://doi.org/10.13031/2013.30575
Hauser, D., Amayenc, P., Nutten, B., Waldteufel, P., 1984. A New Optical Instrument for Simultaneous Measurement of Raindrop Diameter and Fall Speed Distributions. J. Atmos. Ocean. Technol. https://doi.org/10.1175/1520-0426(1984)001<0256:anoifs>2.0.co;2
HAYNES, R.J., SWIFT, R.S., 1990. Stability of soil aggregates in relation to organic constituents and soil water content. J. Soil Sci. https://doi.org/10.1111/j.1365-2389.1990.tb00046.x
Hudson, N.W., 1965. The influence of rainfall on the mechanics of soil erosion : with particular reference to Southern Rhodesia. University of Cape Town.
Iserloh, T., Ries, J.B., Arnáez, J., Boix-Fayos, C., Butzen, V., Cerdà, A., Echeverría, M.T., Fernández-Gálvez, J., Fister, W., Geißler, C., Gómez, J.A., Gómez-Macpherson, H., Kuhn, N.J., Lázaro, R., León, F.J., Martínez-Mena, M., Martínez-Murillo, J.F., Marzen, M., Mingorance, M.D., Ortigosa, L., Peters, P., Regüés, D., Ruiz-Sinoga, J.D., Scholten, T., Seeger, M., Solé-Benet, A., Wengel, R., Wirtz, S., 2013. European small portable rainfall simulators: A comparison of rainfall characteristics. Catena.

https://doi.org/10.1016/j.catena.2013.05.013
Johannsen, L.L., Zambon, N., Strauss, P., Dostal, T., Neumann, M., Zumr, D., Cochrane, T.A., Blöschl, G., Klik, A., 2020. Comparison of three types of laser optical disdrometers under natural rainfall conditions. Hydrol. Sci. J. https://doi.org/10.1080/02626667.2019.1709641
Johannsen, Lisbeth Lolk, Zambon, N., Strauss, P., Dostal, T., Neumann, M., Zumr, D., Cochrane, T.A., Klik, A., 2020. Impact of Disdrometer Types on Rainfall Erosivity Estimation. Water 12, 963. https://doi.org/10.3390/w12040963
Jomaa, S., Barry, D.A., Brovelli, A., Sander, G.C., Parlange, J., Heng, B.C.P., Meerveld, H.J.T., 2010. Effect of raindrop splash and transversal width on soil erosion : Laboratory flume experiments and analysis with the Hairsine – Rose model. J. Hydrol. 395, 117–132. https://doi.org/10.1016/j.jhydrol.2010.10.021
Kemper, W.D., Rosenau, R.C., 1986. Aggregate Stability and Size Dlstributlon', in: Klute, A. (Ed.), Methods of Soil Analysis: Part 1 Physical and Mineralogical Methods. American Society of Agronomy - Soil Science Socity of America, pp. 425–442.
Khaledi Darvishan, A., Sadeghi, S.H., Homaee, M., Arabkhedri, M., 2014. Measuring sheet erosion using synthetic color-contrast aggregates. Hydrol. Process. https://doi.org/10.1002/hyp.9956
Kinnell, P.I.A., 1982. Laboratory studies on the effect of drop size on splash erosion. J. Agric. Eng. Res. 27, 431–439. https://doi.org/10.1016/0021-8634(82)90081-6
Kinnell, P.I.A., 1981. Rainfall Intensity-Kinetic Energy Relationships for Soil Loss Prediction1. Soil Sci. Soc. Am. J. https://doi.org/10.2136/sssaj1981.03615995004500010033x
Kinnell, P.I.A., 1974. Splash Erosion: Some Observations on the Splash-Cup Technique. Soil Sci. Soc. Am. J. https://doi.org/10.2136/sssaj1974.03615995003800040034x
Kinnell, P.I.A., 1973. PROBLEM OF ASSESSING THE EROSIVE POWER OF RAINFALL FROM METEOROLOGICAL OBSERVATIONS. Soil Sci Soc Am Proc. https://doi.org/10.2136/sssaj1973.03615995003700040039x
Klik, A., Truman, C.C., 2003. What is a Typical Heavy Rainstorm?, in: Gabriels, D., Cornelis, W. (Eds.), 25 Years of Assesment of Erosion. Ghent, Belgium, pp. 93–98.
Klute, A., Dirksen, C., 1987. Hydraulic conductivity of Saturated soils, in: Klute, A. (Ed.), Methods of Soil Analysis, Part 1. Physical and Mineralogical Methods. American Society of Agronomy - Soil Science Socity of America, Madison, WI, pp. 694–700.
Koch, A., Mcbratney, A., Adams, M., Field, D., Hill, R., Crawford, J., Minasny, B., Lal, R., Abbott, L., O'Donnell, A., Angers, D., Baldock, J., Barbier, E., Binkley, D., Parton, W., Wall, D.H., Bird, M., Bouma, J., Chenu, C., Flora, C.B., Goulding, K., Grunwald, S., Hempel, J., Jastrow, J., Lehmann, J., Lorenz, K., Morgan, C.L., Rice, C.W., Whitehead, D., Young, I., Zimmermann, M., 2013. Soil Security: Solving the Global Soil Crisis. Glob. Policy 4, 434–441. https://doi.org/10.1111/1758-5899.12096
Lado, M., Ben-Hur, M., 2004. Soil mineralogy effects on seal formation, runoff and soil loss. Appl. Clay Sci. https://doi.org/10.1016/j.clay.2003.03.002
Lado, M., Ben-Hur, M., Shainberg, I., 2004. Soil Wetting and Texture Effects on Aggregate Stability, Seal Formation, and Erosion. Soil Sci. Soc. Am. J. https://doi.org/10.2136/sssaj2004.1992
Lal, R., 1998. Drop size distribution and energy load of rain storms at Ibadan, western Nigeria. Soil Tillage Res. https://doi.org/10.1016/S0167-1987(98)00109-3
Laws, J.O., 1941. Measurements of the fall-velocity of water -drops and raindrops. Trans. Am. Geophys. Union 22, 709. https://doi.org/10.1029/TR022i003p00709
Laws, J.O., Parsons, D.A., 1943. The relation of raindrop-size to intensity. Eos, Trans. Am. Geophys. Union. https://doi.org/10.1029/TR024i002p00452

Le Bissonnais, Y., 2016. Aggregate stability and assessment of soil crustability and erodibility: I. Theory and methodology. Eur. J. Soil Sci. 67, 11–21. https://doi.org/10.1111/ejss.4_12311
Le Bissonnais, Y., Renaux, B., Delouche, H., 1995. Interactions between soil properties and moisture content in crust formation, runoff and interrill erosion from tilled loess soils. CATENA 25, 33–46. https://doi.org/10.1016/0341-8162(94)00040-L
Le Bissonnais, Y., Singer, M.J., 1993. Seal formation, runoff, and interrill erosion from seventeen California soils. Soil Sci. Soc. Am. J. https://doi.org/10.2136/sssaj1993.03615995005700010053x
Le Bissonnais, Y., Singer, M.J., 1992. Crusting, runoff, and erosion response to soil water content and successive rainfalls. Soil Sci. Soc. Am. Bull. https://doi.org/10.2136/sssaj1992.03615995005600060042x
Le Bissonnais, Y., Singer, M.J., Bradford, J.M., 1993. Assessment of soil erodibility: the relationship between soil properties, erosion processes and susceptibility to erosion. Farm L. Eros. Temp. plains Environ. hills. Proc. Symp. Saint-Cloud, Paris, 1992. https://doi.org/10.1016/b978-0-444-81466-1.50012-5
Legout, C., Leguédois, S., Le Bissonnais, Y., Malam Issa, O., 2005. Splash distance and size distributions for various soils. Geoderma 124, 279–292. https://doi.org/10.1016/j.geoderma.2004.05.006
Leguédois, S., Planchon, O., Legout, C., Le Bissonnais, Y., 2005. Splash projection distance for aggregated soils: Theory and experiment. Soil Sci. Soc. Am. J. https://doi.org/10.2136/sssaj2005.0030
Lim, Y.S., Kim, J.K., Kim, J.W., Park, B.I., Kim, M.S., 2015. Analysis of the relationship between the kinetic energy and intensity of rainfall in Daejeon, Korea. Quat. Int. 384. https://doi.org/10.1016/j.quaint.2015.03.021
Liu, H., Lei, T.W., Zhao, J., Yuan, C.P., Fan, Y.T., Qu, L.Q., 2011. Effects of rainfall intensity and antecedent soil water content on soil infiltrability under rainfall conditions using the run off-on-out method. J. Hydrol. 396, 24–32. https://doi.org/10.1016/j.jhydrol.2010.10.028
M. A. Nearing, G. R. Foster, L. J. Lane, S. C. Finkner, 1989. A Process-Based Soil Erosion Model for USDA-Water Erosion Prediction Project Technology. Trans. ASAE 32, 1587–1593. https://doi.org/10.13031/2013.31195
Mazurak, A.P., Mosher, P.N., 1968. Detachment of Soil Particles in Simulated Rainfall. Soil Sci. Soc. Am. J. https://doi.org/10.2136/sssaj1968.03615995003200050036x
Mcintyre, D.S., 1957. Soil splash and the formation of surface crusts by raindrop impact.
McIntyre, D.S., 1958. Soil splash and the formation of surface crusts by raindrop impact. Soil Sci. https://doi.org/10.1097/00010694-195805000-00005
Mermut, A.R., Luk, S.H., Römkens, M.J.M., Poesen, J.W.A., 1997. Soil loss by splash and wash during rainfall from two loess soils. Geoderma 75, 203–214. https://doi.org/10.1016/S0016-7061(96)00091-2
Moghadam, B.K., Jabarifar, M., Bagheri, M., Shahbazi, E., 2015. Effects of land use change on soil splash erosion in the semi-arid region of Iran. Geoderma 241, 210–220.
Montgomery, D.R., 2007. Soil erosion and agricultural sustainability. Proc. Natl. Acad. Sci. U. S. A. https://doi.org/10.1073/pnas.0611508104
Morgan, R.P.C., 2005. Soil erosion and conservation, 3rd ed. Blackwell Publishing company, Oxford.
Morgan, R.P.C., 1995. Soil Erosion and Conservation. Addison-Wesley: London.
Morgan, R.P.C., 1978. FIELD STUDIES OF RAINSPLASH EROSION. Earth Surf Process. https://doi.org/10.1002/esp.3290030308
Morgan, R.P.C., Quinton, J.N., Smith, R.E., Govers, G., Poesen, J.W.A., Auerswald, K., Chisci,

G., Torri, D., Styczen, M.E., Folly, A.J.., 1998. The European Soil Erosion Model (EUROSEM): documentation and user guide.
Nearing, M.A., Bradford, J.M., 1985. Single Waterdrop Splash Detachment and Mechanical Properties of Soils. Soil Sci. Soc. Am. J. 49, 547–552. https://doi.org/10.2136/sssaj1985.03615995004900030003x
Nearing, M.A., Yin, S. qing, Borrelli, P., Polyakov, V.O., 2017. Rainfall erosivity: An historical review. Catena. https://doi.org/10.1016/j.catena.2017.06.004
Palmer, R.S., 1964. The influence of a thin water layer on waterdrop impact forces. IAHS Publ. 65, 141–148.
Panagos, P., Ballabio, C., Borrelli, P., Meusburger, K., 2016a. Spatio-temporal analysis of rainfall erosivity and erosivity density in Greece. Catena 137. https://doi.org/10.1016/j.catena.2015.09.015
Panagos, P., Borrelli, P., Spinoni, J., Ballabio, C., Meusburger, K., Beguería, S., Klik, A., Michaelides, S., Petan, S., Hrabalíková, M., Olsen, P., Aalto, J., Lakatos, M., Rymszewicz, A., Dumitrescu, A., Tadić, M.P., Diodato, N., Kostalova, J., Rousseva, S., Banasik, K., Alewell, C., 2016b. Monthly rainfall erosivity: Conversion factors for different time resolutions and regional assessments. Water (Switzerland) 8. https://doi.org/10.3390/w8040119
Petan, S., Rusjan, S., Vidmar, A., Mikoš, M., 2010. The rainfall kinetic energy–intensity relationship for rainfall erosivity estimation in the mediterranean part of Slovenia. J. Hydrol. 391, 314–321. https://doi.org/10.1016/j.jhydrol.2010.07.031
Pla, I., 1986. A routine laboratory index to predict the effects ofsoil sealing on soil and water conservation., in: Callebaut, C., Gabriels, D., de Boodt, M. (Eds.), Assessment of Soil Surface Sealing and Crusting. University of Ghent, Ghent, Belgium, pp. 154–162.
Poesen, J., 1986. Surface sealing on loose sediments: the role oftexture, slope and position ofstones in the top layer, in: Callebaut, C., Gabriels, D., de Boodt, M. (Eds.), Assessment of Soil Surface Sealing and Crusting. University of Ghent, Ghent, Belgium, pp. 354–352.
Poesen, J., 1985. An improved splash transport model. Zeitschrift fur Geomorphol.
Poesen, J., 1981. Rainwash experiments on the erodibility of loose sediments. Earth Surf. Process. Landforms. https://doi.org/10.1002/esp.3290060309
Poesen, J., Savat, J., 1981. Detachment and transportation of loose sediments by raindrop splash: Part II Detachability and transport ability measurements. Catena.
Poesen, J., Torri, D., 1988. The effect of cup size on splash detachment and transport measurements. Part I: field measurements. Catena Suppl.
Quansah, C., 1981. The effect of soil type, slope, rain intensity and their interactions on splash detachment and transport. J. Soil Sci. https://doi.org/10.1111/j.1365-2389.1981.tb01701.x
Renard, K.G., Foster, G.R., Weesies, G.A., McCool, D.K., Yoder, D.C., 1997. Predicting Soil Erosion by Water: A Guide to Conservation Planning With the Revised Universal Soil Erosion Equation (RUSLE). US Derpartment of Agriculture.
Richter, G., Negendank, J.F.W., 1977. Soil erosion processes and their measurement in the german area of the Moselle river. Earth Surf. Process. 2, 261–278. https://doi.org/10.1002/esp.3290020217
Rodrigo Comino, J., Iserloh, T., Lassu, T., Cerdà, A., Keesstra, S.D., Prosdocimi, M., Brings, C., Marzen, M., Ramos, M.C., Senciales, J.M., Ruiz Sinoga, J.D., Seeger, M., Ries, J.B., 2016. Quantitative comparison of initial soil erosion processes and runoff generation in Spanish and German vineyards. Sci. Total Environ. 565, 1165–1174. https://doi.org/10.1016/j.scitotenv.2016.05.163
Rodrigo Comino, J., Senciales, J.M., Ramos, M.C., Martínez-Casasnovas, J.A., Lasanta, T.,

Brevik, E.C., Ries, J.B., Ruiz Sinoga, J.D., 2017. Understanding soil erosion processes in Mediterranean sloping vineyards (Montes de Málaga, Spain). Geoderma 296. https://doi.org/10.1016/j.geoderma.2017.02.021

Römkens, M.J.M., Helming, K., Prasad, S.N., 2002. Soil erosion under different rainfall intensities, surface roughness, and soil water regimes. Catena 46, 103–123. https://doi.org/10.1016/S0341-8162(01)00161-8

Romkens, M.J.M., Prasad, S.N., Parlange, J.Y., 1990. Surface seal development in relation to rainstorm intensity. Catena Suppl.

Rose, C., Williams, J., Sander, G., Barry, D., 1983. A Mathematical Model of Soil Erosion and Deposition Processes: I. Theory for a Plane Land Element1. Soil Sci. Soc. Am. J. 47, 991–995. https://doi.org/10.2136/sssaj1983.03615995004700050030x

Rose, C.W., 1960. Soil detachment caused by rainfall. Soil Sci. 89, 28–35. https://doi.org/10.1097/00010694-196001000-00005

Ryzak, M., Bieganowski, A., Polakowski, C., 2015. Effect of soil moisture content on the splash phenomenon reproducibility. PLoS One 10, 1–15. https://doi.org/10.1371/journal.pone.0119269

Salles, C., Poesen, J., 2000. Rain properties controlling soil splash detachment. Hydrol. Process. 14, 271–282. https://doi.org/10.1002/(SICI)1099-1085(20000215)14:2<271::AID-HYP925>3.0.CO;2-J

Salles, C., Poesen, J., Govers, G., 2001. A comparison of rain erosivity parameters for predicting soil detachment on interrills. Sustain. Glob. Farm, 10th Int. Soil Conserv. Organ. Meet. My 24–29, 1999 834–837.

Salles, C., Poesen, J., Govers, G., 2000. Statistical and physical analysis of soil detachment by raindrop impact: Rain erosivity indices and threshold energy. Water Resour. Res. 36, 2721–2729. https://doi.org/10.1029/2000WR900024

Salles, C., Poesen, J., Sempere-Torres, D., 2002. Kinetic energy of rain and its functional relationship with intensity. J. Hydrol. 257, 256–270. https://doi.org/10.1016/S0022-1694(01)00555-8

Schjonning P., van den Akker J.J.H., Keller T., et al., Stolte, J., Tesfai, M., Keizer, J., Øygarden, L., Kværnø, S., Verheijen, F., Panagos, P., Ballabio, C., Hessel, R., 2016. Soil compaction. In: Soil threats in Europe. EUR 27607 EN,. JRC Sci. Tech. Reports. https://doi.org/10.2788/828742

Scholten, T., Geißler, C., Goc, J., Kühn, P., Wiegand, C., 2011. A new splash cup to measure the kinetic energy of rainfall. J. Plant Nutr. Soil Sci. 174, 596–601. https://doi.org/10.1002/jpln.201000349

Sempere Torres, D., Salles, C., Creutin, J.D., Delrieu, G., 1992. Quantification of soil detachment by raindrop impact: performance of classical formulae of kinetic energy in Mediterranean storms. Eros. sediment Monit. Program. river basins. Proc. Int. Symp. Oslo, 1992.

Sharma, P.P., Gupta, S.C., 1989. Sand Detachment by Single Raindrops of Varying Kinetic Energy and Momentum. Soil Sci. Soc. Am. J. https://doi.org/10.2136/sssaj1989.03615995005300040003x

Sharma, P.P., Gupta, S.C., Foster, G.R., 1995. Raindrop-Induced Soil Detachment and Sediment Transport from Interrill Areas. Soil Sci. Soc. Am. J. 59, 727. https://doi.org/10.2136/sssaj1995.03615995005900030014x

Sharma, P.P., Gupta, S.C., Rawls, W.J., 1991. Soil Detachment by Single Raindrops of Varying Kinetic Energy. Soil Sci. Soc. Am. J. https://doi.org/10.2136/sssaj1991.03615995005500020001x

Smith, D.D., Wischmeier, W., 1957. Factors affecting sheet and rill erosion. Trans. Am. Geophys. Union 38, 889–896. https://doi.org/10.1029/TR038i006p00889

The World Bank Group, 2016. Agricultural land (% of land area) - European Union [WWW Document]. URL https://data.worldbank.org/indicator/AG.LND.AGRI.ZS?end=2016&locations=EU&most_recent_value_desc=true&start=1961&view=chart (accessed 7.2.20).
Torri, D., Poesen, J., 1992. The effect of soil surface slope on raindrop detachment. Catena. https://doi.org/10.1016/0341-8162(92)90053-E
Torri, D., Sfalanga, M., Del Sette, M., 1987. Splash detachment: Runoff depth and soil cohesion. Catena. https://doi.org/10.1016/S0341-8162(87)80013-9
Truman, C.C., Bradford, J.M., 1990. Effect of antecendet soil moisture on splash detachment under simulated rainfall.
Truman, C.C., Bradford, J.M., Ferris, J.E., 1990. Antecedent Water Content and Rainfall Energy Influence on Soil Aggregate Breakdown. Soil Sci. Soc. Am. J. https://doi.org/10.2136/sssaj1990.03615995005400050030x
Van Asch, T.W.J., 1983. Water erosion on slopes in some land units in a Mediterranean area. Catena Suppl. 4, 129–140.
Van Dijk, A.I.J.M., Bruijnzeel, L.A., Eisma, E.H., 2003. A methodology to study rain splash and wash processes under natural rainfall. Hydrol. Process. 17, 153–167. https://doi.org/10.1002/hyp.1154
Vermang, J., Demeyer, V., Cornelis, W.M., Gabriels, D., 2009. Aggregate Stability and Erosion Response to Antecedent Water Content of a Loess Soil. Soil Sci. Soc. Am. J. 73, 718. https://doi.org/10.2136/sssaj2007.0134
Vigiak, O., Okoba, B.O., Sterk, G., Groenenberg, S., 2005. Modelling catchment-scale erosion patterns in the East African Highlands. Earth Surf. Process. Landforms. https://doi.org/10.1002/esp.1174
Vigiak, O., Sterk, G., Romanowicz, R.J., Beven, K.J., 2006. A semi-empirical model to assess uncertainty of spatial patterns of erosion. Catena. https://doi.org/10.1016/j.catena.2006.01.004
Wang, G., Wu, B., Zhang, L., Jiang, H., Xu, Z., 2014. Role of soil erodibility in affecting available nitrogen and phosphorus losses under simulated rainfall. J. Hydrol. https://doi.org/10.1016/j.jhydrol.2014.04.028
Wischmeier, W., 1976. Use and misuse of the universal soil loss equation. J. soil water Conserv.
Wischmeier, W., Smith, D., 1978. Predicting rainfall erosion losses: a guide to conservation planning, U.S. Department of Agriculture Handbook No. 537. https://doi.org/10.1029/TR039i002p00285
Wischmeier, W H, Smith, D., 1958. Rainfall energy and its relationship to soil loss. Eos, Trans. Am. Geophys. Union.
Wischmeier, Walter H., Smith, D.D., 1958. Rainfall energy and its relationship to soil loss. Eos, Trans. Am. Geophys. Union 39, 285–291. https://doi.org/10.1029/TR039i002p00285
Wu, B., Wang, Z., Zhang, Q., Shen, N., Liu, J., 2019. Evaluating and modelling splash detachment capacity based on laboratory experiments. Catena 176. https://doi.org/10.1016/j.catena.2019.01.009
Wu, J., Zhao, L., Wu, F., Li, Z., 2016. The role of surface microreliefs in influencing splash erosion: A laboratory study. Soil Water Res. 11. https://doi.org/10.17221/280/2014-SWR
Xiao, H., Liu, G., Abd-Elbasit, M.A.M., Zhang, X.C., Liu, P.L., Zheng, F.L., Zhang, J.Q., Hu, F.N., 2017. Effects of slaking and mechanical breakdown on disaggregation and splash erosion. Eur. J. Soil Sci. 68. https://doi.org/10.1111/ejss.12482
Xiao, H., Liu, G., Zhang, Q., Fenli, Z., Zhang, X., Liu, P., Zhang, J., Hu, F., Elbasit, M.A.M.A.,

2018. Quantifying contributions of slaking and mechanical breakdown of soil aggregates to splash erosion for different soils from the Loess plateau of China. Soil Tillage Res. 178, 150–158. https://doi.org/10.1016/j.still.2017.12.026
Yin, S., Xie, Y., Liu, B., Nearing, M.A., 2015. Rainfall erosivity estimation based on rainfall data collected over a range of temporal resolutions. Hydrol. Earth Syst. Sci. 19. https://doi.org/10.5194/hess-19-4113-2015
Zumr, D., Mützenberg, D.V., Neumann, M., Jeřábek, J., Laburda, T., Kavka, P., Johannsen, L.L., Zambon, N., Klik, A., Strauss, P., Dostál, T., 2019. Experimental Setup for Splash Erosion Monitoring—Study of Silty Loam Splash Characteristics. Sustainability 12, 157. https://doi.org/10.3390/su12010157

List of publications

The research performed for this thesis resulted in the publication of the two research articles in peer-reviewed journals as a first author. These articles were the subject of the thesis. In addition, a number of co-authored articles were published in collaboration with colleagues and conference contributions were presented as oral presentations and posters at international conferences.

First author articles:

- Nives Zambon, Lisbeth Lolk Johannsen, Peter Strauss, Tomas Dostal, David Zumr, Martin Neumann, Thomas A. Cochrane and Andreas Klik (2020): Rainfall Parameters Affecting Splash Erosion under Natural Rainfall Conditions, Applied Sciences, 10, 4103, DOI: 10.3390/app10124103

- Nives Zambon, Lisbeth Lolk Johannsen, Peter Strauss, Tomas Dostal, David Zumr, Thomas A. Cochrane and Andreas Klik (2020): Splash erosion affected by initial soil moisture and surface conditions under simulated rainfall, Catena, 196, 104827, DOI: 10.1016/j.catena.2020.104827

Co-authored articles:

1. Lisbeth Lolk Johannsen, **Nives Zambon**, Peter Strauss, Tomas Dostal, Martin Neumann, David Zumr, Thomas A. Cochrane, Günter Blöschl and Andreas Klik (2020): Comparison of three types of laser optical disdrometers under natural rainfall conditions, Hydrological Sciences Journal, 65:4, 524-535, DOI: 10.1080/02626667.2019.1709641.

2. Lisbeth Lolk Johannsen, **Nives Zambon**, Peter Strauss, Tomas Dostal, Martin Neumann, David Zumr, Thomas A. Cochrane and Andreas Klik (2020): Impact of

Disdrometer Types on Rainfall Erosivity Estimations, Water, 12:4, 963, DOI: 10.3390/w12040963.

3. David Zumr, Danilo Vítor Mützenberg, Martin Neumann, Jakub Jeřábek, Tomáš Laburda, Petr Kavka, Lisbeth Lolk Johannsen, **Nives Zambon**, Andreas Klik, Peter Strauss and Tomáš Dostál (2020): Experimental Setup for Splash Erosion Monitoring – Study of Silty Loam Splash Characteristics, Sustainability, 12:1, 157, DOI:10.3390/su12010157.

4. Lorenz Loos, **Nives Zambon** and Andreas Klik (2020): Einfluss von Regenmustern auf Splash-Erosion von sandigem Lehm, submitted to Die Bodenkultur-Journal of Land Management, Food and Environment.
5. Martin Neumann, David Zumr, Petr Kavka, Tomáš Laburda, Lisbeth Lolk Johannsen, **Nives Zambon**, Tomáš Dostál, Peter Strauss and Andreas Klik (2019): Characterization of an artificially generated rainfall used for a soil erosion research (In Czech), Water Management Technical and Economical Information Journal, 61:6, 10-17, ISSN 0322-8916.

Conference contributions:

1. David Zumr, Martin Neumann, Tomáš Laburda, Petr Kavka, Josef Krása, Martina Sobotková, Tomáš Dostál, Lisbeth L. Johannsen, **Nives Balenovic**, Andreas Klik, Peter Strauss, Ondřej Fišer and Zuzana Chládová: Measuring the kinetic energy of rainfall and the soil particles splash. In: TERRAENVISION Abstracts Vol. 1, TNV2018-LD2-343, TERRAenVISION, Barcelona, 29 January-2 February, 2018 [Oral Presentation].

2. **Nives Balenovic**, Lisbeth Lolk Johannsen, Peter Strauss, Tomas Dostal, Jan Devaty, Tomas Laburda, Josef Krasa, David Zumr, Thomas Cochrane, Mike Arnaiz, and Andreas Klik: Splash erosion of three soils under natural rainfall conditions in Central Europe and New Zealand. In: Geophysical Research Abstracts Vol. 20, EGU2018-1845, EGU General Assembly, Vienna, Austria, 8-13 April, 2018 [PICO].

3. Lisbeth Lolk Johannsen, **Nives Balenovic**, Peter Strauss, Tomas Dostal, Martin Neumann, Jakub Jerábek, David Zumr, Mike Arnaiz, Thomas A. Cochrane & Andreas Klik: Investigation of rainfall kinetic energy in Central Europe and New Zealand. In: Geophysical Research Abstracts Vol. 20, EGU2018-4353, EGU General Assembly, Vienna, Austria, 8-13 April, 2018 [Oral presentation].

4. Martin Neumann, David Zumr, Tomáš Laburda, Petr Kavka, Lisbeth L. Johannsen, **Nives Balenovic**, Zuzana Chládová, Ondřej Fišer, Peter Strauss, Tomáš Dostál, and Andreas Klik: Comparison of the rainfall kinetic energy measured by different distrometers. In: Geophysical Research Abstracts Vol. 20, EGU2018-13821, EGU General Assembly, Vienna, Austria, 8-13 April, 2018 [Poster].

5. Tomas Laburda, Josef Krasa, Michal Vrana, **Nives Balenovic**, Lisbeth Lolk Johannsen, Petr Kavka, David Zumr, Jan Devaty, Martin Neumann, Peter Strauss, Andreas Klik, and Tomas Dostal: Photogrammetric measurement of soil surface properties after splash erosion under natural and artificial rainfall. In: Geophysical Research Abstracts Vol. 20, EGU2018-17899, EGU General Assembly, Vienna, Austria, 8-13 April, 2018 [Poster].

6. **Nives Balenovic**, Lisbeth Lolk Johannsen Peter Strauss, Tomas Dostal, Martin Neumann, David Zumr, Jan Devátý, Thomas A. Cochrane, and Andreas Klik: Splash erosion induced by rainfall kinetic energy in Central Europe and New Zealand. Global Soil Erosion Research Forum (GSERF), Yangling, China, 12-16 September, 2018 [Poster].

7. **Nives Balenovic**, Lisbeth Lolk Johannsen, Peter Strauss, Tomas Dostal, David Zumr, Thomas Cochrane, and Andreas Klik: Splash erosion under simulated rainfall affected by different initial soil water content and surface conditions. In: Geophysical Research Abstracts Vol. 21, EGU2019-4137, EGU General Assembly, Vienna, Austria, 7-12 April, 2019 [Poster].

8. Lisbeth Lolk Johannsen, **Nives Balenovic**, Peter Strauss, Tomas Dostal, Martin Neumann, David Zumr, Thomas Cochrane, and Andreas Klik: Comparison of three types of disdrometers under natural rainfall conditions. In: Geophysical Research Abstracts Vol. 21, EGU2019-4157, EGU General Assembly, Vienna, Austria, 7-12 April, 2019 [PICO]

9. Tomas Laburda, Petr Kavka, David Zumr, Josef Krasa, Adam Tejkl, **Nives Balenovic**, Lisbeth Lolk Johannsen, Peter Strauss, Andreas Klik, Jan Devaty, and Michal Vrana: Close-range photogrammetric measurements of the splash and rill soil erosion. In: Geophysical Research Abstracts Vol. 21, EGU2019-15246, EGU General Assembly, Vienna, Austria, 7-12 April, 2019 [Poster].

10. Martin Neumann, David Zumr, Petr Kavka, Tomáš Dostál, Tomáš Laburda, Michal Vrana, **Nives Zambon**, Lisbeth Lolk Johannsen, Peter Strauss and Andreas Klik (2019): Raindrop influence on the soil surface. In: TERRAENVISION Abstracts Vol. 2, TNV2019-LD-2108, TERRAenVISION, Barcelona, 2-7 September, 2019 [Poster].

11. **Nives Zambon**, Lisbeth Lolk Johannsen, Peter Strauss, Tomáš Dostál, David Zumr, Thomas A. Cochrane, and Andreas Klik: Splash erosion experiments with silt loam and loamy snd soil under simulated rainfall produced by two types of rainfall simulators. In: Geophysical Research Abstracts Vol. 22, EGU2020-5103, EGU General Assembly, Online, 4-8 May, 2020 [Online Display].

12. Lisbeth Lolk Johannsen, **Nives Zambon**, Peter Strauss, Tomas Dostal, Martin Neumann, David Zumr, Thomas A. Cochrane, and Andreas Klik: Influence of disdrometer type on rainfall kinetic energy measurement. In: Geophysical Research Abstracts Vol. 22, EGU2020-5317, EGU General Assembly, Online, 4-8 May, 2020 [Online Display].

Appendix 1 – published article on Study 1

Nives Zambon, Lisbeth Lolk Johannsen, Peter Strauss, Tomas Dostal, David Zumr, Martin Neumann, Thomas A. Cochrane and Andreas Klik (2020): Rainfall Parameters Affecting Splash Erosion under Natural Rainfall Conditions, Applied Sciences, 10, 4103, DOI: 10.3390/app10124103.

Author contributions:

NZ set up the experiment, acquired the data, performed the data analysis, evaluated the results, developed the main ideas and wrote the manuscript.
LLJ helped with data acquisition and data analysis, and reviewed the manuscript.
PS added to the main ideas and reviewed the manuscript.
TD added to the main ideas and reviewed the manuscript.
DZ added to the main ideas and reviewed the manuscript.
MN helped with data acquisition and data analysis
TAC added to the main ideas and reviewed the manuscript.
AK gave advice on the data analysis, added to the main ideas and reviewed the manuscript

applied sciences

MDPI

Article

Rainfall Parameters Affecting Splash Erosion under Natural Conditions

Nives Zambon [1,*], Lisbeth Lolk Johannsen [1], Peter Strauss [2], Tomas Dostal [3], David Zumr [3], Martin Neumann [3], Thomas A. Cochrane [4] and Andreas Klik [1]

1 Institute for Soil Physics and Rural Water Management, University of Natural Resources and Life Sciences, 1190 Vienna, Austria; lisbeth.johannsen@boku.ac.at (L.L.J.); andreas.klik@boku.ac.at (A.K.)
2 Institute for Land and Water Management Research, 3252 Petzenkirchen, Austria; peter.strauss@baw.at
3 Faculty of Civil Engineering, Czech Technical University in Prague, 166 29 Prague 6, Czech Republic; dostal@fsv.cvut.cz (T.D.); david.zumr@fsv.cvut.cz (D.Z.); martin.neumann@fsv.cvut.cz (M.N.)
4 Department of Civil and Natural Resources Engineering, University of Canterbury, Christchurch 8140, New Zealand; tom.cochrane@canterbury.ac.nz
* Correspondence: nives.zambon@boku.ac.at

Received: 28 April 2020; Accepted: 10 June 2020; Published: 15 June 2020

Featured Application: Practical and cost-effective splash cup method for splash erosion measurements in field and laboratory conditions.

Abstract: The interaction between rainfall erosivity parameters and splash erosion is crucial for describing the soil erosion process; however, it is rarely investigated under natural rainfall conditions. In this study, we conducted splash erosion experiments under natural rainfall on three sites in Central Europe. The main goal was to obtain the relationship between splash erosion of the bare soil in seedbed condition and commonly used rainfall erosivity parameters (kinetic energy, intensity, and rainfall erosivity (EI_{30})). All sites were equipped with a rain gauge and an optical laser disdrometer where the splash erosion was measured, with modified Morgan splash cups. In order to investigate which parameter best describes the splash erosion process for all sites, a regression analysis was performed. In total, 80 splash erosion events were evaluated. Splash erosion can be described as a linear function of total kinetic energy and a non-linear function of $EI_{30.}$ However, the use of the total kinetic energy led to underestimation of the splash erosion rates for highly intensive rainfalls. Therefore, better results were obtained when using average rainfall intensity as the splash erosion predictor or the kinetic energy divided by the rainfall duration. Minor differences between the replicates during splash erosion measurements indicate that the modified Morgan splash cup provides a good tool for soil erosion assessment.

Keywords: splash erosion; splash cup; kinetic energy; rainfall intensity; rainfall erosivity

1. Introduction

Soil erosion by water is the most common soil degradation process globally, and in arable cropland it is consistently higher than soil formation [1]. Detailed knowledge of the processes that control erosion on arable croplands contributes to better application of soil management techniques that minimize and control soil erosion risk [2]. Splash erosion starts with the raindrop impact on the soil surface, which represents the first stage in soil erosion by water [3]. The detached soil particles transported by raindrop impact are deposited on the near-distance soil surface or are transported further by surface runoff if the infiltration capacity of the soil is reached [4]. The major splash erosion driver is the erosivity of rainfall, which can be expressed by parameters like rainfall intensity [5–7], kinetic energy (*KE*) [8–10], rainfall erosivity (EI_{30}) [11], or raindrop momentum [12]. Apart from the rainfall properties, the detachment of soil particles also depends on soil physico-chemical characteristics, such as infiltration capacity [13,14], initial water content [15,16], the ability to form stable aggregates and crusts [17,18], organic matter content [19], texture, cohesion, porosity, capacity of ionic interchange, and clay content [20].

Splash erosion measurements on a small scale are usually done through splash cups or splash containers [21–26]. Most of the splash erosion studies have been conducted in the laboratories using rainfall simulators, where by controlling the raindrop size and fall height, the *KE* of raindrops is adjusted [12,27–30]. However, rainfall simulators often do not reproduce the same rainfall drop size and velocity distribution characteristics as in nature [31]. As the velocity of raindrops is controlled by the height at which the nozzles are located, due to space or design limitations, sometimes raindrops cannot reach the terminal velocity of natural raindrops [32]. By applying different pressure at the nozzle, the raindrop velocity can be adjusted regarding to the raindrop size; however, large drops are unlikely to reach their terminal velocity, and consequently the *KE*, of natural rainfall [33]. Nevertheless, laboratory experiments improve the consistency of the results by minimizing the effects of the various uncontrolled factors that are present in the field [34], and also allow experiments to be repeated.

Splash erosion experiments under natural rainfall investigate the relationship between rainfall erosivity and splash detachment [3]. Morgan [23] observed the splash erosion under natural rainfall for 100 consecutive days, comparing four different soil textures. The *KE* of rainfall was calculated from the 10 min rainfall intensity values, using the formula from Hudson [35]. Splash erosion of the bare soil was significantly correlated with *KE*. Govers [36] collected data at 21 sites in Belgium using circular splash cups. He found that the product of rainfall *KE* and drop circumference are better at expressing the rainfall erosivity compared to *KE* and intensity, or when the 0.75 power of rainfall intensity is used. However, a detailed drop size distribution (DSD) was not available at the time, and the fall velocities of raindrops were based on data by Laws [37]. Splash erosion under natural conditions is primarily affected by rainfall DSD. The ability of raindrop impact to cause splash erosion (rainfall erosivity) is mainly dependent on drop size and drop fall velocity [12]. Direct measurements of raindrop size and velocity provide precise information about the erosivity of rainstorms—namely, *KE*. When the raindrop size and velocity is not directly measured, the rainfall *KE* is estimated from the experimentally based equations between rainfall intensity and *KE* from other studies. Theoretically obtained rainfall *KE* could underestimate or overestimate the real *KE* [38–40]. Furthermore, DSD obtained from other studies can significantly vary depending on rain type and geographical location [41]. With the development of optical laser techniques (disdrometer), the continuous and direct measurement of raindrop size and velocity has become easily available to assess rainfall *KE*.

A recent study with splash erosion measurements under natural rainfall, using the splash cup technique and rainfall monitoring with a disdrometer, was performed by Fernández-Raga et al. [42]. They used a funnel and cup installed directly in the field for splash erosion measurements, and found a good correlation between splash erosion and rainfall *KE*; however, their findings were based on only nine sampling periods. Angulo-Martínez et al. [43] conducted a study in Spain where the splash erosion of three soil types was measured with Morgan splash cups [23]. A significant relationship was found between splash erosion and the rainfall erosivity index EI_{30}, and high variabilities between the replicates indicated the heterogeneity in splash erosion spatial distribution. According to the results reported from these studies, there are still many uncertainties concerning the changes in surface condition and spatial distribution of splash erosion.

The studies investigating splash erosion under natural rainfall are limited to local conditions. Consequently, monitoring of the rainfall characteristics on higher temporal and spatial resolution is crucial for describing the dominant rainfall parameters on splash erosion related to a specific location. Apart from the field studies of Fernández-Raga et al. [42] and Angulo-Martínez et al. [43], there are very few experiments that include both the monitoring of splash erosion and rainfall characteristics, including DSD, in the same location. Considering the local influences and lack of the data sets on rainfall DSD, it is difficult to define the role of splash in soil erosion process and predict it relative to local conditions. Furthermore, Bauer [44] pointed out that many rain events in Central Europe do not generate overland flow, but splash erosion is initiated already from the first drop impact, which emphasizes the importance of this soil degradation process. Lack of knowledge about the effect of erosive rainfall events on splash detachment in the agriculturally active Central European area was the main motivation for the present study.

This study presents the results from the splash erosion measurements collected during three consecutive summer seasons at three sites in Central Europe. Together with splash erosion, rainfall parameters, including rainfall intensity and *KE*, were monitored at the sites, with the aim of analyzing performance of the most common rainfall erosivity parameters (*KE*, intensity, and rainfall erosivity (EI_{30})), in order to predict splash erosion under natural rainfall.

2. Materials and Methods

2.1. Study Sites

The monitoring of rainfall parameters and splash erosion measurements was located at two sites in Austria and one in the Czech Republic (Figure 1). The Austrian sites, Petzenkirchen (48°9′17″ N, 15°14′46″ E) and Mistelbach (48°34′59″ N, 16°35′15″ E), are situated in the region of Lower Austria, where most of the country agricultural activity takes place. The Czech site was located in Prague (50°6′17″ N, 14°23′15″ E). The long-term, average annual precipitation for the three sites is 902, 537 and 459 mm for Petzenkirchen, Mistelbach, and Prague, respectively [45–47]. According to data measured by Klik and Truman [48] in Lower Austria, most of the erosive storms occurred during the summer period. Panagos et al. [49] also confirmed the highest rainfall erosivity during summer in the Central European region. Therefore, the selected monitoring period was during late spring and summer from 2017 to 2019.

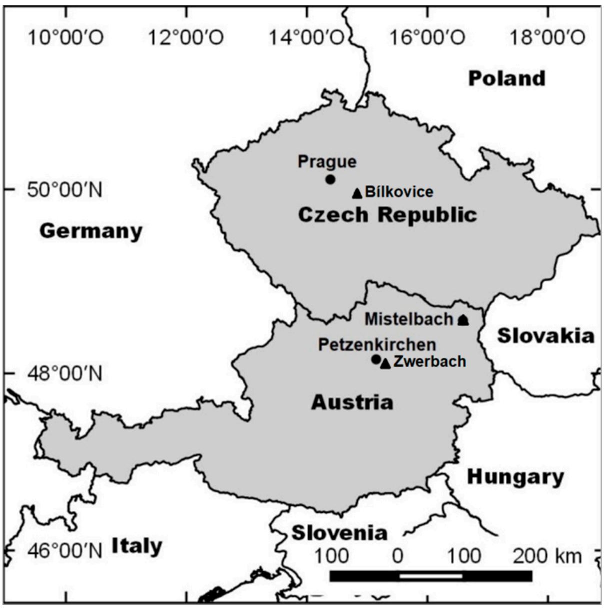

Figure 1. Location map of the study sites in Austria (Petzenkirchen and Mistelbach) and the Czech Republic (Prague), marked with solid dots, and locations of the soil sampling sites (Zwerbach, Mistelbach and Bílkovice), marked with solid triangles.

2.2. Investigated Soils

Soil samples were taken from two locations in Austria close to the experimental sites, Zwerbach (ZW) (48°8′22″ N, 15°14′46″ E) and Mistelbach (MI) (48°35′3″ N, 16°35′16″ E). In the Czech Republic, soil samples were taken within the Central Bohemian Region in Bílkovice (BK) (49°45′41.5″ N, 14°50′20.0″ E). The locations of three sites are marked in Figure 1. The samples were collected from agricultural land in the first 10 cm during April 2017, after seedbed preparation. Soil was dried and sieved through a 10 mm sieve and distributed to the three experimental sites. Particle size distribution was determined with a combined wet sieving and sedimentation method, as defined in the Austrian Norm for soil physical analysis [50,51]. Accordingly, soil textures were determined using the Austrian soil texture triangle [52]. Soil pH was obtained with electrometric pH meter. Total organic carbon was measured according to the Austrian Norm for the determination of soil organic carbon [53], and the aggregate stability of soils was determined with the modified Kemper and Rosenau method [54]. The physical and chemical properties of the soils obtained in the laboratory analysis are listed in Table 1.

Table 1. Soil physical and chemical properties.

Soil	Sand [%]	Silt [%]	Clay [%]	Soil Texture	AS [%]	pH	TOC [%]
Zwerbach	14.0	60.2	25.8	Silt loam	41.4	7.5	1.5
Mistelbach	11.2	70.4	18.4	Silt loam	18.3	8.2	1.6
Bílkovice	41.6	46.3	12.1	Loamy sand	63.3	6.9	1.7

Notes: AS = aggregate stability; TOC = total organic carbon.

2.3. Splash Erosion Measurements

Splash erosion was measured with the splash cup technique proposed by Morgan [23]. The splash cup was produced from a light polypropylene material, with an inner diameter of 10.3 cm and a standing height of 6 cm. On the bottom of the splash cup, holes were drilled to ensure water drainage through the soil; however, two fine meshes (500 and 1000 µm) were placed on the bottom to prevent soil loss trough the holes (Figure 2a). Air-dried and sieved soil (<10 mm) was filled in three layers up to 1 cm below the splash cup edge, to prevent the overflow of soil on the surface during the high intensity rainfall. While levelling it continuously using a long needle, each soil layer was slightly compacted to reach similar conditions (bulk density) as in the field. Aggregates at the top layer surface were randomly distributed to achieve heterogeneous arrangement. For each soil, more or less the same mass was filled into the splash cups, to keep soil density (in seedbed condition) constant within the replicates (Figure 2b). Major differences in the soil structure of the samples prepared for experiment and the original soil in seedbed condition are the aggregate size and their arrangement, due to sieving and sample preparation. However, soil bulk density and porosity were within the same range of the soil in the seedbed condition in the field. Splash cups filled with soils were placed in the middle of a splash collector, with standing height of 30 cm and diameter of 47 cm (Figure 2c). The splash collector had an outlet, ensuring the drainage of rainfall water with splashed soil into collectors placed underneath (Figure 2d). The water collector underneath was completely closed, ensuring that only splashed soil was trapped into the collector. Splash cups were installed in the field in such a way that the soil surface was 1 m above ground level, which corresponds to the same height as the disdrometer (described in next chapter). A detailed splash cup and splash collector design can be found in Zumr et al. [55].

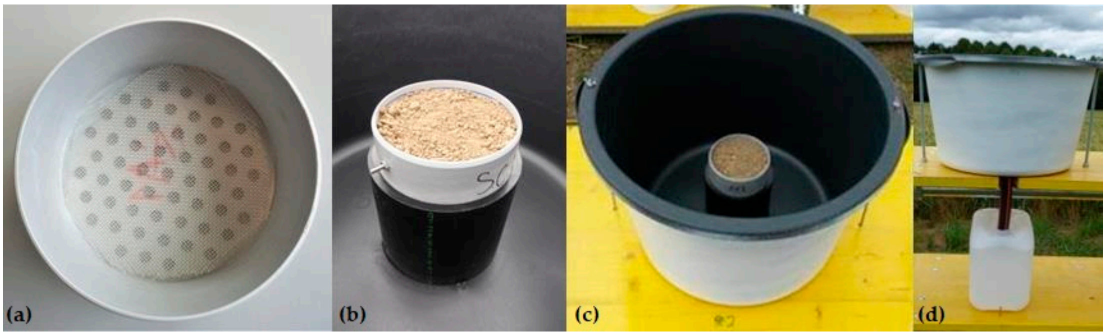

Figure 2. Experimental set-up for splash erosion measurements: (**a**) splash cup with mesh at the bottom; (**b**) splash cup filled with soil; (**c**) splash collector; and (**d**) connection with drainage pipe to water and soil collector.

Splash cups were exchanged, and splashed sediment was collected after each rainfall event, with accumulated precipitation of 5 mm. The events with precipitation lower than 5 mm were considered as erosive if the accumulated rainfall of 2.5 mm was reached after 15 min. This threshold was adopted based on preliminary data analysis and recommended by some European authors [44,56]. The intensity threshold of 12.7 mm (~0.5 in), reported in the Revised Universal Soil Erosion Equation (RUSLE) [11], is too high for European conditions. A rainfall event was defined as the rain period separated between proceeding and succeeding rainfall by 6 h or more. The splashed soil particles on the rim of the splash collector were completely washed off and drained into the water collector with rainfall and sediment. In the laboratory, splashed particles were filtered from water and oven-dried at 40 °C. The average mass of the splashed soil per each rainfall event was calculated from the three or four replicates, depending on the study site.

2.4. Rainfall Parameters

At all sites, rainfall data were collected with a rain gauge (tipping bucket or balance principle). To obtain the *KE* of rainfall, each site was equipped with an optical laser disdrometer, which measures raindrop size and velocity distribution in one-minute intervals. The PWS100 Present Weather Sensors from Campbell Scientific (PWS100) were installed in Mistelbach and Petzenkirchen, and the Laser Precipitation Monitor from Thies Clima (Thies) in Prague. The devices differ in measurement principle, sampling area, and drop size and velocity distribution classes. The PWS100 sampling area was 40 cm^2, in which the drops are categorized in 34 size and 34 velocity classes. The Thies had a sampling area of 44.1 cm^2, with 22 drop sizes and 20 velocity classes. Both disdrometer types differentiate raindrops from hail, ice pellets, and graupel. A detailed description of the disdrometer and rainfall monitoring set-ups at the three sites is given in Johannsen et al. [57].

The rainfall kinetic energy per area, *KE* (J m^{-2}), was calculated for the diameter class *i* and velocity class *j* that are provided by the disdrometer, as follows:

$$KE = \sum N_{i,j} \cdot \frac{1}{12 \cdot A} \cdot \pi \cdot 10^{-6} \cdot \rho \cdot D_i^3 \cdot v_j^2, \quad (1)$$

where $N_{i,j}$ is number of detected raindrops of a certain size class *i* and velocity class *j*; *A* is the sampling area of the disdrometer (m^2); ρ is density of water (g cm^{-3}); D_i is mean drop diameter (mm) of size class *i*; and v_j is mean fall velocity (m s^{-1}) of velocity class *j*. The mass of the raindrop is calculated assuming a spherical drop shape. Total *KE* is the sum of kinetic energies for each drop size and velocity, multiplied by the number of drops in the corresponding classes. Cumulative *KE* of a single rainfall event, KE_{sum} (J m^{-2}), was defined as

$$KE_{sum} = \sum_{i=1}^{n} KE_i, \quad (2)$$

where KE_i represents the i-th minute of the rainfall event. The KE per rainfall duration was calculated as

$$KE_h = \frac{KE_{sum}}{T} \tag{3}$$

where the KE_h is kinetic energy per hour (J m^{-2} h^{-1}) and T is total duration of a rainfall event (h), measured from the beginning of rainfall.

The results obtained in the recent study by Johannsen et al. [57] showed that the differences in rainfall measurements from different disdrometer types, including PWS100 and Thies, influenced the interpretation of rainfall KE. That study concluded that the Thies disdrometer measured higher numbers of smaller drops; therefore, it underestimated the rainfall KE. To ensure comparable results obtained from the two disdrometer types used in this study, we applied the suggested correction factor by Johannsen et al. [57] for the Thies disdrometer. The correction is the ratio of the slope factors obtained from the KE and the intensity relationships for the PWS100 and Thies disdrometers. Accordingly, the final KE for the Thies disdrometer is calculated as in Equation (2) and multiplied with a correction factor of 1.36.

For the periods when the disdrometer data were not available due to disruptions or errors, the KE was calculated based on KE and intensity relationships developed for the three sites, according to the data investigated in Johannsen et al. [40]. The KE is presented as the function of the intensity, which was available from the rain gauge.

The average rainfall intensity I_{av} (mm h^{-1}) of single rainfall event considered the amount of rainfall over a time period, and is expressed as

$$I_{av} = \frac{P}{T}, \tag{4}$$

where P is the cumulative rainfall precipitation (mm) over rainfall duration T (h).

The rainfall erosivity EI_{30} (MJ mm ha^{-1} h^{-1}) [11] for soil erosion estimation was also considered in analysis as an important rainfall parameter affecting splash erosion. The erosivity of a single rainfall event has been defined by the following expression:

$$EI_{30} = KE_{sum} \cdot 100 \cdot I_{30}, \tag{5}$$

where I_{30} is the maximum 30 min rainfall intensity of one rainfall event (mm h^{-1}).

Rainfall erosivity density expresses the mean rainfall erosivity per rainfall unit [49]. The mean monthly erosivity density MED (MJ ha^{-1} h^{-1}) is expressed as:

$$MED = \frac{1}{n} \cdot \sum_{i=0}^{n} \left(\frac{EI_{30}}{P} \right)_i, \tag{6}$$

where n is the number of rainfall events (i) recorded during one month. The total splash erosion rate per one measurement period was calculated as the total amount of the splashed material from the test area per unit area, which is calculated as follows:

$$S = \frac{m_s}{A_s}, \tag{7}$$

where S is average splash erosion rate (g m^{-2}), m_s is the mass of splashed material, and A_s is the area of the splash cup (0.0084 m^2). Splash erosion S_h (g m^{-2} h^{-1}) per rainfall event duration (T) was calculated as

$$S_h = \frac{S}{T}. \tag{8}$$

2.5. Data Analysis

The coefficient of determination (R^2) and the root mean square error (RMSE) were used to validate the efficiency of the influencing rainfall erosivity parameters as the predictors of splash erosion. Pearson correlation analysis was used to estimate the relationship between the splash erosion rates and the sand, silt, or clay content of the three soils. The Kruskal–Wallis [58] test by ranks was used to determinate the differences in splash rates between the three soils.

3. Results

3.1. Rainfall Data

During the splash erosion measurements, the rainiest months were May 2019 in Petzenkirchen, July 2018 in Mistelbach, and June 2018 in Prague (Figure 3). The Mistelbach site had the highest cumulative EI_{30} of 4168 MJ mm ha^{-1} h^{-1}; however, the highest monthly EI_{30} of 1352 MJ mm ha^{-1} h^{-1} was recorded at the Prague site during June 2018.

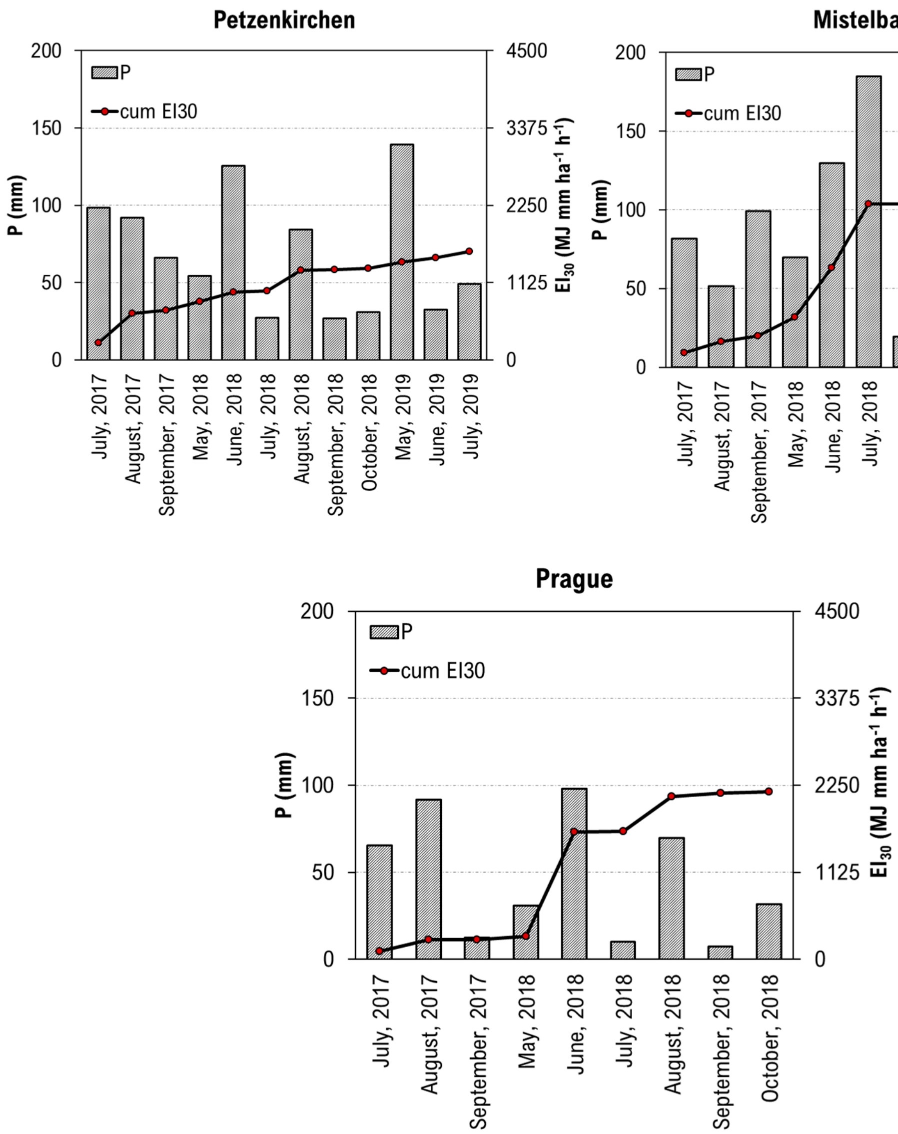

Figure 3. Accumulated monthly rainfall precipitation P (mm) and cumulative rainfall erosivity EI_{30} (MJ mm ha^{-2} h^{-1}) distribution for investigated sites during the measuring period.

During the measuring period, the Mistelbach site had highest average monthly rainfall, KE, EI_{30}, and erosivity density, as well as the largest mean drop diameter (Table 2). Petzenkirchen was the site with the noticeably lowest average monthly EI_{30} and erosivity density. The Prague site had lowest monthly precipitation among the three sites. However, higher average monthly EI_{30} and erosivity density compared to the Petzenkirchen site were caused by intensive storms recorded in June and August 2018 (Figure 3). It should be noted that calculated mean drop diameter could be affected by differences in measured drop size distributions between the disdrometer types used in the study [40].

Table 2. Average monthly rainfall parameters measured at the three study sites.

	Study Sites		
	Petzenkirchen	**Mistelbach**	**Prague**
Number of months measured	12	11	9
Precipitation (mm)	68.7	94.0	46.5
Kinetic energy (J m^{-2})	1026.0	1876.9	661.7
Rainfall erosivity (MJ mm ha^{-1} h^{-1})	131.6	378.9	241.0
Erosivity density (MJ ha^{-1} h^{-1})	1.7	3.8	3.6
Raindrop diameter (mm) *	0.9	1.2	0.6

* According to Johannsen et al. [40].

3.2. Splash Erosion as the Function of Total Kinetic Energy

During the measuring period, 99 splash erosion records of the three soils were obtained from the investigated sites. After the data evaluation, a total of 80 records that had complete rainfall and splash erosion measurements were selected for further data analysis.

For measured KE_{sum}, the mean splash erosion rates ranged between 4 and 2503 g m^{-2} for ZW, 5 to 1972 g m^{-2} for MI, and 12 to 2508 g m^{-2} for BK soils (Figure 4). The variabilities between the splash erosion replicates were larger for the measurements of KE_{sum} above 780 J m^{-2}.

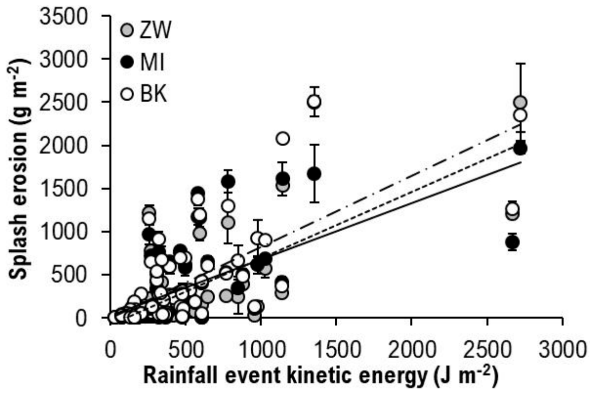

Figure 4. Mean splash erosion for Zwerbach (ZW), Mistelbach (MI), and Bílkovice (BK) soil versus rainfall event cumulative kinetic energy. The dashed–dotted line represents the fitted linear regression line for BK soil, while the dashed line represents ZW, and the solid line represents MI.

Significant ($p < 0.05$) linear regression was obtained for the three soils, as the splash erosion for each soil was positively correlated to KE_{sum} with R^2 of 0.52, 0.50, and 0.45 for the BK, ZW, and MI soils, respectively (Table 3). According to the linear model, BK soil yielded the highest splash erosion, followed by ZW and MI soils. RMSE indicated a high deviation of measured values and values predicted by linear relationships.

Table 3. Main outputs of the regression analysis between splash erosion S (g m^{-2}) for Zwerbach (ZW), Mistelbach (MI), and Bílkovice (BK) soils and rainfall event cumulative kinetic energy KE_{sum} (J m^{-2}). R^2 is the determination coefficient of the regression model, and RMSE (g m^{-2}) indicates the root mean squared error.

Parameter	Soil	Equation	R^2	RMSE
KE_{sum}	ZW	$S = 0.767 \cdot KE_{sum} - 75.968$	0.50	349.25
	MI	$S = 0.653 \cdot KE_{sum} + 22.841$	0.45	326.10
	BK	$S = 0.825 \cdot KE_{sum} - 1.299$	0.52	357.73

3.3. Impact of Rainfall Intensity on Splash Erosion

The points deviating above the fitted linear regression line for the BK soil were mostly measured in Mistelbach (Figure 4). Considering the site-specific differences (Table 2), it was necessary to distinguish the erosive events with higher rainfall intensities from the ones with low intensities having the same KE_{sum}. The example in Figure 5 shows two rainfall events with similar cumulative precipitation and KE_{sum} measured in Mistelbach (Event 1) and Prague (Event 2) with the corresponding splash erosion. The rainfall Event 1 was recorded on June 6, 2018, with a duration of 3.5 h. The rainfall Event 2 was recorded on August 8, 2018, with a duration of 43 min. Cumulative rainfall reached 19 and 20 mm for Event 1 and Event 2, respectively. Corresponding KE_{sum} values were 467 J m^{-2} for Event 1 and 446 J m^{-2} for Event 2. However, during Event 2, up to 86% higher splash erosion rates were measured. Therefore, to compare the effect of kinetic energies characterized by different rainfall intensities on splash erosion, the KE_{sum} was divided by rainfall duration (T) (defined in Equation (3)).

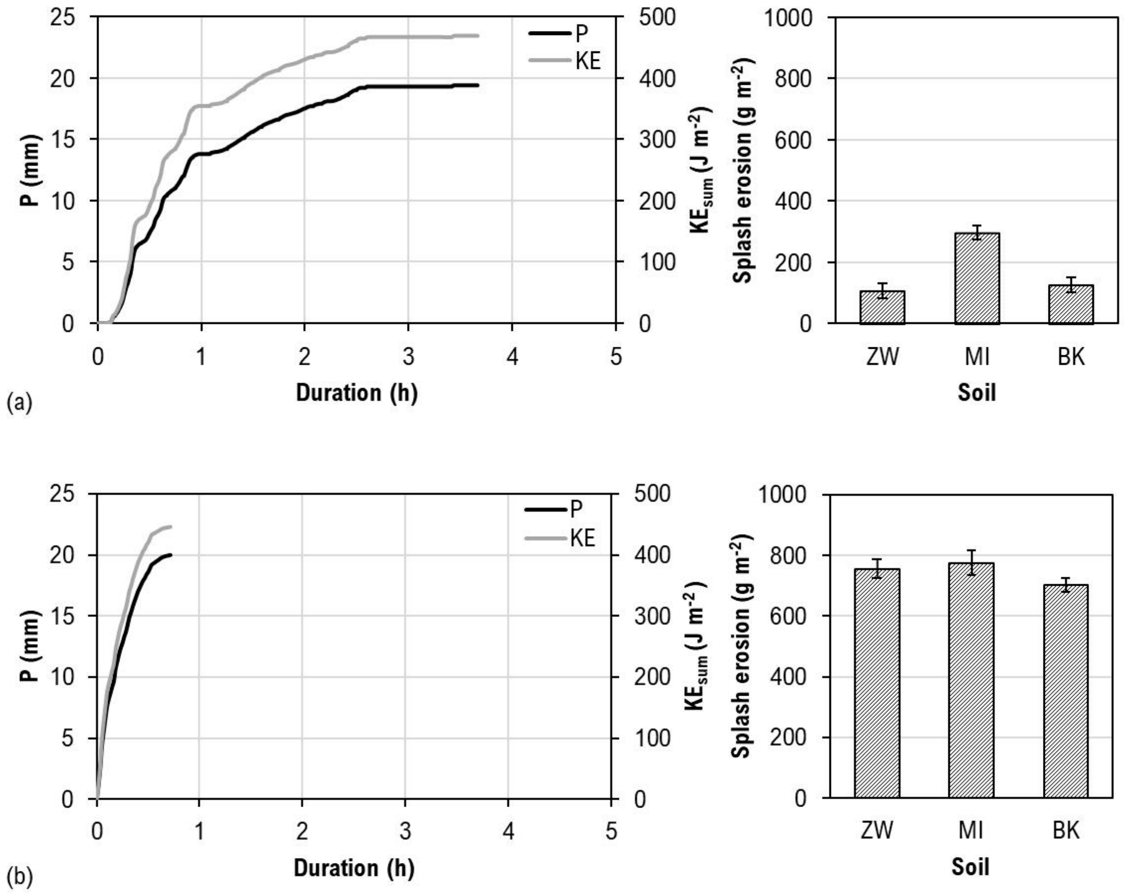

Figure 5. Cumulative rainfall P (mm) and kinetic energy KE_{sum} (J m^{-2}) with corresponding mean splash erosion for Zwerbach (ZW), Mistelbach (MI), and Bílkovice (BK) soil for (**a**) Event 1 and (**b**) Event 2.

3.4. Regression Analysis of Rainfall Erosivity Parameters with Splash Erosion

Previous results have indicated that the KE_{sum} could not represent the realistic ability of rainfall to produce splash erosion. Since rainfall intensity plays an important role in rainfall erosivity, together with I_{av} and EI_{30} the results of regression analysis with KE_h are presented in the following section. KE_h represents the average energy load per rainfall duration.

3.4.1. Splash Erosion and Kinetic Energy Per Rainfall Duration

The relationship between KE_h and splash erosion resulted in a non-linear (power) regression function, with an R^2 of 0.75 for MI soil and 0.76 for ZW and BK soil (Figure 6a, Table 4). The results indicated a less scattered distribution compared to results for KE_{sum} (Figure 4). However, several observations in Figure 6a present a difference of 97% between the lowest and the highest splash erosion rate for a similar range of KE_h (220–280 J m^{-2} h^{-1}). The splash erosion measurement with KE_h of 220 J m^{-2} h^{-1} (E_1 on Figure 6a) was the result of a rainfall event with short duration. Peak intensity of 42 mm h^{-1} was reached at the beginning of a rainfall event, with a short duration of 3 min. This might indicate that the peak intensity duration was too short to produce higher splash erosion rates. High splash erosion rates up to 1044 g m^{-2} h^{-1} were measured for the rainfall event with a KE_h of 223 J m^{-2} h^{-1} (E_2). Maximum intensity for this rainfall event reached 60 mm h^{-1}, where a high percentage of large drops (drop diameter > 3 mm) with high velocities (>6 m s^{-1}) was measured. The splash erosion rates for the event with KE_h of 280 J m^{-2} h^{-1} (Figure 6a, E_3) were remarkably low considering a high amount of the total rainfall of 44 mm.

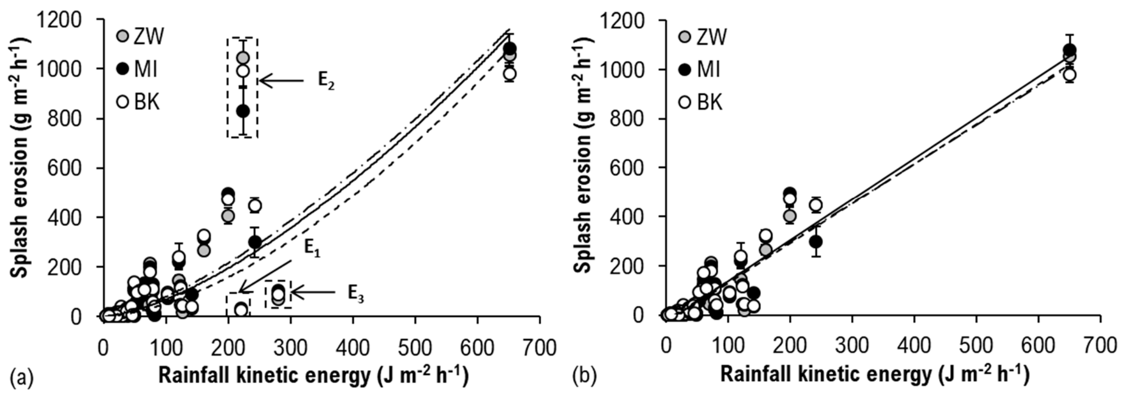

Figure 6. Mean splash erosion for Zwerbach (ZW), Mistelbach (MI) and Bílkovice (BK) soil versus kinetic energy per time unit, including (**a**) all observations (n = 80) and (**b**) without extreme observations (n = 77). The dashed line represents the regression function for ZW, as does the solid line for MI and the dashed–dotted line for BK soil. The points inside the dashed boxes indicate extreme observations (E_1, E_2, and E_3) per soil.

Table 4. Main outputs of the regression analysis between splash erosion S_h (g m^{-2} h^{-1}) for Zwerbach (ZW), Mistelbach (MI), and Bílkovice (BK) soil and rainfall kinetic energy per time unit KE_h (J m^{-2} h^{-1}). The R^2 is the determination coefficient of the regression model, and RMSE (g m^{-2} h^{-1}) indicates the root mean squared error. E_1, E_2, and E_3 denote extreme observations.

Parameter	Soil	Equation	R^2	RMSE
KE_h (including E_1, E_2, E_3)	ZW	$S_h = 0.028 \cdot KE_h^{1.629}$	0.76	112.21
	MI	$S_h = 0.069 \cdot KE_h^{1.498}$	0.75	91.30
	BK	$S_h = 0.113 \cdot KE_h^{1.426}$	0.76	106.27
KE_h (excluding E_1, E_2, E_3)	ZW	$S_h = 1.621 \cdot KE_h - 32.289$	0.91	43.04
	MI	$S_h = 1.668 \cdot KE_h - 27.828$	0.91	43.40
	BK	$S_h = 1.590 \cdot KE_h - 20.586$	0.90	43.10

Excluding these observations from the regression analysis, the resulting relationship between splash erosion and KE_h was linear, with R^2 values of 0.91 for ZW and MI soil, and 0.90 for BK soil (Figure 6b; Table 4). The difference of 62% between the RMSEs for linear and nonlinear models indicates better performance of the splash erosion–KE_h relationship without extreme observations. According to RMSE, correlation coefficients, and slope coefficients of regression equations, fewer minor differences between the soils were noted for the linear than for non-linear regression.

3.4.2. Splash Erosion and Mean Rainfall Intensity

Splash erosion plotted against the I_{av} (calculated according to Equation (4)), resulted in linear relationships for the three soils (Figure 7). Compared to previous results with KE_h, most of the data were grouped in the range of low intensities up to 10 mm h^{-1}, and the highest I_{av} corresponds to a KE_h of 650 J m^{-2} h^{-1}. The three extreme measurements from the previous example with KE_h ($E_{1–3}$) were more linearly distributed with increasing I_{av}; however, they still deviate from the regression lines (Figure 7a).

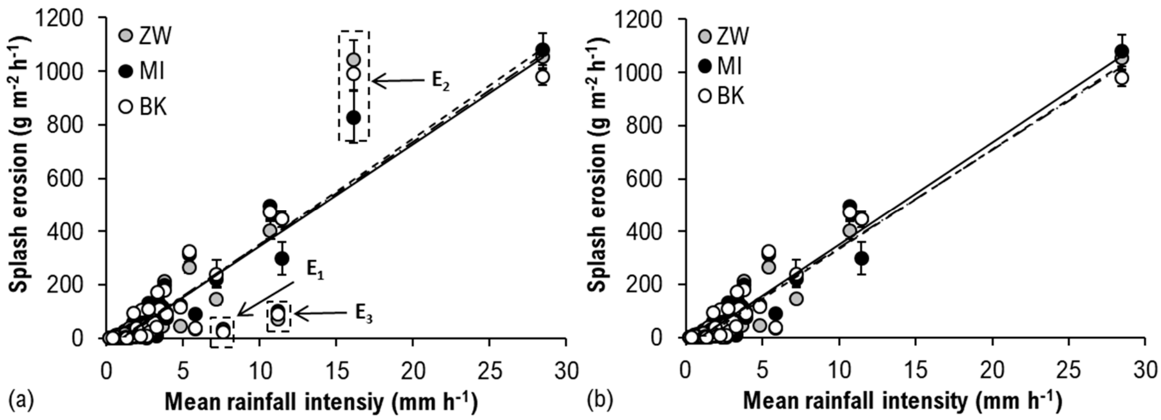

Figure 7. Mean splash erosion for Zwerbach (ZW), Mistelbach (MI), and Bílkovice (BK) soil versus mean rainfall intensity, including (**a**) all observations (n = 80) and (**b**) without extreme observations (n = 77). The dashed line represents the regression function for ZW, as does the solid line for MI and the dashed–dotted line for BK soil. The points inside the dashed boxes indicate extreme observations (E_1, E_2, and E_3) per soil.

The regression analysis without extreme observations did not greatly affect the linear regression for the three soils; nevertheless, R^2 increased for all soils, with the highest increase from 0.81 to 0.93 calculated for the ZW soil (Table 5).

Table 5. Main outputs of the regression analysis between mean splash erosion S_h (g m^{-2} h^{-1}) for Zwerbach (ZW), Mistelbach (MI), and Bílkovice (BK) soil, and mean rainfall intensity I_{av} (mm h^{-1}). The R^2 is the determination coefficient of the regression model, and RMSE (g m^{-2} h^{-1}) indicates the root mean squared error. E_1, E_2, and E_3 denote extreme observations.

Parameter	Soil	Equation	R^2	RMSE
I_{av} (including E_1, E_2, E_3)	ZW	$S_h = 39.765 \cdot I_{av} - 47.492$	0.81	77.08
	MI	$S_h = 38.379 \cdot I_{av} - 39.707$	0.86	62.50
	BK	$S_h = 38.578 \cdot I_{av} - 34.877$	0.82	73.06
I_{av} (excluding E_1, E_2, E_3)	ZW	$S_h = 37.658 \cdot I_{av} - 42.101$	0.93	37.78
	MI	$S_h = 38.691 \cdot I_{av} - 36.893$	0.93	37.68
	BK	$S_h = 36.960 \cdot I_{av} - 30.124$	0.93	37.66

3.4.3. Splash Erosion and Rainfall Erosivity (EI_{30})

The relationship between splash erosion and EI_{30} resulted in a non-linear power function (Figure 8a), with R^2 values of 0.60 for ZW, 0.64 for MI, and 0.65 for BK soil, including the extreme observations (Table 6). Most of the observations were grouped up to an EI_{30} value of 250 (MJ ha mm^{-1} h^{-1}), with high variations in splash erosion (from 5 to 1586 g m^{-2}) between the single observations. Minor differences in R^2 and RMSE between the analysis with and without extreme observations indicated better correlation of extreme splash erosion observations to EI_{30} (Table 6). The highest splash erosion rates were indicated for BK soil, similar to the results obtained with KE_{sum} seen in Figure 4.

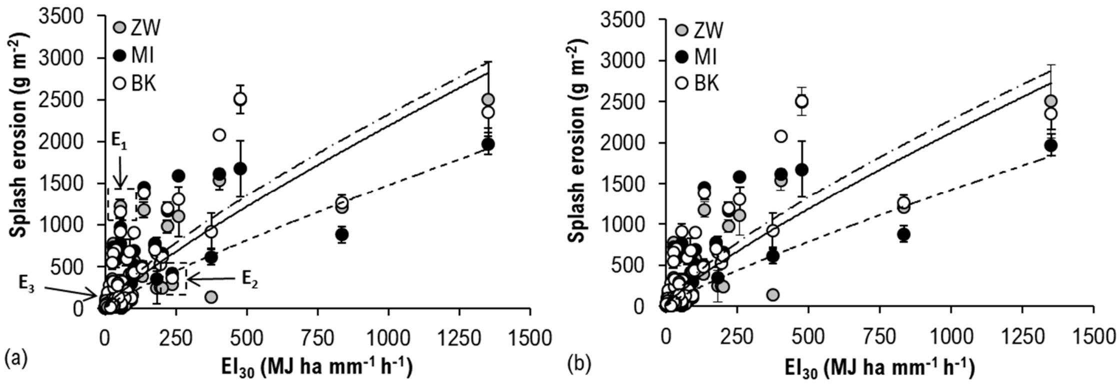

Figure 8. Average splash erosion for Zwerbach (ZW), Mistelbach (MI), and Bílkovice (BK) soil versus mean rainfall erosivity (EI_{30}), including (**a**) all observations (n = 80) and (**b**) those without extreme observations (n = 77). The dashed line represents regression function for ZW, as does the solid line for MI and the dashed–dotted line for BK soil. The points inside the dashed boxes indicate extreme observations (E_1, E_2, and E_3) per soil.

Table 6. Main outputs of the regression analysis between mean splash erosion S (g m^{-2}) for Zwerbach (ZW), Mistelbach (MI), and Bílkovice (BK) soil and rainfall erosivity factor EI_{30} (MJ ha mm^{-1} h^{-1}). R^2 is the determination coefficient of the regression model, and RMSE (g m^{-2}) indicates the root mean squared error. E_1, E_2, and E_3 denote extreme observations.

Parameter	Soil	Equation	R^2	RMSE
EI_{30} (including E_1, E_2, E_3)	ZW	$S = 3.927 \cdot EI_{30}{}^{0.858}$	0.60	335.23
	MI	$S = 6.418 \cdot EI_{30}{}^{0.844}$	0.64	299.95
	BK	$S = 10.233 \cdot EI_{30}{}^{0.785}$	0.65	310.70
EI_{30} (excluding E_1, E_2, E_3)	ZW	$S = 3.899 \cdot EI_{30}{}^{0.854}$	0.60	322.87
	MI	$S = 6.572 \cdot EI_{30}{}^{0.836}$	0.65	287.67
	BK	$S = 10.517 \cdot EI_{30}{}^{0.778}$	0.65	294.55

4. Discussion

Comparable studies to our splash erosion experiments under natural rainfall were made in Portugal by Fernández-Raga et al. [42], and in Spain by Angulo-Martínez et al. [43]. The Thies disdrometer was used in both studies to directly assess rainfall KE. The splash erosion rates measured by Fernández-Raga et al. [42] were between 2.3 and 100 g m^{-2}. In the same range of total KE measured at our sites, splash erosion for loamy sand soil, which was most similar to the texture from the study in Portugal, was between 12 and 2508 g m^{-2}. However, the Portugal study was based on only nine splash erosion records, during which low rainfall intensities characterized by small raindrops (<0.55 mm) were measured. According to findings by Bubenzer and Jones [59], smaller drops produce significantly less splash erosion than larger ones, even for the same amount of KE. This would explain the lower splash erosion rates compared to our measurements, where more erosive rainfall events with larger mean drop sizes (>0.6 mm) were measured. Furthermore, differences in splash erosion measuring principles could also play a role when comparing results. In Portugal, the cup was placed directly on the soil bed, and splashed particles were collected from the surrounding soil. We prepared the soil samples and measured the particles splashed into the collector surrounding the soil. Fernández-Raga et al. [42] described splash erosion as the linear function of total *KE*, with the R^2 being 0.51 and 0.69 for different drop size and intensities thresholds used. That corresponds with our observations for the loamy sand soil, where an R^2 of 0.52 was obtained.

The study from Angulo-Martínez et al. [43] was more comparable to ours, considering that the Morgan splash cups were used for the splash erosion measurements. However, the samples were kept undisturbed during the whole monitoring period, whereas our samples were exchanged after each rainfall event. Splash erosion was measured for three soils with silt, sandy loam, and clay loam textures. The authors suggested EI_{30} as a controlling factor for splash erosion where no differences in detached rates between the soils were reported. Comparable splash erosion rates from our analysis with EI_{30} were found up to 200 MJ ha mm^{-1} h^{-1}; however, with increasing EI_{30}, our splash erosion rates increased up to 2500 g m^{-2}, whereas the rates from Spain remained constant with an average rate of 337 g m^{-2}. The fact that the samples were exchanged between measurements may contribute to higher rates obtained for soils in our study, which was in seedbed conditions.

There is still no general agreement on which rainfall parameters define splash erosion [12]. Parameters dependent on raindrop size and fall velocity, such as rainfall *KE*, momentum, intensity, or a combination of these, are commonly used to describe the raindrop impact on splash detachment. According to our analysis, KE_{sum} could not (Figure 4) explain the variabilities between splash erosion rates obtained for the same amount of *KE*. The reason for that lies in different rainfall intensities between the rainfall events, where high-intensity rainfall produced more splash erosion than low-intensity rainfall (Figure 5). In the field study by Govers [36], it was also concluded that the use of *KE* as an estimate of the rainfall detachment power leads to an underestimation of the relative impact of events with high intensities. From the strong linear relationship between splash erosion and rainfall intensity obtained in our study (Figure 7, Table 5), it can be stated that the splash erosion was more related to rainfall intensity than to other analyzed parameters (KE_{sum}, KE_h and EI_{30}). Nevertheless, we found good agreement between the splash erosion and KE_{sum} divided by rainfall duration (*T*) (Figure 6, Table 4). This indicates that *KE* can also be used as the parameter to predict splash erosion, even when events with different rainfall intensities are analyzed, but its erosive impact has to be expressed through rainfall duration.

The detailed information about drop size distribution allowed us to discern the differences in rainfall characteristics between the study sites. The differences in the splash rates between the rainfall events for the same range of *KE* also contributed to the differing drop size distribution. This was also noticed for the splash rates measured at the Mistelbach site, which is characterized as the site with the highest average raindrop diameter. Another example of this is the extreme event (E_2) reported in the results (Figure 6), where the high splash erosion rates were affected by the large drop size measured for this event. Bubenzer and Jones [59] found that rainfall with larger drops produce more detachment than rainfall with smaller drops, for rainfall having the same total *KE*. Recently, Fu et al. [60] also reported the gradual increase of splash erosion rates with increasing raindrop diameter. Detailed information about raindrop size distribution plays an important role for splash erosion studies like ours, where the direct measurements of the parameters is needed to describe the factors affecting the splash erosion process.

The soil's physical characteristics (texture, soil moisture, organic matter, structure, infiltration capacity, etc.) play an important role in understanding the soil detachment by raindrop splash [2]. Splash erosion of the three soils was positively correlated to the sand content, and significantly ($p < 0.05$) negatively correlated to clay content. For this reason, cumulative splash erosion rates were highest for the BK soil with highest sand content, and significantly different ($p < 0.05$) from ZW soil with the highest clay content (Table 1). Equivalent results were reported in a recent study by Zambon et al. [61], using simulated rainfall on same soils. The high splash detachability of soils with dominating sand content was also confirmed in experiments by Salles et al. [3], Cheng et al. [19], and Xiao et al. [62]. However, the results of the regression and correlation analysis between splash erosion per rainfall duration and KE_h, as well as I_{av}, indicates small differences between the three soils. Other soil properties, such as soil moisture, also have a significant impact on splash erosion [17,63,64]. The results reported by Zambon et al. [61] show that lower splash erosion rates are related to high initial soil water content, followed by surface ponding and changes in saturated hydraulic conductivity induced by surface crusting under high rainfall intensities. Although it was not possible to monitor the changes in soil moisture and surface conditions in the field, these effects probably contributed to results obtained in this field study, especially for the extreme observation E_3. During this observation, two rainfall sub-events were recorded. The second major rainfall sub-event (with total rainfall of 40 mm) occurred 48 h later. Therefore, low splash erosion rates could be related to the long drying period between the first and second rainfall-sub event, resulting in increasing soil surface resistance against the raindrop impact [65]. A more detailed study, including the temporal monitoring of surface changes and soil moisture properties, would possibly contribute to clarifying the complex interaction between soil properties and rainfall controlling the splash erosion process.

Apart from the differences in the rainfall characteristic and soil properties, the experimental design for splash erosion assessment plays an important role when comparing the results from different studies. Recently, a study was published by Fernández-Raga et al. [25] that compared different devices for splash erosion measurements, where the results were strongly affected by the measurement device. This was also visible when comparing our results to the above-described studies. However, low standard deviations between the replicates for each soil obtained in our study confirm that the modified version of the Morgan splash cup provided reliable results for splash erosion measurements.

5. Conclusions

This study analyzed the effect of rainfall parameters on splash erosion under natural rainfall on three sites in Central Europe. Based on the results obtained during the three seasons of measurements, we conclude that splash erosion is more dependent on rainfall intensity than on total kinetic energy and rainfall erosivity (EI_{30}). Still, the kinetic energy of a natural rainfall event can be used as suitable erosivity parameter when dividing it by the rainfall duration. Monitoring of rainfall properties (intensity and kinetic energy) is important to discern the spatial and temporal differences in rainfall characteristics, which influence splash erosion. The dynamic changes in soil moisture, infiltration capacity, and surface roughness affected by weather conditions can lead to uncertainties in the evaluation of splash erosion in the field. Minor differences between the replicates during splash erosion measurements indicate that the modified Morgan splash cup provides a good tool for soil erosion assessment.

Author Contributions: Conceptualization, N.Z. and A.K.; methodology, A.K., T.D., D.Z., T.A.C. and P.S.; formal analysis, N.Z.; investigation, N.Z., L.L.J., and M.N.; resources, P.S., T.D., and A.K.; writing—original draft preparation, N.Z.; writing—review and editing, all authors; visualization, N.Z.; supervision, P.S., T.D., T.A.C. and A.K.; project administration, T.D. and A.K.; funding acquisition, P.S., T.D., and A.K. All authors have read and agreed to the published version of the manuscript.

Funding: This research was performed within the project "Kinetic energy of rainfall as a driving force of soil detachment and transport". Financial support was provided through the Austrian Science Fund (FWF): I 3049-N29 and the Czech Science Foundation (GACR): GF17-33751L. Open access funding was provided by the Austrian Science Fund (FWF).

Acknowledgments: We want to thank the Technical University in Vienna for providing the data from PWS100 and their vehicle during the field campaign in Petzenkirchen (HOAL). Special thanks to Wolfgang Sokol for data processing support, as well as Franz Aigner and other technical and lab personnel for the support during the project.

Conflicts of Interest: The authors declare no conflict of interest.

References

1. Montgomery, D.R. Soil erosion and agricultural sustainability. *Proc. Natl. Acad. Sci. USA* **2007**, *104*, 13268–13272. [CrossRef] [PubMed]
2. Fernández-Raga, M.; Palencia, C.; Keesstra, S.; Jordán, A.; Fraile, R.; Angulo-Martínez, M.; Cerdà, A. Splash erosion: A review with unanswered questions. *Earth Sci. Rev.* **2017**, *171*, 463–477. [CrossRef]
3. Salles, C.; Poesen, J.; Govers, G. Statistical and physical analysis of soil detachment by raindrop impact: Rain erosivity indices and threshold energy. *Water Resour. Res.* **2000**, *36*, 2721–2729. [CrossRef]
4. Morgan, R.P.C. *Soil Erosion and Conservation*, 3rd ed.; Blackwell Publishing Company: Oxford, UK, 2005.
5. Smith, D.D.; Wischmeier, W. Factors affecting sheet and rill erosion. *Trans. Am. Geophys. Union* **1957**, *38*, 889–896. [CrossRef]
6. Rose, C.; Williams, J.; Sander, G.; Barry, D. A Mathematical Model of Soil Erosion and Deposition Processes: I. Theory for a Plane Land Element1. *Soil Sci. Soc. Am. J.* **1983**, *47*, 991–995. [CrossRef]
7. Nearing, M.; Foster, G.R.; Lane, L.J.; Finkner, S.C. A Process-Based Soil Erosion Model for USDA-Water Erosion Prediction Project Technology. *Trans. ASAE* **1989**, *32*, 1587. [CrossRef]
8. Wischmeier, W.H.; Smith, D. Rainfall energy and its relationship to soil loss. *Trans. Am. Geophys. Union* **1958**, *39*, 285–291. [CrossRef]
9. Poesen, J. An improved splash transport model. *Z. Geomorphol.* **1985**, *29*, 193–211.
10. Morgan, R.P.C.; Quinton, J.N.; Smith, R.E.; Govers, G.; Poesen, J.W.A.; Auerswald, K.; Chisci, G.; Torri, D.; Styczen, M.E.; Folly, A.J. *The European Soil Erosion Model (EUROSEM): Documentation and User Guide*; Cranfield University: Silsoe, UK, 1998.
11. Renard, K.G.; Foster, G.R.; Weesies, G.A.; McCool, D.K.; Yoder, D.C. *Predicting Soil Erosion by Water: A Guide to Conservation Planning With the Revised Universial Soil Erosion Equation (RUSLE)*; US Derpartment of Agriculture: Washington, DC, USA, 1997.
12. Salles, C.; Poesen, J. Rain properties controlling soil splash detachment. *Hydrol. Process.* **2000**, *14*, 271–282. [CrossRef]
13. Assouline, S. Infiltration into soils: Conceptual approaches and solutions. *Water Resour. Res.* **2013**, *49*, 1755–1772.
14. Wang, G.; Fang, Q.; Wu, B.; Yang, H.; Xu, Z. Relationship between soil erodibility and modeled infiltration rate in different soils. *J. Hydrol.* **2015**, *528*, 408–418. [CrossRef]
15. Liu, H.; Lei, T.W.; Zhao, J.; Yuan, C.P.; Fan, Y.T.; Qu, L.Q. Effects of rainfall intensity and antecedent soil water content on soil infiltrability under rainfall conditions using the run off-on-out method. *J. Hydrol.* **2011**, *396*, 24–32. [CrossRef]
16. Beczek, M.; Ryżak, M.; Sochan, A.; Mazur, R.; Bieganowski, A. The mass ratio of splashed particles during raindrop splash phenomenon on soil surface. *Geoderma* **2019**. [CrossRef]
17. Le Bissonnais, Y.; Renaux, B.; Delouche, H. Interactions between soil properties and moisture content in crust formation, runoff and interrill erosion from tilled loess soils. *Catena* **1995**, *25*, 33–46. [CrossRef]
18. Le Bissonnais, Y. Aggregate stability and assessment of soil crustability and erodibility: I. Theory and methodology. *Eur. J. Soil Sci.* **2016**, *67*, 11–21. [CrossRef]
19. Cheng, Q.; Cai, Q.; Ma, W. Comparative study on rain splash erosion of representative soils in China. *Chin. Geogr. Sci.* **2008**, *18*, 155–161. [CrossRef]
20. Beguería, S.; Angulo-Martínez, M.; Gaspar, L.; Navas, A. Detachment of soil organic carbon by rainfall splash: Experimental assessment on three agricultural soils of Spain. *Geoderma* **2015**, *245*, 21–30. [CrossRef]
21. Torri, D.; Poesen, J. The effect of cup size on splash detachment and transport measurements. Part II: Theoretical approach. *Catena Suppl.* **1988**, *12*, 113–126.
22. Ellison, W.D. Studies of raindrop erosion. *Agric. Eng.* **1944**, *25*, 131–136.
23. Morgan, R.P.C. Field measurement of splash erosion (Bedfordshire, England). *Eros. Sediment. Transp. Meas. Proc. Florence Symp. (Int. Assoc. Hydrol. Sci. IAHS-AISH)* **1981**, *133*, 373–382.
24. Ma, B.; Liu, Y.; Liu, X.; Ma, F.; Wu, F.; Li, Z. Soil splash detachment and its spatial distribution under corn and soybean cover. *Catena* **2015**, *127*, 142–151. [CrossRef]
25. Fernández-Raga, M.; Campo, J.; Rodrigo-Comino, J.; Keesstra, S.D. Comparative analysis of splash erosion devices for rainfall simulation experiments: A laboratory study. *Water (Switzerland)* **2019**, *11*, 1–21. [CrossRef]

26. Scholten, T.; Geißler, C.; Goc, J.; Kühn, P.; Wiegand, C. A new splash cup to measure the kinetic energy of rainfall. *J. Plant. Nutr. Soil Sci.* **2011**, *174*, 596–601. [CrossRef]
27. Quansah, C. The effect of soil type, slope, rain intensity and their interactions on splash detachment and transport. *J. Soil Sci.* **1981**, *32*, 215–224. [CrossRef]
28. Kinnell, P.I.A. Laboratory studies on the effect of drop size on splash erosion. *J. Agric. Eng. Res.* **1982**, *27*, 431–439. [CrossRef]
29. Sharma, P.P.; Gupta, S.C. Sand Detachment by Single Raindrops of Varying Kinetic Energy and Momentum. *Soil Sci. Soc. Am. J.* **1989**, *53*, 1005–1010. [CrossRef]
30. Fu, Y.; Li, G.; Wang, D.; Zheng, T.; Yang, M. Raindrop energy impact on the distribution characteristics of splash aggregates of cultivated dark loessial cores. *Water (Switzerland)* **2019**, *11*, 1514. [CrossRef]
31. Van Dijk, A.I.J.M.; Bruijnzeel, L.A.; Eisma, E.H. A methodology to study rain splash and wash processes under natural rainfall. *Hydrol. Process.* **2003**, *17*, 153–167. [CrossRef]
32. Iserloh, T.; Ries, J.B.; Arnáez, J.; Boix-Fayos, C.; Butzen, V.; Cerdà, A.; Echeverría, M.T.; Fernández-Gálvez, J.; Fister, W.; Geißler, C.; et al. European small portable rainfall simulators: A comparison of rainfall characteristics. *Catena* **2013**. [CrossRef]
33. Lassu, T.; Seeger, M.; Peters, P.; Keesstra, S.D. The Wageningen Rainfall Simulator: Set-up and Calibration of an Indoor Nozzle-Type Rainfall Simulator for Soil Erosion Studies. *Land Degrad. Dev.* **2015**, *26*, 604–612. [CrossRef]
34. Morgan, R.P.C. Splash detachment under plant covers: results and implications of a field study. *Trans. Am. Soc. Agric. Eng.* **1982**, *25*, 987–991. [CrossRef]
35. Hudson, N.W. The Influence of Rainfall on the Mechanics of Soil Erosion: With Particular Reference to Southern Rhodesia. Master's Thesis, University of Cape Town, Cape Town, South Africa, 1965.
36. Govers, G. Spatial and temporal variations in splash detachment: a field study. *Catena Suppl.* **1991**, *20*, 15–24.
37. Laws, J.O. Measurements of the fall-velocity of water -drops and raindrops. *Trans. Am. Geophys. Union* **1941**, *22*, 709. [CrossRef]
38. van Dijk, A.I.J.M.; Bruijnzeel, L.A.; Rosewell, C.J. Rainfall intensity—Kinetic energy relationships: A critical literature appraisal. *J. Hydrol.* **2002**, *261*, 1–23. [CrossRef]
39. Dunkerley, D. Rain event properties in nature and in rainfall simulation experiments: A comparative review with recommendations for increasingly systematic study and reporting. *Hydrol. Process.* **2008**, *22*, 4415–4435. [CrossRef]
40. Johannsen, L.L.; Zambon, N.; Strauss, P.; Dostal, T.; Neumann, M.; Zumr, D.; Cochrane, T.A.; Klik, A. Impact of Disdrometer Types on Rainfall Erosivity Estimation. *Water* **2020**, *12*, 963. [CrossRef]
41. Kinnell, P.I.A. Problem of Assessing the Erosive Power of Rainfall from Meteorological Observations. *Soil Sci. Soc. Am. Proc.* **1973**, *37*, 617–621. [CrossRef]
42. Fernández-Raga, M.; Fraile, R.; Keizer, J.J.; Varela Teijeiro, M.E.; Castro, A.; Palencia, C.; Calvo, A.I.; Koenders, J.; Da Costa Marques, R.L. The kinetic energy of rain measured with an optical disdrometer: An application to splash erosion. *Atmos. Res.* **2010**, *96*, 225–240. [CrossRef]
43. Angulo-Martínez, M.; Beguería, S.; Navas, A.; Machín, J. Splash erosion under natural rainfall on three soil types in NE Spain. *Geomorphology* **2012**, *175–176*, 38–44. [CrossRef]
44. Bauer, B. Soil splash as an important agent of erosion. *Geogr. Pol.* **1990**, *58*, 99–106.
45. Land Niederösterreich. Wasserstandsnachrichten und Hochwasserprognosen. Messstellendaten. Wieselburg. Available online: https://www.noe.gv.at/wasserstand/#/de/Messstellen/Details/107235/Niederschlag/3Tage (accessed on 25 November 2019).
46. Land Niederösterreich. Wasserstandsnachrichten und Hochwasserprognosen. Messstellendaten. Mistelbach. Available online: https://www.noe.gv.at/wasserstand/#/de/Messstellen/Details/99116541/Niederschlag/3Tage (accessed on 25 November 2019).
47. Czech Hydrometeorological Institute. Prague Clementinum: Basic Data on Prague Clementinum Station. Available online: http://portal.chmi.cz/historicka-data/pocasi/praha-klementinum?l=en# (accessed on 25 November 2019).
48. Klik, A.; Truman, C.C. What is a Typical Heavy Rainstorm? In Proceedings of the 25 Years of Assesment of Erosion, Proceedings of International Symposium, Ghent, Belgium, 22–26 September 2003; Gabriels, D., Cornelis, W., Eds.; Ghent University: Ghent, Belgium, 2003; pp. 93–98.

49. Panagos, P.; Borrelli, P.; Spinoni, J.; Ballabio, C.; Meusburger, K.; Beguería, S.; Klik, A.; Michaelides, S.; Petan, S.; Hrabalíková, M.; et al. Monthly rainfall erosivity: Conversion factors for different time resolutions and regional assessments. *Water (Switzerland)* **2016**, *8*, 119. [CrossRef]
50. ÖNORM L1061-1. *Physikalische Bodenuntersuchungen—Bestimmung der Korngrößenverteilung des Mineralbodens*; Teil 1; Grobboden, Austrian Standards Institute: Vienna, Austria, 2002.
51. ÖNORM L1061-2. *Physikalische Bodenuntersuchungen—Bestimmung der Korngrößenverteilung des Mineralbodens*; Teil 2; Feinboden, Austrian Standards Institute: Vienna, Austria, 2002.
52. ÖNORM L 1050. *Boden als Pflanzenstandort—Begriffsbestimmungen, Untersuchungsverfahren*; Austrian Standards Institute: Vienna, Austria, 1994.
53. ÖNORM L 1080. *Chemische Bodenuntersuchungen—Bestimmung des organischen Kohlenstoffs durch trockene Verbrennung mit und ohne Berücksichtigung von Carbonaten*; Austrian Standards Institute: Vienna, Austria, 1987.
54. Kemper, W.D.; Rosenau, R.C. Aggregate Stability and Size Dlstributlon. In *Methods of soil analysis: Part 1 Physical and Mineralogical Methods*; Klute, A., Ed.; American Society of Agronomy—Soil Science Socity of America: Madison, WI, USA, 1986; pp. 425–442.
55. Zumr, D.; Mützenberg, D.V.; Neumann, M.; Jeřábek, J.; Laburda, T.; Kavka, P.; Johannsen, L.L.; Zambon, N.; Klik, A.; Strauss, P.; et al. Experimental Setup for Splash Erosion Monitoring—Study of Silty Loam Splash Characteristics. *Sustainability* **2019**, *12*, 157. [CrossRef]
56. Richter, G.; Negendank, J.F.W. Soil erosion processes and their measurement in the german area of the Moselle river. *Earth Surf. Process.* **1977**, *2*, 261–278. [CrossRef]
57. Johannsen, L.L.; Zambon, N.; Strauss, P.; Dostal, T.; Neumann, M.; Zumr, D.; Cochrane, T.A.; Blöschl, G.; Klik, A. Comparison of three types of laser optical disdrometers under natural rainfall conditions. *Hydrol. Sci. J.* **2020**, *65*, 524–535. [CrossRef]
58. Kruskal, W.H.; Wallis, W.A. Use of Ranks in One-Criterion Variance Analysis. *J. Am. Stat. Assoc.* **1952**, *47*, 583–621. [CrossRef]
59. Bubenzer, G.D.; Jones, B. Drop size and impact velocity effects on the detachment of soils under simulated rainfall. *Trans. Am. Soc. Agric. Eng.* **1971**, *14*, 625–628. [CrossRef]
60. Fu, Y.; Li, G.; Zheng, T.; Li, B.; Zhang, T. Splash detachment and transport of loess aggregate fragments by raindrop action. *Catena* **2017**, *150*, 154–160. [CrossRef]
61. Zambon, N.; Johannsen, L.L.; Strauss, P.; Dostál, T.; Zumr, D.; Cochrane, T.A.; Klik, A. Splash erosion affected by initial soil moisture and surface conditions under simulated rainfall. *Catena*. under review.
62. Xiao, H.; Liu, G.; Zhang, Q.; Fenli, Z.; Zhang, X.; Liu, P.; Zhang, J.; Hu, F.; Elbasit, M.A.M.A. Quantifying contributions of slaking and mechanical breakdown of soil aggregates to splash erosion for different soils from the Loess plateau of China. *Soil Tillage Res.* **2018**, *178*, 150–158. [CrossRef]
63. Ryzak, M.; Bieganowski, A.; Polakowski, C. Effect of soil moisture content on the splash phenomenon reproducibility. *PLoS ONE* **2015**, *10*, 1–15. [CrossRef]
64. Assouline, S.; Mualem, Y. Modeling the dynamics of seal formation and its effect on infiltration as related to soil and rainfall characteristics. *Water Resour. Res.* **1997**, *33*, 1527–1536. [CrossRef]
65. Caron, J.; Kay, B.D.; Stone, J.A. Improvement of Structural Stability of a Clay Loam with Drying. *Soil Sci. Soc. Am. J.* **1992**, *56*, 1583–1590. [CrossRef]

Appendix 2 – published article on Study 2

Nives Zambon, Lisbeth Lolk Johannsen, Peter Strauss, Tomas Dostal, David Zumr, Thomas A. Cochrane and Andreas Klik (2020): Splash erosion affected by initial soil moisture and surface conditions under simulated rainfall, Catena, 196, 104827, DOI: 10.1016/j.catena.2020.104827.

Author contributions:

NZ set up the experiment, acquired the data, performed the data analysis, evaluated the results, developed the main ideas and wrote the manuscript.

LLJ helped with data acquisition and data analysis, and reviewed the manuscript.

PS added to the main ideas and reviewed the manuscript.

TD added to the main ideas and reviewed the manuscript.

DZ added to the main ideas and reviewed the manuscript.

TAC gave advice on the data analysis, added to the main ideas and reviewed the manuscript.

AK gave advice on the data analysis, added to the main ideas and reviewed the manuscript.

Catena 196 (2021) 104827

Contents lists available at ScienceDirect

Catena

journal homepage: www.elsevier.com/locate/catena

Splash erosion affected by initial soil moisture and surface conditions under simulated rainfall

Nives Zambon[a,*], Lisbeth Lolk Johannsen[a], Peter Strauss[b], Tomas Dostal[c], David Zumr[c], Thomas A. Cochrane[d], Andreas Klik[a]

[a] University of Natural Resources and Life Sciences, Department of Water, Atmosphere & Environment, Vienna, Austria
[b] Institute for Land and Water Management Research, Petzenkirchen, Austria
[c] Czech Technical University in Prague, Faculty of Civil Engineering, Prague, Czech Republic
[d] University of Canterbury, Department of Civil and Natural Resources Engineering, Christchurch, New Zealand

ARTICLE INFO

Keywords:
Splash erosion
Rainfall kinetic energy
Rainfall simulator
Saturated hydraulic conductivity
Surface sealing
Ponding

ABSTRACT

Soil erosion by water is one of the most severe soil degradation processes. Splash erosion is the initial stage of soil erosion by water, resulting from the destructive force of rain drops acting on soil surface aggregates. Apart from rainfall properties, constant soil physical properties (texture and soil organic matter) are crucial in understanding the splash erosion. However, there is lack of information about the effect of variable soil properties such as soil initial water content and surface condition (seal formation) on splash erosion. The objective of the present study was to determine how initial water content and surface condition affected soil splash erosion under simulated rainfall. The changes in soil surface condition were characterized by hydraulic variability (saturated hydraulic conductivity) due to surface seal formation. Slit loam and loamy sand soil textures were used in the experiment. The soil samples were collected from the top layer; air dried, and filled into modified Morgan splash cups for splash erosion measurements. Rainfall was created in the laboratory using two types of rainfall simulators covering intensity range from 28 to 54 mm h^{-1} and from 35 to 81 mm h^{-1}. The soil samples were exposed to three consecutive rainfall simulations with different time intervals between simulations and different initial water content and surface conditions (air-dried, wet-sealed, and dry-crusted). Wet-sealed soil samples had up to 70% lower splash erosion rate compared to air-dried samples, due to surface ponding followed by seal formation. A significant decrease in soil saturated hydraulic conductivity indicated the formation of surface seal for silt loam soils. A non-significant decrease in saturated hydraulic conductivity for loamy sand soil was attributed to earlier formation of stable seals. Two different rainfall simulators produced different amount of splash erosion rates; however, the splash erosion development for increasing rainfall intensity was almost equal considering same initial surface condition. These results provide insight into dynamic changes of individual soil parameters affected by rainfall, and could find wider application for more complex soil erosion prediction models.

1. Introduction

Detachment of soil by rain drop impact is the first stage of the soil erosion process by water (Quansah, 1981). According to Rose (1960) and Hairsine and Rose (1991), splash has more influence on detached soil particles than surface runoff, before the stage of rill and gully erosion is reached. Bare soil surface exposed to rain drops changes its structural and hydraulic properties, which remarkably influences soil infiltration, soil water repellency, overland flow, and final soil erosion rates (Fernández-Raga et al., 2019). The main driver for the splash detachment process is the kinetic energy (KE) of rainfall, which depends on the amount, size, and fall velocities of the drops according to Wischmeier et al. (1971), Ghadiri and Payne (1977) and Morgan (2005). Together with rainfall characteristics, soil physical parameters are crucial in defining the soil erosion process. Wischmeier and Smith (1978) concluded that particle size distribution and organic matter content were the most dominant indicators of soil erodibility. Le Bissonnais (2016) also reported that soil mineralogy, soil texture, organic matter content and initial water content (θ_a) influence the formation of aggregates, where higher θ_a increases the resistance of aggregates against the rain drop impact.

At the beginning of rainfall, KE of rain drops has to exceed a

* Corresponding author at: Institute for Soil Physics and Rural Water Management (SoPhy), University of Natural Resources and Life Sciences (BOKU), Muthgasse 18, 1190 Vienna, Austria.
E-mail address: nives.zambon@boku.ac.at (N. Zambon).

https://doi.org/10.1016/j.catena.2020.104827
Received 12 December 2019; Received in revised form 29 July 2020; Accepted 3 August 2020

threshold, in order to induce destruction of soil aggregates (Kinnell, 2005). If detached soil particles are deposited on the soil surface, they can cause pore filling and clogging by wash-in of fine soil particles (Assouline, 2004; McIntyre, 1958). Soil infiltration rate is then reduced with incipient surface ponding. During ponding the soil surface is rapidly sealed and the crust formation is dependent on cumulative rainfall KE (Baumhardt et al., 1990). Development of seal on soil surface depends on the soil characteristics, being mostly common for soils with high silt content and low organic matter (Armenise et al., 2018). When observing the interaction of splash erosion and seal development, Cheng et al. (2008) discovered that the splash erosion fluctuations are related to surface crust development, where the final splash rates were lower for the soils suspected to surface sealing. Furthermore, several researches have investigated the effect of ponding on soil erosion. For instance, Gao et al. (2003) proved that shallow water layer can accelerate the rain drop impact force on soil erosion, until it reaches a critical depth when the soil detachability decreases. However, they did not consider surface seal formation during ponding phase. Proposed by Guy et al. (1987), the defined critical ponding depth on soil surface is rainfall dependent and equal to three drop diameter.

During the rainfall, soil hydraulic and structural properties define the soil erosion and runoff production. Different approaches have been developed to describe the water movement through the soil affected by surface sealing. Assouline and Mualem (1997) related the seal formation to increase in soil bulk density. Furthermore, in later study (Assouline and Mualem, 2002), they proved that the use of saturated hydraulic conductivity (K_s) for an infiltration model can sufficiently describe the heterogeneity in soil hydraulic properties.

Many experimental studies (e.g. Kinnell, 1982; Salles et al., 2001; Salles and Poesen, 2000; Sharma et al., 1991) have been dealing with rainfall properties controlling splash erosion. However, there is still scarce information in most of these studies about the influence of soil physical properties (moisture, texture, structure, infiltration capacity etc.) on splash erosion. Few authors (Beczek et al., 2019; Truman and Bradford, 1990; Vermang et al., 2009) investigated the effect of different soil moisture on splash erosion, however, different results reported could be contributed to particular conditions in the experiment. Variable results were mainly concerning the different preventing mode, soil organic carbon and clay content of soil samples (Vermang et al., 2009), which can affect the result interpretation. Furthermore, there is lack of studies relating splash erosion with sealing and crust formation and its influence on infiltration (Fernández-Raga et al., 2017).

The main aim of this study is to investigate the effect of different soil moisture content and surface condition (seal formation) on splash erosion for three soils under simulated rainfall. The changes on soil surface were related to changes in soil K_s. Consequently, second objective is to quantify the differences in soil K_s affected by different rainfall intensities and corresponding KE. According to the recent knowledge of authors, the influence of different rainfall characteristics produced by two rainfall simulators on splash erosion development has never been investigated within one study. Therefore, a third objective is to quantify the differences between rainfall characteristics produced by two rainfall simulators and their impact on soil splash erosion for different soil initial conditions.

2. Materials and methods

2.1. Soil sampling

Soil samples were taken from three different locations. Two locations, Zwerbach (15°14′46.09″E, 48° 8′21.91″N) and Mistelbach (16°35′16.07″E, 48°35′2.60″N), are located in agricultural parts of Lower Austria. Third location is situated in Býkovice (14°50′20.0″E, 49°45′41.5″N) within the Central Bohemian Region in Czech Republic. Further on, the soils from Mistelbach, Zwerbach and Býkovice will be referred as MI, ZW and BK, respectively. The samples were collected in spring 2017, after seed-bed preparation from the top soil layer (0–10 cm), air dried and sieved through 10 mm sieve. Particle size distribution was determined with a combined wet sieving and sedimentation method (ÖNORM L 1061-1; ÖNORM L 1061-2, 2002). Soil textures varied from silt loam to loamy sand (ÖNORM L 1050, 2016).[1] According to World Reference Base (WRB) classification (IUSS Working Group WRB, 2014) soils MI, ZW and BK are classified as Calcic Chernozem, Dystric Planosol and Dystirc Cambisoil, respectively.

Samples for chemical analyses were air-dried, crushed, mixed and passed through a 2 mm sieve. Total carbon content was analysed by dry combustion (ÖNORM L 1080, 2013, 2013) using a C/N Analyzer (Vario Max CN, Elementar). Soil organic carbon content (OC) was obtained by subtracting inorganic carbon content measured volumetrically by the Scheibler method with a Calcimeter (ÖNORM L 1084, 2016) from total carbon content measured by C/N Analyzer. Further, the calcium carbonate was measured with the calcimeter using the method by Scheibler (ÖNORM L 1084, 2016). Soil pH was determined in a 1:2.5 soil to water solution, using a glass electrode by Metrohm. Cation exchange capacity (CEC) was estimated by extraction of the effective exchangeable cations by barium chloride solution following ÖNORM L 1086-1, 2014. Aggregate stability (AS) of soils was determined with the wet sieving method according to Kemper and Koch (1966) in modified form. The physical and chemical properties of soils obtained from laboratory analysis are listed in Table 1.

2.2. Experimental design

The experiments took place at the Institute for Soil Physics and Rural Water Management at University of Natural Resources and Life Sciences in Vienna, Austria (BOKU) and the Institute of Land and Water Management Research in Petzenkirchen, Austria (BAW). Modified Morgan splash cups (Morgan, 1981) were used for the splash erosion measurements. The splash cups were constructed from PVC drainage pipe tops with the inner diameter of 10.5 cm (Fig. 1-a) and height of 5 cm (Fig. 1-b). In the bottom of the splash cup, holes were drilled, to ensure water drainage through the soil layer during the rainfall. First, two nylon meshes (500 and 1000 µm) were placed on the bottom of the splash cup, to prevent soil loss trough the holes (Fig. 1-a). Air-dried and sieved (aggregates < 10 mm) soil material was filled into the splash cups. The soil was loosely packed in three layers to reach similar bulk density as in seedbed condition (1–1.2 g cm^{-3}) for each corresponding soil. Soil layers were levelled with a long metal needle. Top layer was filled up to 1 cm below the splash cup edge to prevent surface overflow during high intensities (Fig. 1-c). At the top layer soil aggregates were randomly distributed to achieve heterogeneous arrangement of the all fractions (from fine to coarse).

Splash cups were placed in the middle of a splash collector, with standing height of 30 cm and diameter of 45.5 cm (Fig. 1-d). Splash collector had an outlet, ensuring the drainage of rainfall water with detached soil into buckets placed underneath. After the exposure to rainfall, eroded soil was rinsed from the collector rim, filtered and oven dried at 105 °C. The splash weighted from the filters corresponds to splashed soil from the splash cup surface of 86.6 cm^2.

Fig. 2 illustrates schematic overview of experiments made with two rainfall simulators. The three soils (MI, ZW, BK) were subjected to three rainfall simulations of 30 min, with various rainfall intensities across the positions under the rainfall simulator and different initial soil surface conditions. The first rainfall simulation was performed on air-dried soil surface (AD, $\theta < 5\%$). Second rainfall simulation followed after 24 h on wet-sealed (WS, $\theta_a \sim 30\%$) and final (third) simulation on dry-

[1] Primary classifications of particle size distribution following ÖNORM L 1050, 2016 (1994): sand (particle sizes from 0.2 mm − 0.063 mm diameter), silt (particle sizes from 0.063 mm − 0.002 mm diameter), clay (particle sizes smaller than 0.002 mm).

Table 1
Physical and chemical properties of soil material (0–10 cm soil depth) including: particle size distribution, aggregate stability (AS), alkalescence (pH), calcium carbonate content ($CaCO_3$), organic carbon (OC) and cation exchange capacity (CEC).

Soil location	Sand [%]	Silt [%]	Clay [%]	Soiltexture	AS [%]	$CaCO_3$ [%]	pH	OC [%]	CEC [cMol/kg]
Mistelbach	11.2	70.4	18.4	Silt loam	18.3	10.3	7.7	1.6	26.2
Zwerbach	14.0	60.2	25.8	Silt loam	41.4	3.9	7.7	1.5	25.8
Býkovice	41.6	46.3	12.1	Loamy sand	63.3	< 0.92	7.2	1.7	20.7

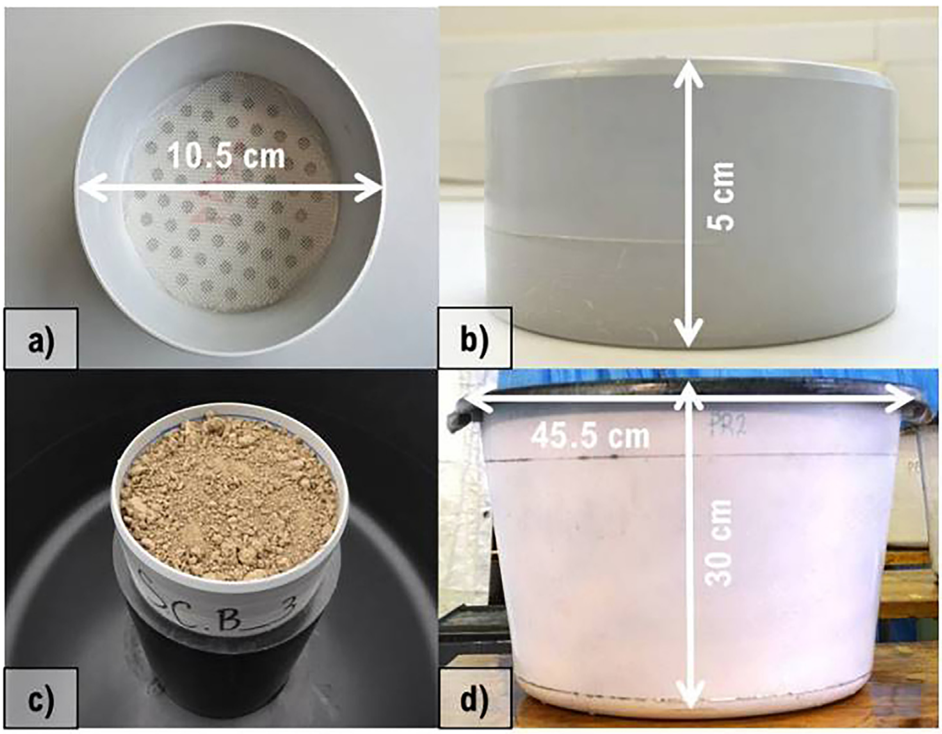

Fig. 1. Figure showing: (a) splash cup design from above; (b) splash cup design from side; (c) splash cup filled with soil and (d) splash collector design.

crusted soil surface (DC, 5% < θ_a < 10%) after approximately ten days of drying. A total of 9, 6 and 3 replications of splash erosion measurements were made for the AD, WS and DC surface condition, respectively. At the end of each rainfall simulation, K_s of soil samples was measured using constant head method, according to description by Klute and Dirksen (1987) at the BAW. Each measurement of soil K_s was replicated three times. Furthermore, the changes in soil infiltration rate were observed by measuring the time from the beginning of the rainfall until the appearance of surface ponding (accumulated water layer). This was defined as ponding time (t_p). Ponding was recorded by two cameras installed on the corners of experimental area under the BAW rainfall simulator. The cameras recorded a photo in one-minute interval during the rainfall simulation. Photos from the camera were analysed and the t_p was registered. Additionally, ponding was visually observed during the rainfall simulation where t_p for each soil sample was noted. The final t_p form camera and visual observation varied in ± 1 min, therefore t_p form the camera observations were taken as a reference.

Ponding was not temporary observed under the rainfall simulator at BOKU due to technical reasons; it was only noted if the samples had surface ponding or not after each experiment.

2.3. Rainfall simulators

For generating artificial rainfall two types of rainfall simulators were used. Norton Ladder type of rainfall simulator located at the BOKU consisted of four oscillating VeeJet 80100 spray nozzles, arranged in two rows and elevated 2.3 m above the splash cups. The simulated rainfall was operated with a pressure of 0.45 bar at the nozzles and the water was distributed from deionized water supply. Totally, nine different positions were arranged under the rainfall simulator for splash erosion measurements, as presented on the Fig. 3-a.

The rainfall simulator at BAW was equipped with one FullJet nozzle (½ HH-30WSQ), where intensity was controlled electronically by discontinuous spraying (Strauss et al., 2000). This design was deviating from normal use (three nozzles) to produce as much heterogeneity in rainfall intensity as possible. The nozzle was elevated 2.3 m above the splash cups and six positions were selected for splash erosion measurements (Fig. 3-b). The BAW rainfall simulator used deionized water with a constant water pressure of 0.25 bar at nozzles.

Rainfall simulations were performed for 30 min with a constant rainfall intensity rate. The maximum rainfall intensity tended to be between 40 and 80 mm h^{-1}, since it was attempted to keep the average intensity equal to those measured (data not shown) under natural rainfall at the locations from which the soil samples were collected. Real distribution of rainfall intensities below the simulators was measured for each position defined for splash erosion measurements, as shown on Fig. 3. Intensities were calculated from the accumulated water volume captured by the splash collectors and drained into the buckets beneath during 30 min rainfall simulation. Total volume of accumulated water in the buckets below the splash collectors was divided by the splash collector area (1625 cm^2). The intensities under the rainfall simulator at BOKU were measured after each experiment with soil samples. The mean of totally three replicates per soil type and initial condition for defined position was used in the results. Under the

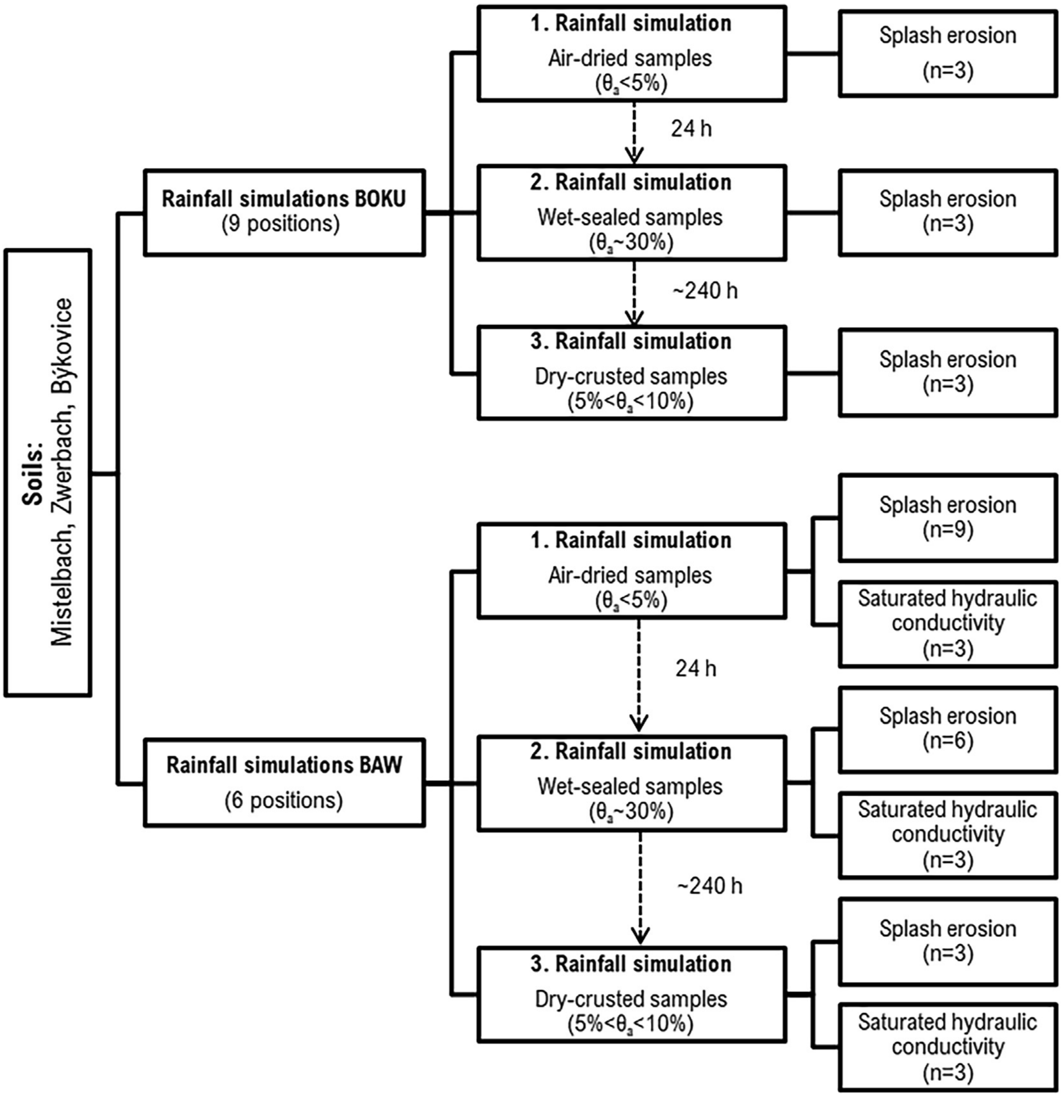

Fig. 2. Schematic overview of the splash erosion experiments for two rainfall simulators. The numbers in the parenthesis under splash erosion and saturated hydraulic conductivity indicate the number of replications per each soil. θ_a denotes the initial soil water content.

rainfall simulator at BAW, the intensity for defined positions of splash cups was calculated as the mean value obtained from totally six rainfall simulations (independent from soil or initial condition).

Rainfall KE, mean drop diameter, median drop diameter and mean drop fall velocity were derived from drop size distribution (DSD) measured with an optical laser disdrometer Weather Sensor OTT Parsivel Version 1 (Parsivel) by OTT Messtechnik. Parsivel disdrometer has a measuring area of 54 cm^2 and categorises the drops into 32 drop size and velocity classes (OTT, 2005). The KE under both rainfall simulators was obtained for each position defined for splash erosion measurements, as shown in Fig. 3. Disdrometer was centred on the positions of corresponding splash cups, which were previously marked on the ground. It was ensured that the height of the disdrometer laser beam is equal to the height of soil surface in the splash cup. For each position 15 min of rainfall was measured with the disdrometer.

The kinetic energy $KE_{i,j}$ (J m^{-2}) of rainfall per minute was computed for the diameter class i and velocity class j, that are provided by disdrometer, as follows:

$$KE_{i,j} = \frac{1}{2} m_i v_j^2 = \sum N \bullet \frac{1}{12 \bullet A} \bullet \pi \rho_w \bullet 10^{-6} \bullet D_i{}^3 \bullet v_j{}^2 \quad (1)$$

where m_i is the mean mass [g] corresponding to the drop diameter class i; N is number of detected raindrops of a certain size class i and velocity class j; A is the is the sampling area of the disdrometer (m^2); ρ_w is density of water (g cm^{-3}); D_i is mean drop diameter (mm) of size class i; and v_j is mean fall velocity (m s^{-1}) of velocity class j. The mass of raindrop was calculated assuming a spherical drop shape. Total KE is the sum of KEs for each drop size and velocity, multiplied with number of drops in the corresponding classes.

2.4. Statistical analysis

Statistical analyses were performed in R Studio (R Development Core Team, 2015). The Kruskal and Wallis (1952) test (one-way ANOVA on ranks) was used to identify statistical differences in K_s for different intensity rates (positions). Each position under the rainfall simulator represented one group of data for which the K_s was obtained. The positions (groups) differ in intensity rates which they are exposed to. The comparison is based on three replicates ($n = 3$) of K_s values obtained for each group (intensities). Multiple comparison between groups (post hoc) was further conducted with Dunn's test (Dunn, 1964) with p-adjustments of Benjamini-Hochberg (Benjamini and Hochberg, 1995). The differences in splash erosion rates between the three soils were analysed using the Student's t-test.

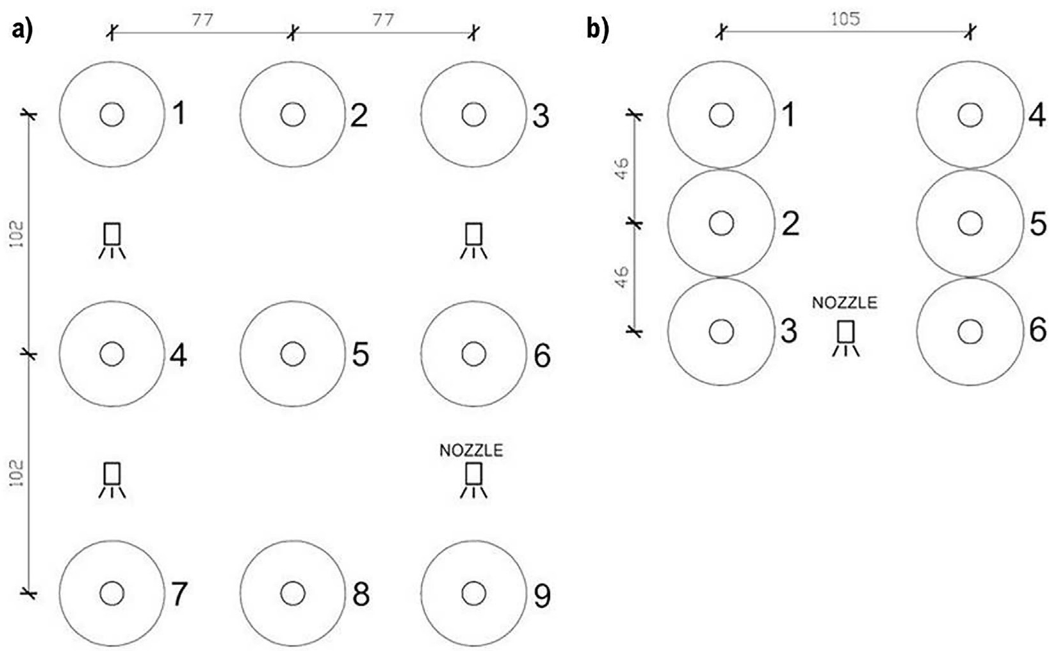

Fig. 3. Schematic representation of splash collectors (outer circle) and splash cup (inner circle) under positions marked for rainfall simulator at (a) BOKU and (b) BAW.

3. Results

3.1. Intensity and kinetic energy

According to intensity measurements, the rainfall simulators at BOKU and BAW covered intensity range from 28.2 to 54.2 mm h^{-1} (Table 2) and 35.3 to 81.2 mm h^{-1} (Table 3), respectively. Drop size distribution indicated that the rainfall simulator at BAW produced higher percentage of drops with drop diameter larger than 0.6 mm (Fig. 4-a), however, rainfall simulator at the BOKU had higher percentage of drops with velocity greater than 5.2 mm s^{-1} (Fig. 4-b). This resulted in larger mean and median drop size obtained for positions under the BAW rainfall simulator (Table 2) and higher mean raindrop velocity for positions under the BOKU rainfall simulator (Table 3). Distribution of mean drop velocity per drop size class (Fig. 5), indicated that 14% of total drops with diameter larger than 1.3 mm under the BAW rainfall simulator did not reach their terminal velocity, as specified by Atlas et al. (1973). Since the rainfall simulator at the BOKU produced higher velocity of larger drops, the resulting KE per mm of rainfall was on average 62% higher (Table 2) compared to KE per mm of rainfall for rainfall simulator at the BAW (Table 3). Total KE ranged between 504.4 and 923.1 J m^{-2} h^{-1} for the BOKU rainfall simulator (Table 2), and between 375.8 and 961.8 J m^{-2} h^{-1} for the BAW rainfall simulator (Table 3).

3.2. Splash erosion

Due to higher KE per mm of rainfall measured under the rainfall simulator at the BOKU, overall splash erosion rates were almost twice as high compared to results obtained with BAW simulator as shown on Fig. 6 (excluding the ZW soil for AD condition on Fig. 6-d).

For the rainfall simulator at BOKU, the MI soil had widest range of splash rates (0.06–0.58 kg m^{-2} h^{-1}) compared to ZW (0.02–0.31 kg m^{-2} h^{-1}) and BK (0.12–0.43 kg m^{-2} h^{-1}) soil. Splash erosion under the BAW rainfall simulator ranged similarly between three soils (0.02–0.23 kg m^{-2} h^{-1}) for AD initial condition (Fig. 6-a,d,g). The highest splash erosion was measured for samples exposed to KE of 667 J m^{-2} h^{-1} with largest drop diameter (Table 3). Relationship between splash erosion for three soils and KE was linear for the BOKU rainfall simulator, and non-linear for the BAW rainfall simulator (Table 4). Highest coefficient of determination (R^2) was calculated for ZW soil, considering both rainfall simulators. Between 60 and 72% less splash erosion, compared to simulation with AD initial condition, was measured for three soils with WS initial condition under both rainfall simulators. This reduction was evident for samples exposed to KE > 660 J m^{-2} h^{-1}, which were affected by surface ponding. However,

Table 2
Rainfall properties measured with collectors (intensity) and optical laser disdrometer under rainfall simulator at BOKU.

Position	Intensity [mm h^{-1}]	Kinetic energy [J m^{-2} h^{-1}]	Mean drop diameter* [mm]	Median drop diameter [mm]	Mean drop velocity** [m s^{-1}]	Kinetic energy/intensity [J m^{-2} mm^{-1}]
1	28.3	504.4	0.7	0.5	4.2	17.8
2	37.8	619.0	0.7	0.6	4.3	16.4
3	35.3	681.0	0.7	0.5	4.4	19.3
4	42.5	701.0	0.8	0.6	4.4	16.5
5	49.6	716.5	0.8	0.7	4.4	14.4
6	54.2	923.1	0.8	0.6	4.4	17.0
7	28.2	566.3	0.7	0.5	4.3	20.0
8	32.3	546.3	0.7	0.6	4.3	16.9
9	35.9	712.2	0.7	0.5	4.4	19.8

* The standard deviations of mean drop diameter were < 0.1 mm.
** The standard deviations of mean drop diameter were < 0.1 m s^{-1}.

Table 3
Rainfall properties measured with collectors (intensity) and optical laser disdrometer under rainfall simulator at BAW.

Position	Intensity [mm h^{-1}]	Kinetic energy [J m^{-2} h^{-1}]	Mean drop diameter [mm]	Median drop diameter* [mm]	Mean drop velocity** [m s^{-1}]	Kinetic energy/intensity [J m^{-2} mm^{-1}]
1	70.2	773.6	0.8	0.7	4.1	11.0
2	81.2	961.8	1.0	0.8	4.2	11.8
3	56.7	667.0	1.3	1.0	4.3	11.8
4	35.3	375.8	1.2	1.0	4.3	10.6
5	43.5	421.2	0.8	0.8	4.1	9.7
6	56.3	560.7	0.7	0.6	4.0	10.0

* The standard deviations of mean drop diameter were < 0.1 mm.
** The standard deviations of mean drop diameter were < 0.1 m s^{-1}.

splash erosion increased for samples exposed to lower KE. This was particularly noted for MI and ZW soil under the BOKU rainfall simulator (Fig. 6-b,e). Reduction in splash erosion for WS initial condition resulted in negative linear function between splash and KE with low R^2 (mostly < 0.10) considering both rainfall simulators (Table 4). The splash erosion for the samples with DC surface condition increased with KE, except for BK soil under the BOKU rainfall simulator (Fig. 6-i). Similarly to splash erosion results with WS condition, MI and ZW soil showed increase of roughly 50% in splash erosion rates for the samples exposed KE < 660 J m^{-2} h^{-1} (Fig. 6-c,f). Highest R^2 between splash erosion for three soils and KE was obtained for samples under the BAW rainfall simulator (Table 4).

3.3. Saturated hydraulic conductivity

Splash erosion affected by surface ponding during the rainfall simulations was contributed to different θ_a and changes in soil hydraulic properties. To quantify this changes soil K_s was measured after each rainfall simulation with different soil initial condition. Fig. 7 represents average K_s (n = 3) for the three soils and three initial conditions. Highest K_s between three soils were measured for ZW soil with the maximum of 1,102.9 mm h^{-1} obtained for initial AD surface condition (Fig. 7-d). Lowest values were measured for DC surface condition (Fig. 7-f). Similar trend was observed for MI soil, where highest K_s of 461.7 mm h^{-1} decreased to 56.3 mm h^{-1} for DC surface condition (Fig. 7-a,c). Generally, BK soil exhibited lowest K_s between three soils with maximum K_s of 193 mm h^{-1} for WS initial surface condition (Fig. 7-g-i). When comparing the K_s values measured for individual surface conditions it was observed that the samples exposed to lower (< 56.7 mm h^{-1}) intensities had higher K_s than samples exposed to high intensities. These differences were significant (P < 0.05) for MI soil with AD samples (Fig. 7-a), including ZW soil with WS and DC samples (Fig. 7-e,f). Furthermore, high variations between the replicates, typical for the samples exposed to lower intensities (< 56.7 mm h^{-1}), could result in no significant (P > 0.05) difference between K_s obtained for AD and WS surface condition considering three soils (Fig. 7-b,d,h).

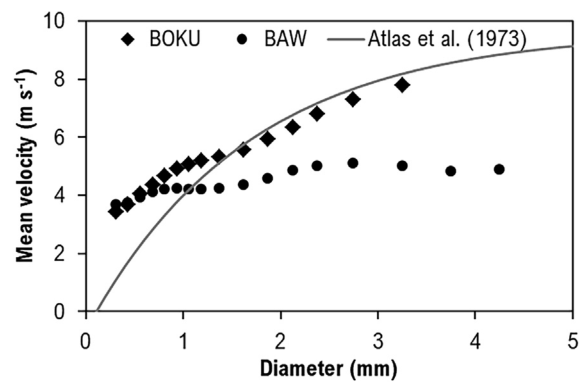

Fig. 5. Mean drop velocity of each drop size class for all positions measured under rainfall simulator at BAW and BOKU and terminal fall velocity line drawn according to Atlas et al. (1973). The velocities are shown for drop size classes within the total drops amount was larger than 100.

3.4. Relationship between soil saturated hydraulic conductivity and rainfall kinetic energy

As shown in previous results, the K_s of soil samples tend to decrease with the increasing intensity and after subsequent exposure to rainfall. To investigate the impact of KE on K_s, total KE applied on soil surface during the three rainfall simulations was plotted against K_s measured for each soil initial condition (Fig. 8). The relationship obtained for MI, ZW and BK soil can be described as a power function of accumulated KE, which agrees best for MI and ZW soil with R^2 of 0.54 and 0.74, respectively, where for BK soil low R^2 of 0.22 was obtained.

From the KE-K_s functions obtained, the decrease in K_s with increasing KE was observed until reaching a steady state, where KE had no impact on further K_s reduction. Assuming that the decrease in K_s was accompanied with a surface sealing, constant K_s values would indicate a final stage in the surface seal formation. The amount of KE needed for fully developed surface sealing could be calculated by considering the impact of KE on soil K_s. After a certain amount of KE applied on the soil

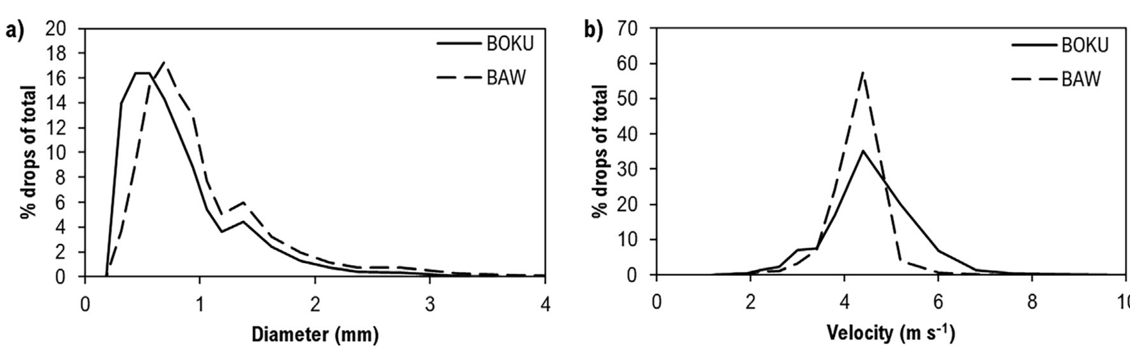

Fig. 4. Mean drop size and velocity distribution including all positions under rainfall simulator at BOKU and BAW. Each drop size and velocity class is percentage of drops within the class out of the total drops amount (classes with < 100 drops were not considered).

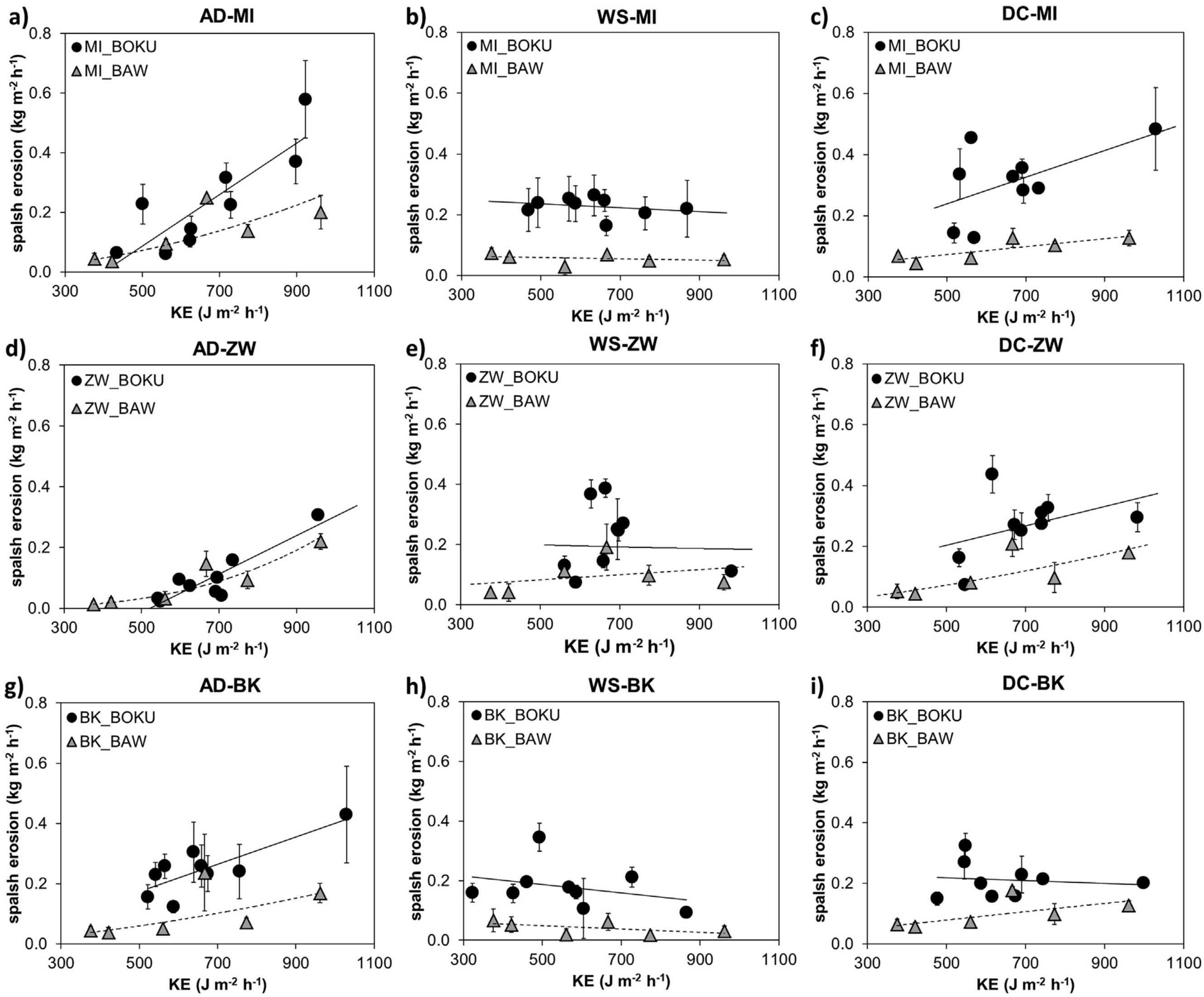

Fig. 6. Mean splash erosion plotted against rainfall kinetic energy (KE) obtained under rainfall simulator at BOKU and BAW. Splash erosion is shown for: (a-c) Mistelbach (MI), (d-f) Zwerbach (ZW) and (g-i) Býkovice (BK) soil with respect to air-dried (AD), wet-sealed (WS) and dry-crusted (DC) surface initial condition. Whiskers indicate ± standard deviation of mean splash erosion within replicates (n = 3, 6, 9).

Table 4
Linear and nonlinear regression with associated determination coefficient (R^2) between kinetic energy (KE) ($kJ\ m^{-2}\ h^{-1}$) and splash erosion (S) ($kg\ m^{-2}\ h^{-1}$) obtained for two rainfall simulators, at BOKU and BAW institute, and Mistelbach (MI), Zwerbach (ZW) and Býkovice (BK) soil with air-dried (AD), wet-sealed (WS) and dry-crusted (DC) soil initial condition (IC).

Soil	IC	BOKU	R^2	BAW	R^2
MI	AD	S = 9E-04 KE − 0.35	0.73	S = 5E-07 KE ^ 1.92	0.77
ZW	AD	S = 6E-04 KE − 0.33	0.80	S = 2E-10 KE ^ 3.02	0.90
BK	AD	S = 5E-04 KE − 0.05	0.65	S = 3E-06 KE ^ 1.59	0.56
MI	WS	S = -6E-05 KE + 0.27	< 0.10	S = -2E-05 KE + 0.07	< 0.10
ZW	WS	S = -1E-04 KE + 0.31	< 0.10	S = 9E-05 KE + 0.04	0.11
BK	WS	S = -1E-04 KE + 0.25	< 0.10	S = -6E-05 KE + 0.08	0.32
MI	DC	S = 4E-04 KE − 0.02	0.32	S = 1E-04 KE + 0.07	0.68
ZW	DC	S = 3E-04 KE − 0.04	0.18	S = 7E-06 KE ^ 1.48	0.70
BK	DC	S = -5E-05 KE + 0.24	< 0.10	S = 3E-03 KE ^ 0.90	0.56

surface, K_s significantly ($P < 0.05$) varied for increasing KE until reaching a constant value (Fig. 8). This amount of KE was addressed as the threshold value required for fully developed seal formation and it represented the transformation point between variable and constant soil K_s. Accordingly, the calculated threshold value of accumulated kinetic energy (KE_0) was found to be 0.39 $kJ\ m^{-2}$ for MI soil and 0.59 $kJ\ m^{-2}$ for ZW soil (Fig. 8-a,b). The BK soil showed no significant impact of increasing KE on K_s; therefore, the threshold value could not be obtained (Fig. 8-c).

3.5. Surface ponding

Present surface ponding was mostly concentrated within samples in central positons under the rainfall simulator at BOKU (e.g. positon 2, 4, 5, 6, and 8), where the drops overlapped (Table 2). For these positons higher KE and lower final splash erosion rates were measured, compared to positons with no surface ponding. During the rainfall simulation at the BAW, t_p was recorded for each soil sample in splash cup (Table 5). Generally, highest t_p was measured for the AD and DC surface condition, and lowest for WS surface condition. This was expected considering that samples with AD and DC initial condition had higher infiltration capacity due to lower θ_a and samples with WS initial condition had lower infiltration capacity due to higher θ_a. Furthermore, this results correlated to the K_s values obtained for the three soils. The shortest t_p was measured for BK soil, which had the lowest K_s and longest t_p for the ZW soil with highest K_s compared to other soils.

Measured t_p for the samples with WS initial condition was related to

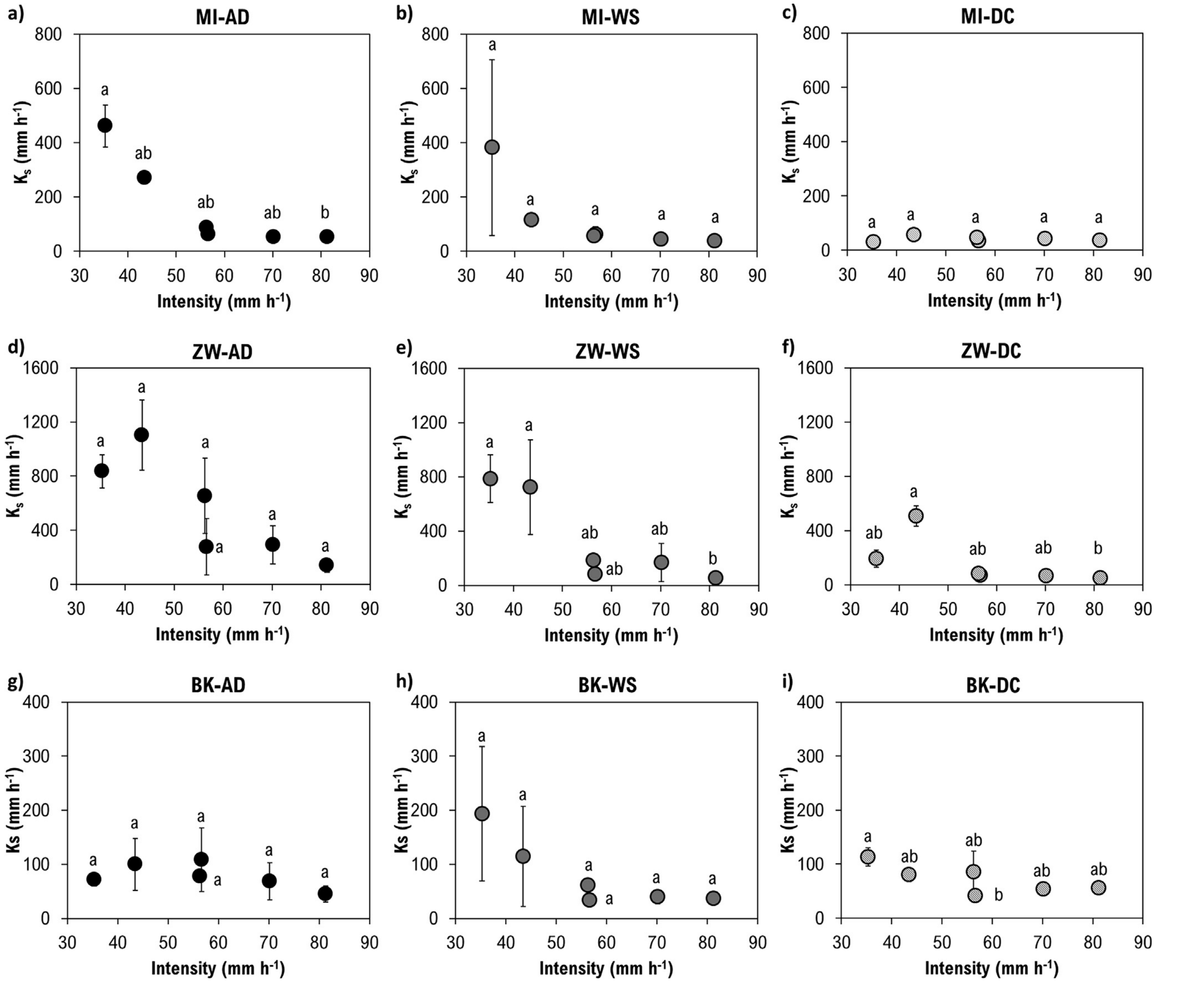

Fig. 7. Mean soil saturated hydraulic conductivity (K_s) obtained for (a-b) Mistelbach (MI), (d-f) Zwerbach (ZW) and (g-i) Býkovice (BK) soil with (AD), wet-sealed (WS), and dry-crusted (DC) surface initial condition. Letters indicate difference at significance level $P < 0.05$ between Ks obtained for different intensity rates under BAW rainfall simulator. Whiskers indicate ± standard deviation of the mean K_s within replicates (n = 3).

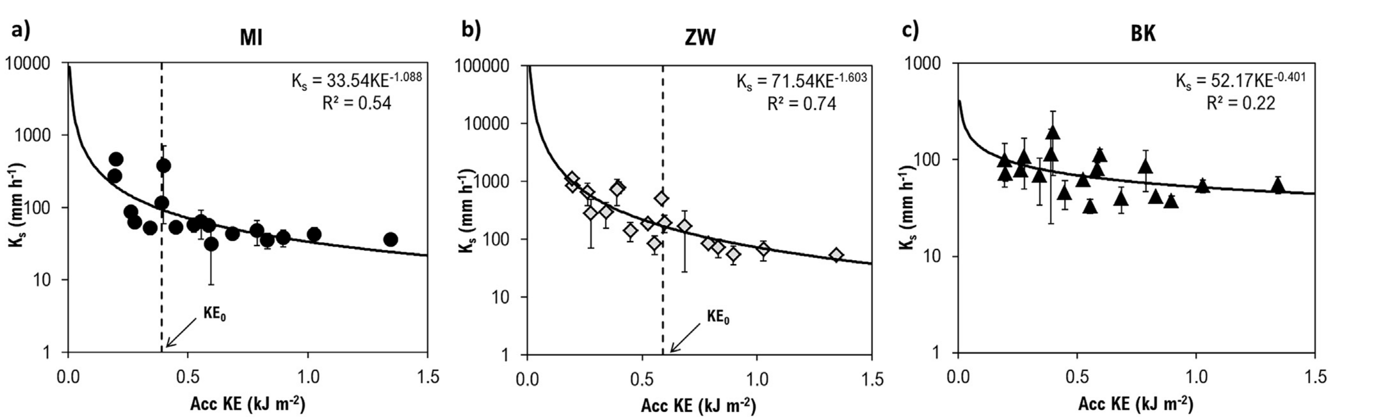

Fig. 8. Regression analysis of mean soil saturated hydraulic conductivity (K_s) in logarithmic scale plotted against accumulated rainfall kinetic energy (Acc KE) for: (a) Mistelbach (MI), (b) Zwerbach (ZW) and (c) Býkovice (BK) soil. The dashed line shows the threshold (KE_0) separating the variable from constant K_s values. Whiskers represent ± standard deviation of mean K_s within replicates (n = 3).

Table 5
Average time to ponding (t_p) (± standard deviation) from three observations (n = 3) during rainfall simulation with Mistelbach (MI), Zwerbach (ZW) and Býkovice (BK) soil obtained for three different soil initial conditions: air-dried (AD), wet-sealed (WS) and dry-crusted (DC). Positons with soil samples where no ponding was detected are marked as (−) under the column t_p.

Soil	Position	Intensity [mm h^{-1}]	t_p AD [min]	t_p WS [min]	t_p DC [min]
MI	1	70.2	21 (± 0)	6 (± 1)	17 (± 3)
MI	2	81.2	20 (± 2)	4 (± 0)	10 (± 3)
MI	3	56.7	23 (± 0)	6 (± 0)	18 (± 2)
MI	4	35.3	–	27 (± 0)	–
MI	5	43.5	–	11 (± 0)	–
MI	6	56.3	–	8 (± 2)	28 (± 1)
ZW	1	70.2	–	10 (± 2)	24 (± 0)
ZW	2	81.2	–	6 (± 2)	22 (± 2)
ZW	3	56.7	–	8 (± 2)	–
ZW	4	35.3	–	–	–
ZW	5	43.5	–	–	–
ZW	6	56.3	–	25 (± 0)	–
BK	1	70.2	24 (± 2)	4 (± 0)	18 (± 1)
BK	2	81.2	18 (± 3)	3 (± 0)	10 (± 0)
BK	3	56.7	21 (± 1)	4 (± 0)	20 (± 0)
BK	4	35.3	–	–	–
BK	5	43.5	–	11 (± 5)	–
BK	6	56.3	20 (± 0)	7 (± 0)	21 (± 3)

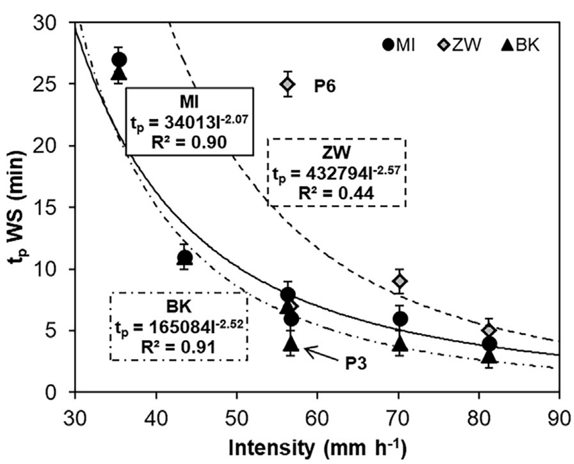

Fig. 9. Regression analysis of mean ponding time (t_pWS) for soil samples with wet-sealed (WS) surface initial condition and Mistelbach (MI), Zwerbach (ZW) and Býkovice (BK) soil, in correlation with rainfall intensity obtained under rainfall simulator at BAW. P3 and P6 show results obtained for positions 3 and 6 under rainfall simulator, respectively. Whiskers represent ± standard deviation of mean t_p within replicates (n = 3).

the intensity rates (Fig. 9). The results showed high agreement between t_p and rainfall intensity with R^2 of 0.90 and 0.91 obtained for MI and BK soil, respectively. The R^2 for ZW soil was remarkably lower, due to high difference in t_p between the positons 3 and 6, with same intensity rate of 56 mm h^{-1} (P3, P6 on Fig. 9). Larger drop diameter measured for position 3 (Table 3) could contribute to greater surface compaction during the previous simulation with AD initial condition. This eventually resulted in lower K_s for positon 3 and therefore, shorter t_p during the simulation with WS samples (Fig. 7-e). Similar results of t_p for position 3 and 6 were also observed for MI soil during the simulation with AD initial condition (Table 5).

4. Discussion

4.1. Effect of rainfall kinetic energy produced by two rainfall simulators on splash erosion

The results of splash erosion obtained from both rainfall simulators revealed comparable trend of splash development in relation with KE (Fig. 6). However, twice as high splash erosion rates were measured for the rainfall simulator at BOKU. The velocities of raindrops were crucial in defining rainfall kinetic energy, where higher velocities contributed to higher KE for BOKU rainfall simulator (Fig. 4-b). The differences in drop size-velocity distribution between different rainfall simulators can result in the significantly different splash erosion rates. This should be considered when comparing the splash erosion results from different studies.

The rainfall KE produced by rainfall simulator is often defined by (uniform) drops of different size and fall height, while the KE obtained in the field conditions depends primarily on drop size distribution (Van Dijk et al., 2003). Similar was observed with the two rainfall simulators used in present study. The drop distribution of rainfall simulator at the BAW was too uniform to describe the natural rainfall and the velocities of larger drops (> 1.3 mm) were far from the terminal velocity, defined by Atlas et al. (1973). On the contrary, the BOKU rainfall simulator produced higher velocities for most of drops in the same diameter class. However, large drops were still under the terminal velocity line (Fig. 5). Related to drop terminal velocity under the simulated rainfall, Iserloh et al. (2013) concluded that larger drops produced by different rainfall simulators are usually not able to reach their terminal velocity (mostly due to low fall height). For this reason, the rainfall KE produced in the laboratory cannot completely represent KE of natural rainfall.

4.2. Effect of soil water content and surface condition on splash erosion

Fluctuations in splash rates obtained from individual rainfall simulator were combined effect of θ_a and seal development affected by KE. Lower θ_a (AD initial condition) contributed to greater splash erosion for samples exposed to high intensities and KE. Therefore, splash erosion could be described as a linear or power function of increasing KE for AD initial condition, which was also obtained in previous studies (Fernández-Raga et al., 2010; Sharma et al., 1991; Zumr et al., 2019). However, appearance of surface ponding in the last stage of rainfall simulation indicated the reduction in soil infiltration rate, characterized by lower soil permeability due to surface seal formation (Assouline, 2004; Liu et al., 2011; Sharma et al., 1995). Surface seal was easily observable on the soil samples exposed to high intensities (> 50 mm h^{-1}) with completely smooth soil surface after the rainfall simulation. In addition, significantly lower K_s (Fig. 7) for the samples exposed to high intensities indicated the beginning of surface seal formation.

In the following rainfall simulation with WS soil samples splash erosion decreased with increased rainfall KE (Fig. 6-b,e,h). The final splash erosion rates for samples exposed to highest KE were evidently lower compared to rates for AD surface condition. According to results in Table 5, surface ponding was initiated earlier than for AD and DC initial condition. This was contributed to high θ_a, where early surface ponding at higher θ_a results from rapid decline in the hydraulic gradient for intensive rainfall in combination with a lower storage capacity (Liu et al., 2011; Vermang et al., 2009). Furthermore, partly formed seals (for MI and ZW soil) from previous simulation with AD soil samples probably resulted in higher resistance of soil surface to splash erosion prior to surface ponding. Following surface ponding eventually lowered the raindrop impact on soil surface preventing the further splash erosion (Poesen, 1981). Similar results were reported by Vermang et al. (2009), where soil detachment decreased along with surface seal development and formation of shallow water layer by surface runoff.

During the simulation with DC initial condition, the influence of the

θ_a on reduction in t_p could be excluded, since the initial θ_a was approximately three times lower. Therefore, the reduction in infiltration rates followed by surface ponding (Table 5) may be due to already developed seals, after previous exposure of the samples to rainfall (with AD and WS initial condition). Unlikely to splash erosion for WS initial condition, the reduction in splash erosion rates was noticed only for BK soil under the BOKU rainfall simulator (Fig. 6-i). Results for other soils, however, suggested the increase in splash erosion compared to samples with AD initial condition under lower rainfall intensities. Opposite results were reported by Le Bissonnais et al. (1995), where drying of aggregates increased the stability against aggregate breakdown. According to Lado et al. (2004), the wetting rate in combination with initial water content determined the magnitude of slaking forces causing aggregate break down. These forces are greater if the aggregates are drier. Therefore, it could be hypothesized that the higher splash erosion rates during the rainfall simulation with DC initial condition for the MI and ZW samples could be contributed to aggregate destruction by slaking.

Generally splash erosion increased or did not vary between the simulations on samples with different initial conditions which were not affected by surface ponding. This was related mostly to samples exposed to lower intensity and KE (< 660 J m^{-2} h^{-1}). High θ_a for WS samples may result in higher splash erosion (compared to AD initial condition) for the slow ponding soil samples considering both ZW and MI soil (Fig. 6-a-f). The findings of Beczek et al. (2019) and Gao et al. (2003) confirmed that the mass of monitored eroded material increased with higher θ_a due to lower cohesion between soil particles, considering that no surface seal was present.

Following the above lines discussed, it is difficult to select one factor that describes the differences in splash erosion rates for different initial conditions and soils. Soil conditions before rainfall and their variability during the rainfall will contribute to variation in splash characteristics. Depending on rainfall, soil structure, physico-chemical properties and θ_a, response of the soil to raindrop impact will vary. Nevertheless, for the three soils studied under rainfall conditions in this experiment can be concluded that reduction in splash erosion was primarily attributed to surface ponding initiated by high rainfall intensities and subsequent sealing formation. High initial θ_a reduced soil infiltration capacity and induced faster surface ponding (for WS initial condition) with decrease in splash erosion rates (Walker et al., 2007). In the case of the three soils studied here, initially lower K_s for MI and BK soil could be attributed to lower porosity considering lower clay content (12–18%) than for ZW soil, as indicated by Wei et al. (2015). Furthermore, it should be noted that beside the soil texture other soil properties, such as OC and calcium cations (Ca^{2+}) could affect the soil hydraulic properties (Wuddivira and Camps-Roach, 2007) and eventually splash erosion rates. However, we could not establish correlation between K_s and OC or $CaCO_3$ (contains Ca^{2+}) for the three soils presented here (Table 1, Fig. 7).

4.3. Effect of soil properties on surface seal formation

Soil detachment is depended on aggregate strength and after seal development on seal strength (Vermang et al., 2009). The both are highly related to soil physico-chemical properties (Mualem et al., 1990). Stability of aggregates obtained for three soils could not explain differences in the splash rates or the seal development in the present study. For example, BK soil had highest ratio of stable aggregates (Table 1), however, the splash erosion rates for AD surface condition did not significantly ($P < 0.05$) differ compared to MI soil with lowest AS. High OC and $CaCO_3$ content could be favourable for higher soil AS (Le Bissonnais et al., 1993). Similar OC content between the soils (Table 1) and low $CaCO_3$ soil could not explain higher AS for BK. However, it might be considered that higher clay content for MI and ZW soil could promote the slaking forces during the wet-sieving and decrease of the AS. Furthermore, the K_s obtained for BK was lowest compared to other two soils and did not vary between the simulations (Fig. 8-c, Fig. 7-g-i). On the one hand, this could indicate that the KE did not have major effect on the surface seal formation. On the other hand, stable surface seal formation could be initiated in early stage of rainfall simulation with AD soil samples. Therefore, further development (decrease) was not detected. In addition to that, the BK soil had visibly smaller aggregates compared to other two soils. For this reason, the lower KE was needed to destroy aggregates and to form crust. In the study by Fox et al. (2007), smaller fractions were more susceptible to surface crusting and splash erosion than the coarser fractions. Furthermore, lower surface roughness due to smaller aggregates might indicate smaller depressional storage, which induced earlier surface runoff (Truman and Bradford, 1990).

ZW soil showed lowest splash erosion rates and high K_s for AD surface condition compared to three soils. Le Bissonnais et al. (1995) reported that soils with high OC content have lowest erosion rate in AD conditions. Similar values of OC content were obtained for three soils (Table 1). Considering this, low splash erosion rates for ZW soil in AD condition were not contributed to OC content. However, according to Vermang et al. (2009) and Xiao et al. (2018) during the fast wetting period on dry surface, formation stable aggregates is affected by cementing effect of clay particles trough the surface water tension. This may be the reason for higher resistance of the ZW soil to soil erosion and seal development.

Manny studies provided the evidence that formation of sealing was characteristics of soils with high silt content (Cheng et al., 2008; Rodrigo Comino et al., 2017; Truman and Bradford, 1990). This could be also applied on results obtained in this study for MI soil, characterized by high silt content and low AS (Table 1). Assuming that the decrease in splash erosion and K_s was affected by surface seal formation, the MI soil showed highest reduction in K_s between the rainfall simulations among the three soils.

4.4. Effect of rainfall kinetic energy on surface seal formation

The obtained threshold values of KE required to form stable seal formation, confirmed the assumption of greater seal development under the soil surfaces exposed to higher KE. This was also stated by Bedaiwy (2008), where the important influence of KE on surface formation was highlighted. Constant or increasing splash erosion rates obtained for all three soils exposed to low intensity rates (< 35.3 mm h^{-1}) implied that accumulated KE throughout the simulations was lower than critical KE to initiate surface seal formation. However, high deviations between the replicates for K_s require more measurements in order to more precisely describe the process of surface crust development for certain scenarios.

5. Conclusion

In this study different scenarios of splash erosion development were obtained by applying simulated rainfall produced from two different rainfall simulators on soil samples with air-dried, wet-sealed and dry-crusted surface condition. Both rainfall simulators exhibited same trend of splash erosion development by applying similar range of intensities, though the total amount of splash rates where significantly different. This was contributed to differences in drop and velocity spectrum resulting in different kinetic energy produced for the same rainfall amount. Since splash erosion in primarily affected by raindrop impact, a special attention should be given when comparing the results obtained with different rainfall simulators due to variabilities in drop and velocity distribution.

The splash erosion rates increased with increasing kinetic energy for air-dried and dry-crusted soil samples with lower initial water content. Higher initial water content contributed to decrease (up to 70%) in splash erosion rates for the wet-sealed initial condition due to early surface ponding and sealing. Time to ponding measurements verified that decrease in soil infiltration rate for wet-sealed condition is the function of increasing intensity with R^2 of 0.90 and 0.91 for silt loam and loamy sand soil, respectively. The formed seal layer can be reflected on decrease in saturated hydraulic conductivity, where the predominant factor for its reduction was kinetic energy. We identified a threshold rainfall kinetic energy from which stable surface seals are formed, which equals to 0.39 and 0.59 kJ m^{-2} h^{-1} for two silt loam soils used in this experiment. Considering high variability among replicates for saturated hydraulic conductivity measurements, it is difficult to identify clear relationship for some scenarios. Further experiments comparing more soil types should be conducted in order to precisely define soil specific properties controlling the splash erosion. In natural conditions soil is exposed to frequent changes in soil moisture and surface structure due to variable weather impacts. This research presents that the conditions before rainfall such as initial water content and surface condition highly affect soil erodibility, infiltration and final splash erosion. Therefore, including these parameters into soil erosion prediction models could significantly improve their accuracy.

Declaration of Competing Interest

The authors declare that they have no known competing financial interests or personal relationships that could have appeared to influence the work reported in this paper.

Acknowledgements

This research was performed within the project “Kinetic energy of rainfall as driving force of soil detachment and transport“, jointly funded by the Austrian Science Fund (FWF), grant number I 3049-N29 and the Czech Science Foundation (GACR), grant number GF17-33751L. The authors would like to thank to editors and anonymous reviewers for their useful comments and suggestions.

References

Armenise, E., Simmons, R.W., Ahn, S., Garbout, A., Doerr, S.H., Mooney, S.J., Sturrock, C.J., Ritz, K., 2018. Soil seal development under simulated rainfall: Structural, physical and hydrological dynamics. J. Hydrol. 556, 211–219. https://doi.org/10.1016/j.jhydrol.2017.10.073.

Assouline, S., 2004. Rainfall-induced soil surface sealing: a critical review of observations, conceptual models, and solutions. Vadose Zo. J. 3, 570–591. https://doi.org/10.2113/3.2.570.

ÖNORM L 1080, 2013. Chemische Bodenuntersuchungen – Bestimmung des organischen Kohlenstoffs durch trockene Verbrennung mit und ohne Berücksichtigung von Carbonaten. Austrian Standards, Vienna, Austria.

ÖNORM L 1050, 2016. Boden als Pflanzenstandort – Begriffsbestimmungen, Untersuchungsverfahren. Austrian Standards, Vienna, Austria.

Assouline, S., Mualem, Y., 2002. Infiltration during soil sealing: The effect of areal heterogeneity of soil hydraulic properties. Water Resour. Res. 38, 22-1-22–9. https://doi.org/10.1029/2001wr001168.

Assouline, S., Mualem, Y., 1997. Modeling the dynamics of seal formation and its effect on infiltration as related to soil and rainfall characteristics. Water Resour. Res. 33 (7), 1527–1536. https://doi.org/10.1029/96WR02674.

Atlas, D., Srivastava, R.C., Sekhon, R.S., 1973. Doppler radar characteristics of precipitation at vertical incidence. Rev. Geophys. 11, 1–35. https://doi.org/10.1029/RG011i001p00001.

Baumhardt, R.L., Römkens, M.J.M., Whisler, F.D., Parlange, J.-Y., 1990. Modeling infiltration into a sealing soil. Water Resour. Res. 26 (10), 2497–2505. https://doi.org/10.1029/WR026i010p02497.

Beczek, M., Ryżak, M., Sochan, A., Mazur, R., Bieganowski, A., 2019. The mass ratio of splashed particles during raindrop splash phenomenon on soil surface. Geoderma. https://doi.org/10.1016/j.geoderma.2019.03.028.

Bedaiwy, M.N.A., 2008. Mechanical and hydraulic resistance relations in crust-topped soils. Catena 72, 270–281. https://doi.org/10.1016/j.catena.2007.05.012.

Benjamini, Y., Hochberg, Y., 1995. Controlling the False Discovery Rate: A Practical and Powerful Approach to Multiple Testing. J. R. Stat. Soc. Ser. B. https://doi.org/10.1111/j.2517-6161.1995.tb02031.x.

Cheng, Q., Cai, Q., Ma, W., 2008. Comparative study on rain splash erosion of representative soils in China. Chin. Geogr. Sci. 18, 155–161. https://doi.org/10.1007/s11769-008-0155-9.

Dunn, J.O., 1964. Multiple comparison using rank sums. Technometrics.

Fernández-Raga, M., Campo, J., Rodrigo-Comino, J., Keesstra, S.D., 2019. Comparative analysis of splash erosion devices for rainfall simulation experiments: A laboratory study. Water (Switzerland) 11, 1–21. https://doi.org/10.3390/w11061228.

Fernández-Raga, M., Fraile, R., Keizer, J.J., Varela Teijeiro, M.E., Castro, A., Palencia, C., Calvo, A.I., Koenders, J., Da Costa Marques, R.L., 2010. The kinetic energy of rain measured with an optical disdrometer: An application to splash erosion. Atmos. Res. https://doi.org/10.1016/j.atmosres.2009.07.013.

Fernández-Raga, M., Palencia, C., Keesstra, S., Jordán, A., Fraile, R., Angulo-Martínez, M., Cerdà, A., 2017. Splash erosion: A review with unanswered questions. Earth-Sci. Rev. https://doi.org/10.1016/j.earscirev.2017.06.009.

Fox, D.M., Darboux, F., Carrega, P., 2007. Effects of fire-induced water repellency on soil aggregate stability, splash erosion, and saturated hydraulic conductivity for different size fractions. Hydrol. Process. https://doi.org/10.1002/hyp.6758.

Gao, B., Walter, M.T., Steenhuis, T.S., Parlange, J.Y., Nakano, K., Rose, C.W., Hogarth, W.L., 2003. Investigating ponding depth and soil detachability for a mechanistic erosion model using a simple experiment. J. Hydrol. 277, 116–124. https://doi.org/10.1016/S0022-1694(03)00085-4.

Ghadiri, H., Payne, D., 1977. Raindrop impact stress and the breakdown of soil crumbs. J. Soil Sci. https://doi.org/10.1111/j.1365-2389.1977.tb02233.x.

Guy, B.T., Dickinson, W.T., Rudra, R.P., 1987. Roles of rainfall and runoff in the sediment transport capacity of interrill flow. Trans. Am. Soc. Agric Eng. https://doi.org/10.13031/2013.30575.

Hairsine, P.B., Rose, C.W., 1991. Rainfall detachment and deposition: sediment transport in the absence of flow-driven processes. Soil Sci. Soc. Am. J. https://doi.org/10.2136/sssaj1991.03615995005500020003x.

Iserloh, T., Ries, J.B., Arnáez, J., Boix-Fayos, C., Butzen, V., Cerdà, A., Echeverría, M.T., ernández-Gálvez, J., Fister, W., Geißler, C., Gómez, J.A., Gómez-Macpherson, H., Kuhn, N.J., Lázaro, R., León, F.J., Martínez-Mena, M., Martínez-Murillo, J.F., Marzen, M., Mingorance, M.D., Ortigosa, L., Peters, P., Regüés, D., Ruiz-Sinoga, J.D., Scholten, T., Seeger, M., Solé-Benet, A., Wengel, R., Wirtz, S., 2013. European small portable rainfall simulators: A comparison of rainfall characteristics. Catena 110, 100–112. https://doi.org/10.1016/j.catena.2013.05.013.

IUSS Working Group WRB, 2014. World Reference Base for Soil Resources 2014. World Soil Resources Report. FAO, Rome.

Kemper, W.D., Koch, E.J., 1966. Aggregate stability of soils from western United States and Canada. United State Dep. Agric.

Kinnell, P.I.A., 2005. Raindrop-impact-induced erosion processes and prediction: A review. Hydrol. Process. 19, 2815–2844. https://doi.org/10.1002/hyp.5788.

Kinnell, P.I.A., 1982. Laboratory studies on the effect of drop size on splash erosion. J. Agric. Eng. Res. 27, 431–439. https://doi.org/10.1016/0021-8634(82)90081-6.

Klute, A., Dirksen, C., 1987. Hydraulic conductivity of Saturated soils. In: Klute, A. (Ed.), Methods of Soil Analysis, Part 1. Physical and Mineralogical Methods. American Society of Agronomy - Soil Science Socity of America, Madison, WI, pp. 694–700.

Kruskal, W.H., Wallis, W.A., 1952. Use of ranks in one-criterion variance analysis. J. Am. Stat. Assoc. https://doi.org/10.1080/01621459.1952.10483441.

Lado, M., Ben-Hur, M., Shainberg, I., 2004. Soil wetting and texture effects on aggregate stability, seal formation, and erosion. Soil Sci. Soc. Am. J. https://doi.org/10.2136/sssaj2004.1992.

Le Bissonnais, Y., 2016. Aggregate stability and assessment of soil crustability and erodibility: I. Theory and methodology. Eur. J. Soil Sci. 67, 11–21. https://doi.org/10.1111/ejss.4_12311.

Le Bissonnais, Y., Singer, M.J., Bradford, J.M., 1993. Assessment of soil erodibility: the relationship between soil properties, erosion processes and susceptibility to erosion. Farm L. Eros. Temp. plains Environ. hills. Proc. Symp. Saint-Cloud, Paris, 1992. https://doi.org/10.1016/b978-0-444-81466-1.50012-5.

Le Bissonnais, Y., Renaux, B., Delouche, H., 1995. Interactions between soil properties and moisture content in crust formation, runoff and interrill erosion from tilled loess soils. Catena 25, 33–46. https://doi.org/10.1016/0341-8162(94)00040-L.

Liu, H., Lei, T.W., Zhao, J., Yuan, C.P., Fan, Y.T., Qu, L.Q., 2011. Effects of rainfall intensity and antecedent soil water content on soil infiltrability under rainfall conditions using the run off-on-out method. J. Hydrol. 396, 24–32. https://doi.org/10.1016/j.jhydrol.2010.10.028.

McIntyre, D.S., 1958. Soil splash and the formation of surface crusts by raindrop impact. Soil Sci. https://doi.org/10.1097/00010694-195805000-00005.

Morgan, R.P.C., 2005. Soil Erosion and Conservation, third ed. Blackwell Publishing company, Oxford.

Morgan, R.P.C., 1981. Field measurement of splash erosion. Int. Assoc. Sci. Hydrol. Publ. 133, 373–382.

Mualem, Y., Assouline, S., Rohdenburg, H., 1990. Rainfall induced soil seal (A) A critical review of observations and models. Catena. https://doi.org/10.1016/0341-8162(90)90008-2.

ÖNORM L 1084, 2016. Chemische Bodenuntersuchungen - Bestimmung von Carbonat unter Berücksichtigung von Luftdruck und Temperatur. Austrian Standards, Vienna, Austria.

ÖNORM L1061-1, 2002. Physikalische Bodenuntersuchungen – Bestimmung der Korngrößenverteilung des Mineralbodens; Teil 1: Grobboden. Austrian Standards, Vienna, Austria.

ÖNORM L1061-2, 2002. Physikalische Bodenuntersuchungen – Bestimmung der Korngrößenverteilung des Mineralbodens; Teil 2: Feinboden. Austrian Standards, Vienna, Austria.

ÖNORM L 1086-1, 2014. Chemische Bodenuntersuchungen - Extraktion der effektiv austauschbaren Kationen Ca^{++}, K^{+}, Mg^{++}, Na^{+} sowie Al^{+++}, Fe^{+++}, Mn^{++} und H^{+} mit Bariumchlorid-Lösung und Ermittlung der Austauschkapazität. Wien.

OTT, 2005. Operating instructions. Present weather sensor Parsivel. Kempten.

Poesen, J., 1981. Rainwash experiments on the erodibility of loose sediments. Earth Surf. Process. Landforms. https://doi.org/10.1002/esp.3290060309.

Quansah, C., 1981. The effect of soil type, slope, rain intensity and their interactions on splash detachment and transport. J. Soil Sci. https://doi.org/10.1111/j.1365-2389.1981.tb01701.x.

R Development Core Team, 2015. R: A language and environment for statistical computing. R Foundation for Statistical Computing, Vienna, Austria. URL http://www.R-project.org/. R Found. Stat. Comput. Vienna, Austria. https://doi.org/10.1007/978-3-540-74686-7.

Rodrigo Comino, J., Senciales, J.M., Ramos, M.C., Martínez-Casasnovas, J.A., Lasanta, T., Brevik, E.C., Ries, J.B., Ruiz Sinoga, J.D., 2017. Understanding soil erosion processes in Mediterranean sloping vineyards (Montes de Málaga, Spain). Geoderma 296. https://doi.org/10.1016/j.geoderma.2017.02.021.

Rose, C.W., 1960. Soil detachment caused by rainfall. Soil Sci. 89, 28–35. https://doi.org/10.1097/00010694-196001000-00005.

Salles, C., Poesen, J., 2000. Rain properties controlling soil splash detachment. Hydrol. Process. 14, 271–282. https://doi.org/10.1002/(SICI)1099-1085(20000215)14:2 < 271::AID-HYP925 > 3.0.CO;2-J.

Salles, C., Poesen, J., Govers, G., 2001. A comparison of rain erosivity parameters for predicting soil detachment on interrills. Sustain. Glob. Farm, 10th Int. Soil Conserv. Organ. Meet. My 24–29, 1999 834–837.

Sharma, P.P., Gupta, S.C., Foster, G.R., 1995. Raindrop-induced soil detachment and sediment transport from interrill areas. Soil Sci. Soc. Am. J. 59, 727. https://doi.org/10.2136/sssaj1995.03615995005900030014x.

Sharma, P.P., Gupta, S.C., Rawls, W.J., 1991. Soil detachment by single raindrops of varying kinetic energy. Soil Sci. Soc. Am. J. 55, 301. https://doi.org/10.2136/sssaj1991.03615995005500020001x.

Strauss, P., Pitty, J., Pfeffer, M., Mentler, A., 2000. Rainfall simulation for outdoor experiments. Curr. Res. methods to assess Environ. fate Pestic. 329–333.

Truman, C.C., Bradford, J.M., 1990. Effect of antecendet soil moisture on splash detachment under simulated rainfall.

Van Dijk, A.I.J.M., Bruijnzeel, L.A., Eisma, E.H., 2003. A methodology to study rain splash and wash processes under natural rainfall. Hydrol. Process. 17, 153–167. https://doi.org/10.1002/hyp.1154.

Vermang, J., Demeyer, V., Cornelis, W.M., Gabriels, D., 2009. Aggregate stability and erosion response to antecedent water content of a loess soil. Soil Sci. Soc. Am. J. 73, 718. https://doi.org/10.2136/sssaj2007.0134.

Walker, J.D., Walter, M.T., Parlange, J.Y., Rose, C.W., van Meerveld, H.J.T., Gao, B., Cohen, A.M., 2007. Reduced raindrop-impact driven soil erosion by infiltration. J. Hydrol. 342, 331–335. https://doi.org/10.1016/j.jhydrol.2007.06.003.

Wei, Y., Wu, X., Cai, C., 2015. Splash erosion of clay-sand mixtures and its relationship with soil physical properties: The effects of particle size distribution on soil structure. Catena 135, 254–262. https://doi.org/10.1016/j.catena.2015.08.003.

Wischmeier, W., Smith, D., 1978. Predicting rainfall erosion losses: a guide to conservation planning, U.S. Department of Agriculture Handbook No. 537. https://doi.org/10.1029/TR039i002p00285.

Wischmeier, W.H., Johnson, C.B., Cross, B.V., 1971. Soil erodibility nomograph for farmland and construction sites. J. Soil Water Conserv.

Wuddivira, M.N., Camps-Roach, G., 2007. Effects of organic matter and calcium on soil structural stability. Eur. J. Soil Sci. 58, 722–727. https://doi.org/10.1111/j.1365-2389.2006.00861.x.

Xiao, H., Liu, G., Zhang, Q., Fenli, Z., Zhang, X., Liu, P., Zhang, J., Hu, F., Elbasit, M.A.M.A., 2018. Quantifying contributions of slaking and mechanical breakdown of soil aggregates to splash erosion for different soils from the Loess plateau of China. Soil Tillage Res. 178, 150–158. https://doi.org/10.1016/j.still.2017.12.026.

Zumr, D., Mützenberg, D.V., Neumann, M., Jeřábek, J., Laburda, T., Kavka, P., Johannsen, L.L., Zambon, N., Klik, A., Strauss, P., Dostál, T., 2019. Experimental setup for splash erosion monitoring—study of silty loam splash characteristics. Sustainability 12, 157. https://doi.org/10.3390/su12010157.